



TRIBHUVAN UNIVERSITY
INSTITUTE OF ENGINEERING
PULCHOWK CAMPUS

THESIS NO: M-326-MSREE-2017/2020

**Analysis of Small Signal Stability on Wind Power Integration to Integrated
Nepal Power System**

by

Bishwas Pokhrel

**A THESIS SUBMITTED TO THE DEPARTMENT OF MECHANICAL AND
AEROSPACE ENGINEERING IN PARTIAL FULLFILMENT OF THE
REQUIREMENTS FOR THE DEGREE OF MASTERS OF SCIENCE IN
RENEWABLE ENERGY ENGINEERING**

DEPARTMENT OF MECHANICAL AND AEROSPACE ENGINEERING

LALITPUR, NEPAL

JULY 2020

COPYRIGHT

The author has agreed that the library, Department of Mechanical and Aerospace Engineering, Pulchowk Campus, Institute of Engineering may make this thesis freely available for inspection. Moreover, the author has agreed that permission for extensive copying of this thesis for scholarly purpose may be granted by the professor(s) who supervised the work recorded herein or, in their absence, by the Head of the Department wherein the thesis was done. It is understood that the recognition will be given to the author of this thesis and to the Department of Mechanical and Aerospace Engineering, Pulchowk Campus, and Institute of Engineering in any use of the material of the thesis. Copying or publication or the other use of this research for financial gain without approval of the Department of Mechanical and Aerospace Engineering, Pulchowk Campus, Institute of Engineering and author's written permission is prohibited.

Request for permission to copy or to make any other use of this thesis in whole or in part should be addressed to:

Head

Department of Mechanical and Aerospace Engineering

Pulchowk Campus, Institute of Engineering

Lalitpur, Nepal

TRIBHUVAN UNIVERSITY
INSTITUTE OF ENGINEERING
PULCHOWK CAMPUS

DEPARTMENT OF MECHANICAL AND AEROSPACE ENGINEERING

The undersigned certify that they have read, and recommended to the Institute of Engineering for acceptance, a thesis entitled “Analysis of Small Signal Stability on Wind Power Integration to Integrated Nepal Power System” submitted by Bishwas Pokhrel in partial fulfillment of the requirements for the degree of Master of Science in Renewable Energy Engineering.

Supervisor, Assoc. Prof. Dr. Nawraj Bhattarai
Head of Department,
Department of Mechanical and Aerospace Engineering

Supervisor, Assoc. Prof. Dr. Shree Raj Shakya
Department of Mechanical and Aerospace Engineering

External Examiner, Dr. Narayan Prasad Adhikari
Director
Alternative Energy Promotion Centre (AEPC)

Committee Chairperson, Dr. Nawraj Bhattarai
Head of Department,
Department of Mechanical and Aerospace Engineering

Date: 29th July 2020

ABSTRACT

In power system, the wind energy and its technology integration begins to significantly influence the power system structure and parameters. Wind energy system has diverged generator technologies than the hydro power plants which are conventional. The power system stability, steady-state, transient dynamics and small-signal dynamics will be affected considerably. When the power system dynamics is connected with the wind energy system its stability are more concerned in practical way.

The wind turbines are incorporated with doubly-fed induction generator (DFIG) in modern era and, therefore, the simplified model of the DFIG incorporated with wind turbine is modelled and presented by differential algebraic relations. The model is validated against literature and references and then with the system characteristics.

The power system is non-linear and therefore, it is linearized with state space relations and then incorporated with the DFIG locations and differential size. Eigen value analysis is used to identify the stability of the DFIG and voltage limits are checked whether it is under limit or not.

In technical analysis, the IEEE standard test system is chosen for validation and then the paradigm is used to analyze the INPS system incorporated with wind energy system at different locations. The small signal stability, effect on voltage and power flow, and operating point variations are observed.

In financial analysis, project life is considered 20 year and wind energy production variation is considered in a range which is under Betz limit of generation. Different scenario for subsidy on total cost of the system is considered during financial analysis. The wind power system is feasible only if majority is financed under subsidy. The payback period of the project is attractive under high subsidy scheme only.

ACKNOWLEDGEMENT

I am taking take this opportunity to extend sincere thanks and indebtedness to all those persons who helped me during the entire period of thesis work. Primarily, I would like to express my gratitude to my project supervisors Dr. Nawraj Bhattarai & Dr. Shree Raj shakya for their continuous guidance and support throughout this study.

I would like to express my deep sense of gratitude to the Department of Mechanical and Aerospace Engineering, Pulchowk Campus, Institute of Engineering (IOE) for including the thesis work in my master's degree. I would also like to thank MSREE Coordinator Dr. Ajay Kumar Jha for providing us guidelines and teaching us Research Methodology which helped me in shaping up the research work. I would also like to thank all the esteemed faculty members of Department of Mechanical and Aerospace Engineering for guiding and encouraging us throughout period of my study.

I also acknowledge indebtedness to my family members, my roommates, colleagues for their continuous help, support and inspiration throughout my study period.

TABLE OF CONTENTS

COPYRIGHT	2
ABSTRACT	4
ACKNOWLEDGEMENT	5
LIST OF FIGURES	9
LIST OF TABLES	10
LIST OF PUBLICATIONS	11
LIST OF ABBREVIATIONS	12
LIST OF SYMBOLS	13
CHAPTER ONE: INTRODUCTION	14
1.1 Background.....	14
1.2 Problem Statement	15
1.3 Research Gap	15
1.4 Objectives	16
1.4.1 Main Objective.....	16
1.4.2 Specific Objective	16
1.5 Limitations.....	16
1.6 Thesis Organization	17
CHAPTER TWO: LITERATURE REVIEW	18
2.1 Bus Classification	21
2.2 Analysis Methods	22
2.3 Literature Survey	23
2.4 Wind Integration and Power Flow	25
2.5 Transient Stability.....	25
2.6 Voltage Stability and Small Signal Stability	27
CHAPTER THREE: RESEARCH METHODOLOGY	28

3.1 Description of Methodology.....	28
3.2 Block Diagram.....	28
3.3 Small Signal Stability Analysis	29
3.3.1 Formation of System State Matrix.....	29
3.3.2 Differential Algebraic Equations (DAE) of DFIG	31
3.3.3 Modal Matrices	32
3.3.4 Eigen value Sensitivity.....	33
3.3.5 Participation Factor.....	33
3.3.6 Network Equations for Generation and Load Bus.....	33
3.4 Power Flow Analysis	34
3.5 Methodological tool.....	36
CHAPTER FOUR: RESULTS AND DISCUSSION.....	37
4.1 General.....	37
4.1 DFIG integrated to IEEE 9 Bus System.....	37
4.2 DFIG integrated to INPS System	40
4.2.1 Case 1: [Balaju] DFIG Connected to Bus 5 with P=0.5 and Q=0.2	42
4.2.2 Case 2: [Bhaktapur] DFIG Connected to Bus 10 with P=0.5 and Q=0.2	45
4.2.3 Case 3: [Nawalparasi] DFIG Connected to Bus 31 with P=0.1 and Q=0.04 ..	48
4.2.4 Case 4: [Makwanpur] DFIG Connected to Bus 26 with P=0.1 and Q=0.04..	51
4.2.5 Case 5: [Acham] DFIG Connected to Bus 15 with P=0.2 and Q=0.08	53
4.3 Financial Analysis of Wind Energy.....	56
CHAPTER FIVE: CONCLUSION AND RECOMMENDATIONS.....	61
REFERENCES.....	62
APPENDIX A: Research Paper	64
APPENDIX B: Load and Generation Data of INPS System.....	72
APPENDIX C: Line Data of INPS System	74

APPENDIX D: Financial Analysis	77
APPENDIX E: MATLAB Codes.....	78
APPENDIX D: Plagiarism Report	131

LIST OF FIGURES

Figure 1: Classification of stability	20
Figure 2: Power Flow Simulation DFIG and Substation.....	25
Figure 3: Methodological block diagram for thesis	28
Figure 4: Flow Chart for Stability Analysis.....	30
Figure 5: Flow Chart for Newton Raphson Method of Power Flow	35
Figure 6: IEEE machine having 9 bus system	37
Figure 7: Eigenvalues Without DFIG.....	39
Figure 8: Eigenvalues With DFIG.....	39
Figure 9: Voltage profile for base load flow solution of INPS system	41
Figure 10: Eigen value plot of INPS system without DFIG	42
Figure 11: Eigen value plot of INPS system with DFIG for case 1: Balaju	43
Figure 12: Eigen sensitivity plot for Balaju	43
Figure 13: Eigen value plot of INPS system with DFIG for case 2: Bhaktapur	45
Figure 14: Eigen sensitivity for Bhaktapur	46
Figure 15: Eigen value plot of INPS system with DFIG for case 3: Nawalparasi	48
Figure 16: Eigen sensitivity plot for different DFIG Power for Nawalparasi	49
Figure 17: Eigen value plot of INPS system with DFIG for case 4: Makwanpur.....	51
Figure 18: Eigen sensitivity plot for different DFIG Power for Makwanpur	52
Figure 19: Eigen value plot of INPS system with DFIG for case 5: Acham.....	53
Figure 20: Eigen sensitivity plot for different DFIG Power for Acham.....	56
Figure 21: Levelized cost of energy versus project capacity factor	57
Figure 22: Approximate Cumulative Cash Flow versus project year	58

LIST OF TABLES

Table 1: Literature Survey and Findings of the research.....	23
Table 2: Base Case load flow solution	38
Table 3: Eigen Values for IEEE 9 bus system.....	38
Table 4: Load flow solution when DFIG connected	39
Table 5: Base load flow solution of INPS system.....	40
Table 6: Load flow solution with DFIG Integration for Balaju	44
Table 7: Load flow solution with DFIG Integration for Bhaktapur	46
Table 8: Wind Turbine Capacity and Location in Nepal.....	48
Table 9: : Load flow solution with DFIG Integration for Nawalparasi.....	49
Table 10: : Load flow solution with DFIG Integration for Makwanpur	52
Table 11: : Load flow solution with DFIG Integration for Acham	54
Table 12: Summary Sheet of Financial Analysis	57

LIST OF PUBLICATIONS

1. **Bishwas Pokhrel**, Assoc. Prof. Dr. Shreeraj Shakya, and Assoc. Prof. Dr. Nawaraj Bhattarai (2020). Analysis of Small Signal Stability on Wind Power Integration to Integrated Nepal Power System (INPS). *International Journal of Engineering and Applied Science (IJEAS)*, Vol. 7, 2394-3361.

LIST OF ABBREVIATIONS

B/C	Benefit to Cost Ratio
DFIG	Doubly Fed Induction Generator
DG	Distributed Generation
FACTS	Flexible AC Transmission System
GW	Giga Watt
HC	Hosting Capacity
HEP	Hydro Electric Project
IEEE	Institute of Electrical and Electronics Engineers
INPS	Integrated Nepal Power System
IRR	Internal Rate of Return
kVA	Kilo Volt Ampere
kW	Kilo Watt
LDC	Load Dispatch Centre
MATLAB	MATrix LABORatory
MW	Mega Watt
NEA	Nepal Electricity Authority
NREL	National Renewable Energy Laboratory
NPV	Net Present Value
PSO	Particle Swarm Optimization
Pu	Per Unit
PV	Photo-Voltaic
SLD	Single Line Diagram

LIST OF SYMBOLS

Symbol	Description	Dimension / Unit
c_1	Constant	[-]
c_2	Constant	[-]
I	Current	[A]
J	Jacobian Metrix	[-]
J_i	Current at Node i	[A]
P	Active Power	[kW]
P_{DG}	DG Size (Specified Active Power)	[kW]
$P_{totalload}$	Total Active Load	[kW]
$P_{totalloss}$	Total Active Power Loss	[kW]
Q	Reactive Power	[kVAR]
Q_{DG}	DG Size (Specified Reactive Power)	[kVAR]
$Q_{totalload}$	Total Reactive Load	[kVAR]
$Q_{totalloss}$	Total Reactive Power Loss	[kVAR]
S	Apparent Power	[VA]
V	Voltage	[V]
Y	Shunt Admittance	$[\Omega^{-1}]$
Z	Impedance	$[\Omega]$
Λ	The Real and Reactive Power Demand	[-]

CHAPTER ONE: INTRODUCTION

1.1 Background

The small signal stability of a power system is the capability of power system that maintains the system stable while small variation of disturbances is created in the system. When the disturbances are increased indefinitely the instability of the system increases. The initial operating conditions of the wind energy system, characteristics of control devices incorporated and strength of components electrical in the system affects small signal stability of power system. It is inevitable that the power system cannot be operated if the system is unstable in terms of small signal stability. The steadiness of power system consisting synchronous machine has a major attention in past and also will obtain an immense attention in future too. The small signal stability programs and its simulation programs can be used for controller design, stability status and system dynamics. The present trend in power system restructuring and deregulation has increased operation efficiency. The higher penetration of distributed generation (DG) like renewable such as wind turbine generators (WTGs) has an impact on system stability. The use of controllers on WTGs or use of FACT devices at an appropriate position enables the system stability and security.

In 2019, capacity of 60.4 GW of wind energy systems was installed globally with the 19% increase in installation than the previous year. China and US remain the world's largest onshore and offshore wind markets, together accounting for more than 60% of new installed capacity in 2019. Offshore wind is driving global wind installations and play important role with the installation record of 6.1 GW in 2019, which accounts for 10 % share of new installations record.

Among all renewable technology and energy system, wind energy has become economical and proven renewable energy technology in recent years and are intermittent source of energy. Now-a-days, one of the secure and sustainable electricity supply are wind energy systems and those are proven and tested technology of energy system. The environment is resource and may generation cost include complete generation technology capital.

The tentative wind resource potential in Nepal is mapped by Solar and wind energy resources assessment (SWERA) project. The report presents a very good potential of

wind energy development in the country. The predicted wind energy potential in Nepal is about 3000 MW with potential area of about 6074 km². The wind power density greater than 300 W/m² shares 10 % of entire area and has been analyzed with consideration of the installed capacity of 5MW/km².

1.2 Problem Statement

While defining the small signal stability, synchronism and small disturbances are considered and is defined in previous section 1.1. The small disturbances may be either change in consumer's load or generation power of generating stations. The system may become unstable due to steady and gradual upsurge in generator rotor angle because of deficiency in synchronizing torque results affected by damping torque. In integrated power system with newer technologies, especially wind turbines, adverse effect on power system are introduced due to the spinning reserves requirements and scheduling and energy storage because wind energy resource is variable and difficult to predict. The positioning and alternating nature of wind turbine generators creates voltage dips, grid frequency variation beyond the limits. Hence, the disturbances due to integration of wind turbine in integrated power system must be studied to imply the problems and also probable solutions to overcome the problem.

1.3 Research Gap

The wind turbines are very much using in the world, in the scenario of Nepal wind power is limited growth in small scale. The wind turbine standalone is useful but when it is linked to the grid then it impacts on the stability of the grid. The research gap in the thesis is how the stability changes while wind turbines are added to grid and how much power can be integrated at the prescribed location and is not studied in Nepalese power system. The more the connection point of wind turbine system into the grid, then how it affects the participation factor and small signal stability of the grid.

1.4 Objectives

1.4.1 Main Objective

The main objective of the thesis is to study the small signal stability effect on the Integrated Nepal Power System (INPS) due to wind power integration into grid.

1.4.2 Specific Objective

1. To study the influence on voltage profile, and stability of electric power grid.
2. To study the effects on small signal stability with participation factor and Eigen value analysis in INPS due to wind power integration.
3. To study the sway of wind power sensitivity in the Integrated Nepalese Power System (INPS).
4. To perform financial analysis of wind turbo-generator system.

1.5 Limitations

This dissertation discusses on the WTG impact on the system stability but restricted to technical discussion on voltage profile Eigen value analysis and Eigen sensitivity analysis. The thermal limit of existing grid the current handling capacity cables and conductors, grid sensitivity effect due to impedance match and series/parallel harmonic resonance is not considered. It only provides information about whether system is stable or not while integration or adding a wind power to the grid. It does not provide information and specification of the protection system that could be incorporated for wind generation unit and grid system. The effect in power flow in network due to reconfiguration of grid system is not well-thought-out in the analysis. The variable renewable energy (VRE) sources are not considered due to its inability to supply more or less constant power at all periods.

1.6 Thesis Organization

The thesis organization is categorized in five chapters as follows:

Chapter 1 explains the presents the introduction of power system with energy scenario, distributed generation (DG) and wind turbine generation (WTG). The difficulties raised when WTG integration is linked into grid is discussed and express the objective of this dissertation with scope and limitation of the study.

Chapter 2 comprises of literature review based on the background of the distributed generation and wind turbine integration, power system stability, and power flow analysis. In stability, small signal stability, voltage stability, and transient stability are deliberated.

Chapter 3 proposes the methodology for the power flow analysis, small signal stability analysis and the stability analysis, Eigen value and participation factor analysis in integrated power system with WTG. The methodological tools which are used for proposed paradigm are discussed under this chapter.

Chapter 4 discusses on the stability variation due to WTG size and its location in the integrated Nepalese power system and the related results are presented and also provides the discussion and summary of the DFIG analysis in IEEE and INPS system.

Chapter 5 delivers the conclusion with recommendations for future works.

CHAPTER TWO: LITERATURE REVIEW

In Nepal, the potential of hydro energy is in topmost position. The technical potential of hydro power is 83,000 MW and techno-economical feasible is 42,000 MW. NEA's hydropower plants and small power plants altogether generated 2,548.11 GWh of electricity in FY 2018/19, an increase by 10.39 % over the generation in FY 2017/18. These all generators are interconnected at 220 kV and 132 kV transmission line voltage level and known as national grid of the country. The line length is 2337.7 km. The system in whole is controlled and regulated by the Integrated Nepal Power System (INPS). The government of Nepal (GON) has kept the power generation as well as renovation or extension of grid strength. The transmission voltage of many 220 kV & 400kV is under construction and also many are proposed. The peak demand of the INPS is 1320.28 MW in 2019 and the annual energy generation is 2548.11 GWh at 2019. The more power required is purchased from independent power producers (IPP) and cross-border trade with India. At the remote areas of Nepal, the power supplied to consumer based on isolated mode system and generations are from micro hydro power, solar and wind energy (*Annual report of Nepal Electricity Authority, 2018/19, 2019*). The power developed from such sources has now in influential stage and a concept of 'mini grid' can be integrated to existing INPS. This grid can increase the load factor, system stability and security.

The integration of generating stations at appropriate position can increase small signal stability margin. The power failure or even cascading power failure is due to the instability of system. The low stability margin may undergo unstable when the small changes in dynamic state variables.

Energy Access, as defined by IEA is: "The user having a dependable and reasonable access to regular activities, where first priority is to connect electricity and then increasing over the time depending upon consumption." IEA's definition comes as a requirement for developing an Energy Development Index and focuses on household energy access, with emphasis on access for household utility and electricity connection.

In the World Economic Outlook 2012, the level of consumption increases over time which is fixed at a minimum level as 250 kWh per year for rural household and 500 kWh for municipal household in order to reach the area average. The utility of electricity in replace of advanced cook-stoves (biomass used), LPG stoves and biogas

systems for cooking are also taken into account in which GTF is defined under electricity access and access to modern cooking solutions separately. Electricity Access as “Principal source of lighting and accessibility of an electricity connection at home” and the modern one as “depending on non-solid fuels for cooking primarily”. Limitations: defined separately, solid fuels may be sustainable and clean. Like gasifiers. Hence, to achieve sustainable development, energy should be considered as an enabler for development as well as a potential source of challenges to sustainability. Energy is thus an important factor in sustainable development, and since access to energy enables productivity, energy access is an important consideration for sustainable development. With the motto to achieve global sustainable development, seventeen Sustainable Development Goals (SDGs) were approved by UN General Assembly in 2015 which has to be achieved till 2030. The goals of universal energy access were addressed by the goal number 7 of the 17.

The aim of Sustainable Development Goal (SDG) number 7 is “Universal access to affordable, reliable, and sustainable modern energy by 2030”. To track the progress of those goals, SE4ALL Global Tracking Framework (GTF) was created as an initiative led by international development partners like World Bank and International Energy Agency. Energy data is gathered at regular intervals to measure baseline and progress. Multi-tier Framework was developed by ESMAP, under the SEEforALL initiative for monitoring and evaluation of energy access. MTF has redefined energy access from a traditional one to a multidimensional one, as “the capability to benefit energy that is sufficient, available when necessary, consistent, having good quality, appropriate, inexpensive, lawful, healthy and harmless for all required energy services”.

For power system stability study, a detailed DFIG wind turbine model is proposed having the stator flux transient in *V. Akhmatov* PhD thesis. However, this presentation possesses a difficult situation for positive sequence fundamental frequency simulation tools because of incompatibility and very small time step stipulation with standardized power system components (Akhmatov, 2003). *I. Erlich et. al* proposed another DFIG wind turbine in reduced order model, where for normal simulation, the stator transients are omitted. However, the incorporation of a current controller in DFIG system still require a small step-size for the simulation. This model excludes both the rotor flux dynamics and stator from the DFIG model, which is equivalent to the steady state

system representation. However, instantaneous rotor current controller is still assumed. An repetition procedure is required to solve the algebraic loops among grid system including the generator prototype and the grid prototype, which is not desirable for the model implementation (Erlich, Kretschmann, Fortmann, Mueller-Engelhardt, & Wrede, 2007). Time lags are presented by *Y. Lei et. al*, which represent the delays of current controller and are introduced to avoid algebraic loops. Thus, the rotor dynamics are omitted (Lei, Mullane, Lightbody, & Yacamini, 2006).

According to the power system point of view, whenever the power system is affected by the external or internal physical disturbance, the capability of an electric power system to regain the state of operating equilibrium is defined as the power system stability. Power system stability is classified as shown in Figure 1.

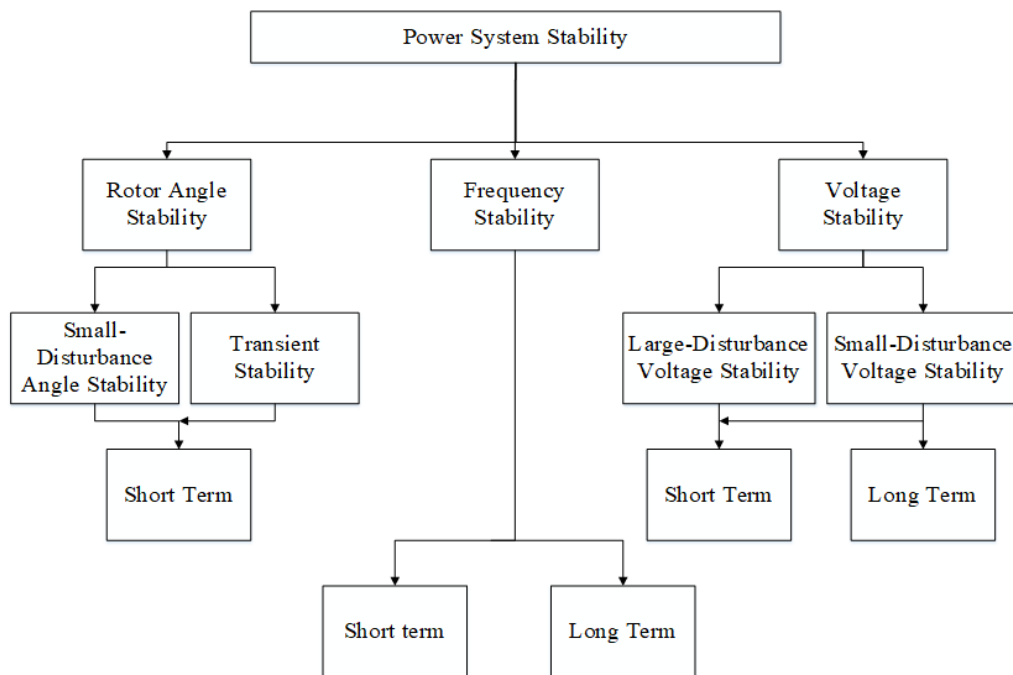


Figure 1: Classification of stability

When the synchronous machines of an interconnected the grid network is able to remain steady while subjecting a disturbance then it is referred to be total angle stability of power system. The system become unstable due to loss of synchronization with other generators when the angular swings of few generators increases. Hence, it is recommended to maintain the synchronization of each generators when two machines or multi machines are used in a system.

Load/power flow analysis is usually used to identify the parameters of each node in every connection. This method of analysis incorporates the power flow calculation and voltage of a transmission network of definite bus conditions or terminal. The four quantities namely: active power, reactive power, voltage magnitude, and power angle are associated with each bus in balanced system.

2.1 Bus Classification

When one or many lines, loads and generators are interconnected to a point, it is defined as a bus also known as node. As mentioned earlier, the four quantities: active power, reactive power, voltage magnitude, and power angle are used in power system in the load flow problem. Power flow equation is used to identify the two quantities out of mentioned four where as other two are specified. Depending upon these four parameters, the buses are categorized into 3 phases as: Generation bus, Slack bus, and Load bus. The loads are taken constant while solving the equations of power system. The solutions of power flow provide the information of four quantities and are known for all nodes.

Load Buses: The generation of real 12 reactive power are taken as null and they have no generation connected to them. The negative sign represents the power flows out of bus where the loads are depicted by real power ($-P_L$) and reactive power ($-Q_L$) when the loads are connected to these buses.

Voltage Controlled Buses: The generation system is connected either in the active power generation or reactive power generation or both in this type of buses. This bus is also called generation bus or PV bus. In order to keep the constant power and constant bus voltage, the prime mover controls the power generation and excitation system controls the terminal voltage.

Slack or Swing Bus: It is the reference bus to other buses and all the information of load, voltage controlled and generation buses are referenced to slack bus information. However, the reference is set against angles of other bus and the voltages are measured. Slack bus has angle zero degree for the reference unless otherwise not defined.

2.2 Analysis Methods

The analysis of voltage stability is introduced by dynamic and static analysis which have their own pros and cons. Time domain analysis and information of the parameters variation on time bases is introduced in dynamic analysis. Coordination of equipment's with time frame overlapping are used in dynamic simulations. Generator controls, under voltage load shedding and switched capacitor banks can be taken as an example for equipment's with time frame overlapping. The performance during the final stages of collapse like changes in load, motor stalling etc. and recovery resulting in voltage collapse or stability can be extracted using dynamic simulations. The limitation of dynamic simulation includes the complexity due to extra dimension of time frame in the model, requirement of detailed information for each parameters and large system of equation. Extensive computing technology and methods should be incorporated to determine the parameter and solving the equations.

The slower performance on voltage stability and steady state parameters of the system is addressed by the static analysis. The important phenomenon in the instability is areas susceptible to voltage instability can be defined by generating the indices which are also used to indicate the elements. Due to the less rigorous computation, static analysis is suitable for online and offline application.

2.3 Literature Survey

The table 1 shows the proposed approach and corresponding findings on the following literature.

Table 1: Literature Survey and Findings of the research

Reference/Articles	Proposed Method	Findings	Gap
Shi LB, Wanc C, <i>et al</i> , 2011	Probabilistic approach is presented for the analysis of small signal stability.	DFIG based generation intermittence is incorporated in test system and system becomes unstable with the increase of real power output.	It fails to decide the reactive power and oscillation stability is not considered.
Lingling F, Chanxia Z, Lee ZM, Minqiang H., 2011 Zhu C, Hu M, Wu Z., 2012	An eigenvalue analysis and dynamic simulation is carried to study the effect of induction generator (IG) and torsional interaction in series compensated power system for different compensation levels.	The network resonant frequency likely to increase for higher compensation level and low wind speed, which results in poor damping; while higher wind speed improves the networks' damping, resonant mode and compensation level.	Eigenvalues are used for mechanical stability analysis but fails to the electrical stability.

Tsourakis G, Nomikos BM, Vournas CD., 2009	Differential geometry theory is introduced for a non-linear controller which is used for DFIG wind power connection to grid.	System damping as well as the fault ride-through capability of DFIG is improved.	Grid stability is improved but fails for signal stability.
Suriyaarachchi DHR, <i>et al</i> , 2012 Faried SO, Unal I, Rai D, Jean M., 2012	Small signal stability analysis is used to analyze the sub-synchronous resonance between a DFIG wind power connection and a series compensated power line is presented.	The sub-synchronous interaction between DFIG wind turbine-generator system and series compensated power systems is due to controller interactions.	It deals with the compensation on wind farm not to decide the grid system behavior.
Mishra Y, Mishra S, <i>et al</i> , 2009 Yang L, Yang GY, <i>et al</i> , 2010 Fan L, Yin H, Zhixin M., 2011	A model for small signal stability system is developed and then an eigen value based objective function is optimized by using optimization techniques: PSO, BF, and DE to tune the parameters of DFIG controller.	The dynamic performance of wind turbine system improves and provides the fault ride through capability to DFIG.	Optimization as performed based on eigenvalues but not discuss about the voltage.
Bhukya J, Mahajan V, 2017	Small signal stability analysis with consideration of three – phase fault.	DFIG induces oscillatory instability in the system and it is improved using excitation controller.	Lacks to define the location of DFIG.

2.4 Wind Integration and Power Flow

For power/load flow analysis with wind integration, wind turbine generator system is modeled which provides fixed power and is integrated into the system as a load bus by assuming it as a negative load. The model studies real power (P) level and reactive power is injected based on power factor ranging 0.85 - 0.9 lagging. The reactive power is fulfilled by the shunt capacitors for reactive power consumption. Voltage source inverters are introduced in DFIG is modeled by PV bus with appropriate reactive power limits. Although, a single substation is depicted for the wind energy generation system because wind farms are used to deliver bulk power. The aggregated model is applicable for the active power flow to grid network. Figure 2 shows the simplified representation of collected system in a single model of a GE WTG.

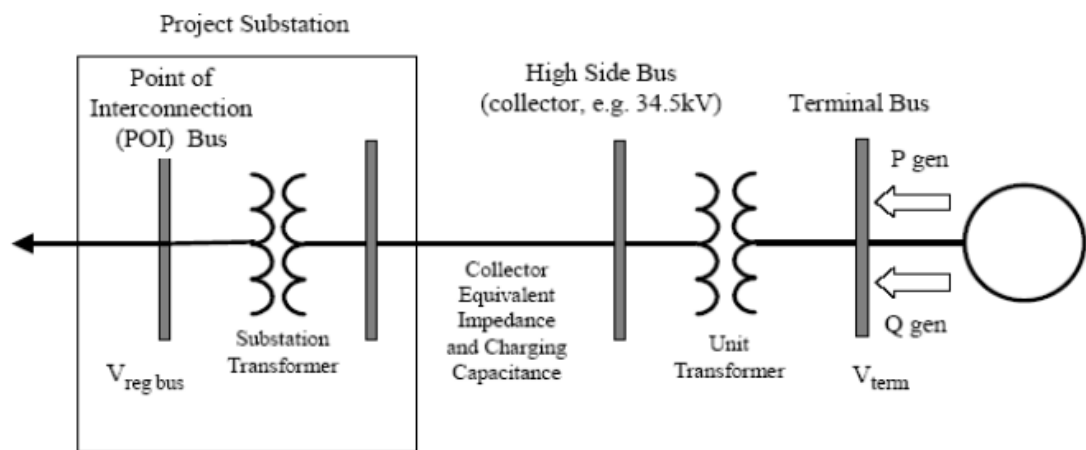


Figure 2: Power Flow Simulation DFIG and Substation

The power system uses mainly Gauss-Siedel method and Newton Raphson (NR) method in the integrated network. The Fast De-coupled method is also used in newer system which have more lateral branching network.

2.5 Transient Stability

Transient stability is defined as the power systems' ability to maintain synchronism whenever exposed to a severe disruption/disturbance which can result in large deviation of generator rotor angle. Equipment damage and load changes can be taken as an example for severe disruption. The system responds based on the power rotor angle variation. The initial operating state and the disturbance severity creates the transient

effect which effects the stability of system. The insufficient synchronizing torque creates transient instability in the system and results in a periodic rotor angular separation. The 3 to 5 seconds disturbance study is interested in transient stability studies and time duration may be extended to 10-20 seconds for large system (Ghennam, Berkouk, & François, 2009). When the electrical torque drops below the mechanical torque due to network disturbance in a synchronous machine, the rotor is accelerated resulting the increase in speed of rotor and deviating the position (angular) of rotor flux vector. When the rotor angle is increased the generator load torque also increases. This mechanism leads to increment in electrical torque to tally the mechanical torque. Talking about the wind energy system incorporated with DFIG, the speed and position of the rotor varies due to the load disturbance created by generator. But, asynchronous operation excludes the dependency of position of rotor flux vector on the physical position of rotor. And there is no any existence of characteristics of synchronizing torque angle (Tapia, Tapia, Xabier Ostolaza, & Sáenz, 2003). Due to increased DFIG penetration, impact of disturbances is high and can be reduced by proper mechanism or technique. The dynamic characteristics depicted by DFIG in the network can be matched with the synchronous machines by orienting the wind farms in well manner (Slootweg, De Haan, Polinder, & Kling, 2001; Tapia et al., 2003). In traditional system of protection in wind farm, wind turbo-generator sets were disconnected while any grid fault occurs. In order to handle the wind turbines and ride through temporary faults, a new protection system is required. The new protection must be able to enhance the stability in grid transient, power oscillation and damping of system. The factors like network parameter and fault conditions also affect the stability of an interconnected system with wind turbine-generator in transient state. In transient stability simulation incorporated with wind energy technology/system, the wind speed is considered to be constant throughout the period. Since the generator speed varies, the mechanical torque cannot be considered constant. (Lima, Luna, Rodriguez, Watanabe, & Blaabjerg, 2010) . Recent researches have identified that transient stability of the system can be improved by replacing the fixed-speed turbines with variable speed wind turbines technology which uses DFIG. The sensitivity of such system is considered as major drawback as they are very vulnerable due to grid-connected power electronic converter. This is because, the rush of active power to the converter results in faults. Power flows through the capacitor linking the two converters in a direction of the rotor side converter to the grid side converter. The grid side converter is maintained at low

voltage because of machine terminals and it cannot transfer extra power to grid which leads to increment in the charging on capacitor further leading to high voltage across the terminals (Lima et al., 2010; Tapia et al., 2003). The converter is protected to avoid the further damages using a crowbar. The crowbar provides a safe route to high transient currents by short circuiting itself when the rotor current exceeds the protection limits. (Bieker, Peitz, Brunton, Kutz, & Dellnitz, 2019).

2.6 Voltage Stability and Small Signal Stability

Voltage stability is defined sometimes as load balancing system (Hauer, 1991). Voltage instability involves voltage dynamics which is opposed to synchronous stability of rotor angle. The Voltage collapse in the system is defined as the mechanism in which very low voltage profile is generated by a voltage instability which is a vital portion of the system. The limits of voltage instability and maximum power transmission of the grid are not interconnected directly (Hauer, 1991; Taylor, 1994). The large complex system cannot be analyzed practically. For the simplicity, the systems examined in power system are approximately linearized with small deviation occurring at the equilibrium although they are not of a linear nature. When the failure occurs, the system's ability to return to its former state in a short period is defined as the stability. The stability of signals i.e. small signal stability and large signal stability is analyzed using the Lyapunov linearization method. A new proposal to predict the combined stability of small and large signal stability problem was presented by the authors (Che et al., 2017; Chi-Tsong, 1984; Wilems, 1971). When the system is stable in a power system, an equilibrium is generated between the mechanical momentum which is incoming and electrical momentum which is outgoing. But, it remains to be concisely static stability when the short circuit faults are also incorporated the balance between the incoming momentum and outgoing momentum are eliminated and the equilibrium is explained in term of static stability. This type of problem is elucidated by largest Lyapunov based approach which uses the data from large systems alone. (Dheer, Doolla, & Bandyopadhyay, 2017; Haung, Chen, Ma, Zhang, & Chen, 2018).

CHAPTER THREE: RESEARCH METHODOLOGY

3.1 Description of Methodology

The outline of this work begins from the literature review, in which the wind power generation and the impact on the grid, when integrated to the existing grid is studied. At the review stage, issues of wind farm integration are investigated, the methodologies for system impact study relevant to small signal stability integration is explored.

3.2 Block Diagram

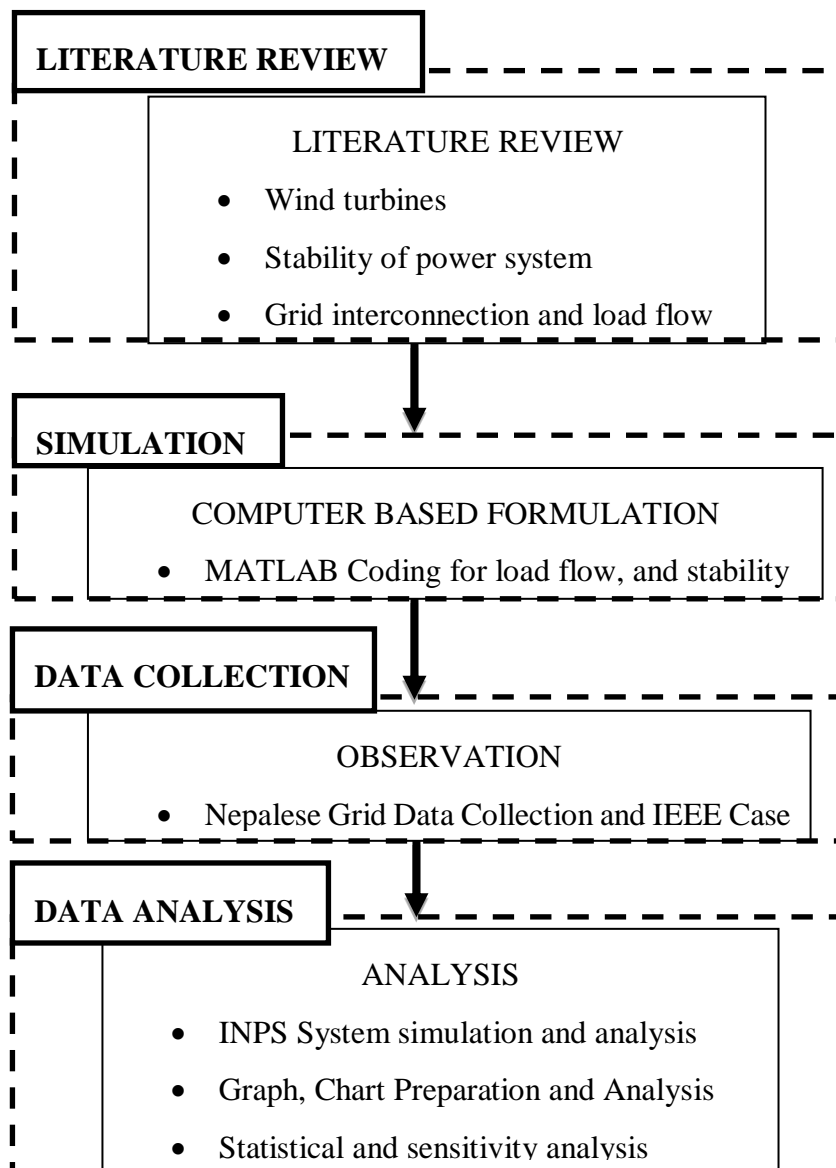


Figure 3: Methodological block diagram for thesis

Figure 3 is the diagrammatic representation of methodology. The block diagram consists of four parts: Literature review, Simulation, Data Collection and Data Analysis. In Literature, wind turbine characteristics, wind turbine power generation capability, power system stability and methods for power flow are studied. MATLAB is used to formulate and simulate the prescribed process of methods to study the stability. The data of wind turbine power generation and its feasibility is collected from Alternative Energy Promotion Centre (AEPC) and the integrated Nepalese power system data is collected from Nepal Electricity Authority (NEA). A formulated simulation is done into the INPS and WTG data and analysis is performed for the integrated system.

3.3 Small Signal Stability Analysis

The stability analysis for the power system is performed under the condition that the DFIG is added to the grid. In stability analysis, the Eigen values and its vector, participation factor are important for the study. The system data is arranged and then the load flow is performed without and integration of DFIG and stability of the system is studied. After that, the DFIG is integrated to the grid and then the load flow is performed to check the power flow in the network and stability is checked from Eigen value analysis. If the system is found stable, then the results are saved so can be used further. If system is not found to be stable, then the DFIG parameters are varied with respect to the power and the DFIG reactance. The figure 3 shows the methodology for the stability analysis and subsections 3.3.1 to 3.3.6 are used to describe the involved equations and mathematical formulations.

3.3.1 Formation of System State Matrix

The non-linear model of whole system can be represented by non-linear equations. The equations are in state space form are as follows:

$$\dot{x} = f(x, y, u) \quad (1)$$

$$0 = g(x, y) \quad (2)$$

Where, x , y and u are the variables for state, output and input respectively.

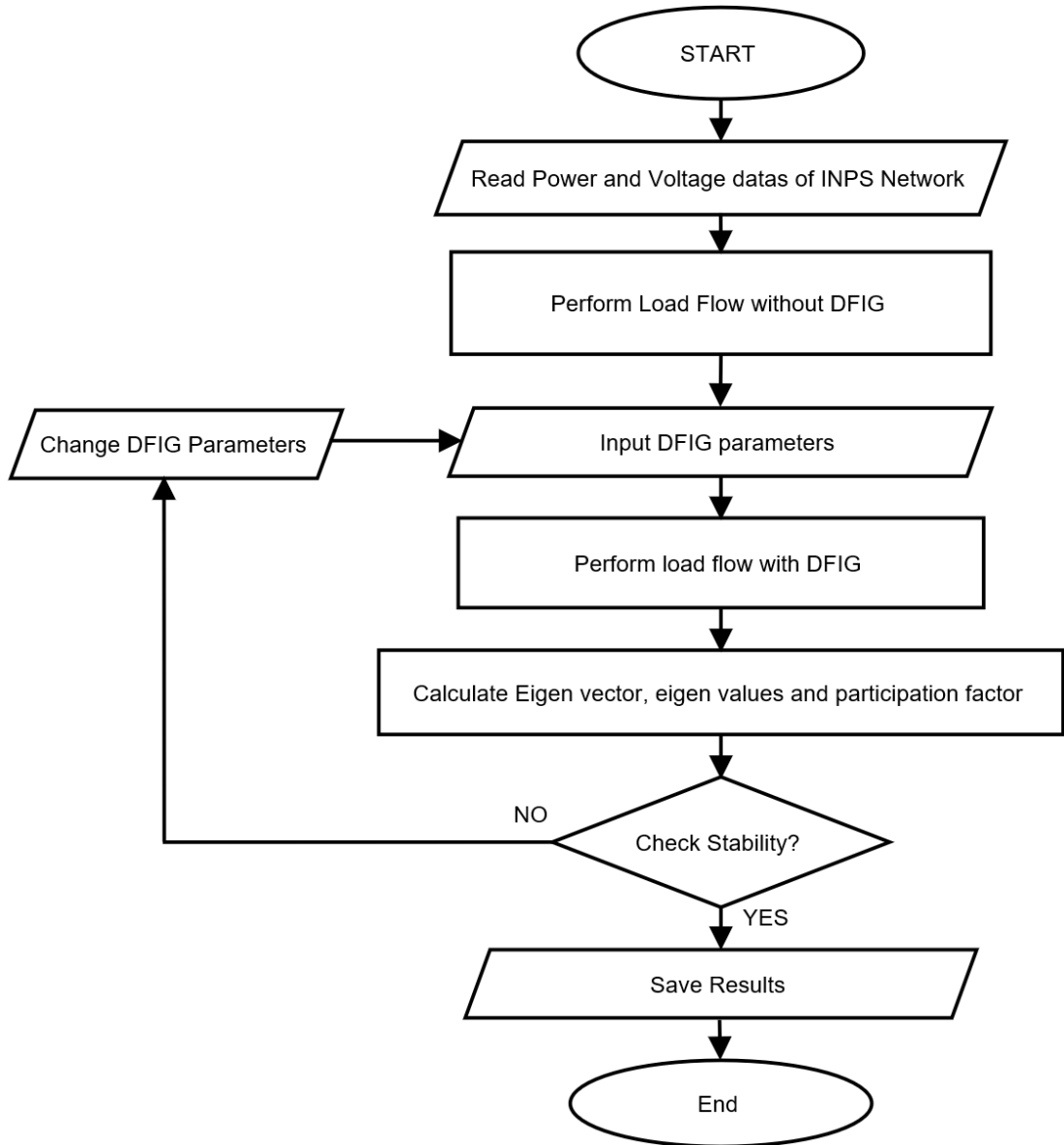


Figure 4: Flow Chart for Stability Analysis

The equations (1) and (2) are linearized and system state matrix A_{sys} is formed.

$$\dot{\Delta x} = A_{sys}\Delta x \quad (3)$$

The Eigen value of A_{sys} is calculated for the computation for the small signal stability. The Eigen values are may be real or complex or zero. The complex Eigen values appear always in complex conjugate pair. For stable operation of system, all eigenvalues λ_i must be in the left half plane. $\lambda_i = (\sigma_i \pm j\omega_i)$ and $\sigma_i < 0$. The time constant T [s], damping ratio ζ and oscillating frequency f [Hz] of Eigen value is given by:

$$T = \frac{1}{|\sigma|} \quad (4)$$

$$\zeta = \frac{-\sigma}{\sqrt{\sigma^2 + \omega^2}} \quad (5)$$

$$f = \frac{\omega}{2\pi} \quad (6)$$

3.3.2 Differential Algebraic Equations (DAE) of DFIG

The DFIG wind1power is linked to load (PQ) bus through a transformer and a bus. If n_{dfg} is the number of DFIGs then the total number of buses is increased by n_{dfg} . The following equations represent the DAEs and DFIG:

$$\frac{di_{qsi}}{dt} = \frac{\omega_{elB}}{L'_{si}} (-R_i i_{qsi} + \omega_s L'_{si} i_{dsi} + \frac{\omega_{ri}}{\omega_s} e'_{qsi} - \frac{1}{T_{ri} \omega_s} e'_{dsi} - v_{qsi} + K_{mrrri} v_{qri}) \quad (7)$$

$$\frac{di_{dsi}}{dt} = \frac{\omega_{elB}}{L'_{si}} (-R_i i_{qsi} - \omega_s L'_{si} i_{qsi} + \frac{\omega_{ri}}{\omega_s} e'_{dsi} + \frac{1}{T_{ri} \omega_s} e'_{qsi} - v_{dsi} + K_{mrrri} v_{dri}) \quad (8)$$

$$\frac{de'_{qsi}}{dt} = \omega_{elB} \omega_s \left(R_{2i} i_{dsi} - \frac{e'_{qsi}}{T_{ri} \omega_s} + \left(1 - \frac{\omega_{ri}}{\omega_s} \right) e'_{dsi} + K_{mrrri} v_{dri} \right) \quad (9)$$

$$\frac{de'_{dsi}}{dt} = \omega_{elB} \omega_s \left(-R_{2i} i_{qsi} - \frac{e'_{dsi}}{T_{ri} \omega_s} + \left(1 - \frac{\omega_{ri}}{\omega_s} \right) e'_{qsi} + K_{mrrri} v_{qri} \right) \quad (10)$$

$$\frac{d\omega_{ri}}{dt} = \frac{1}{2H_{gi}} (k_{shi} \theta_{twi} + c_{shi} \omega_{elB} (\omega_{ti} - \omega_{ri}) - T_{ei}) \quad (11)$$

$$\frac{d\theta_{twi}}{dt} = \omega_{elB}(\omega_{ti} - \omega_{ri}) \quad (12)$$

$$\frac{d\omega_{ti}}{dt} = \frac{1}{2H_{ti}} (-k_{shi}\theta_{twi} - k_{shi}\omega_{elB}(\omega_{ti} - \omega_{ri}) + T_{mi}) \quad (13)$$

The total powers delivered to grid in terms of active and reactive powers are as follows:

$$P_{tot} = P_s + P_r = v_{qs}i_{qs} + v_{ds}i_{ds} + v_{qr}i_{qr} + v_{dr}i_{dr} \quad (14)$$

$$Q_{tot} = Q_s + Q_{GSC} = Q_s = -v_{qs}i_{ds} + v_{ds}i_{qs} \quad (15)$$

Where, the grid side converter reactive power is operated at the unity power factor and is zero. The P_s represent stator active power and Q_s represent reactive powers. The rotor currents are:

$$i_{qr} = -\left(\frac{e'_{ds}}{X_m}\right) - k_{mrr}i_{qs} \quad (16)$$

$$i_{dr} = \left(\frac{e'_{qs}}{X_m}\right) - k_{mrr}i_{ds} \quad (17)$$

Here ω_{elB} refers electrical base speed, ω_s synchronous speed, v_{qs} , v_{ds} are stator quadrature & v_{qr} , v_{dr} rotor quadrature and direct voltages, i_{qs} , i_{ds} & i_{qr} , i_{dr} stator & rotor quadrature and direct currents, e'_{qs} and e'_{ds} equivalent quadrature and direct voltage sources behind transient impedance.

3.3.3 Modal Matrices

The following matrices are introduced to express the Eigen properties of A_{sys} .

$$\Phi = [\Phi_1 \Phi_2 \dots \Phi_n] \quad (18)$$

$$\Psi = [\Psi_1^t \Psi_2^t \dots \Psi_n^t]^t \quad (19)$$

$\Lambda = \text{diag. matrices, with eigenvalue } \lambda_1 \lambda_2, \dots, \lambda_n \text{ as diag. elements}$

$$A_{sys} = \Phi \Lambda \quad (20)$$

$$\Psi\Phi = I, \Psi = \Phi^{-1} \quad (21)$$

so from equation (20) and (21),

$$\Phi^{-1}A_{sys}\Phi = \Lambda \quad (22)$$

3.3.4 Eigen value Sensitivity

Let the element of matrix be a_{kj} , (k -th row and j -th column element of A_{sys}). By taking partial derivative to a_{kj} in both in sides we get,

$$\frac{\partial \lambda_i}{\partial a_{kj}} = \Psi_{ik}\Phi_{ji} \quad (23)$$

3.3.5 Participation Factor

The contribution of dominant states (row-wise) to particular modes (eigenvalue in column-wise) is determined by participation factor (pf). The combination of right eigenvector and left eigenvector forms the participation matrix (P) as:

$$P = [p_1 p_2 \dots p_n] \quad (24)$$

$$\text{with } p_i = \begin{bmatrix} p_{1i} \\ p_{2i} \\ \vdots \\ p_{ni} \end{bmatrix} = \begin{bmatrix} \Phi_{i1}\Psi_{1i} \\ \Phi_{i2}\Psi_{2i} \\ \vdots \\ \Phi_{in}\Psi_{ni} \end{bmatrix} \quad (25)$$

When p_{ki} is normalized to get participation factor of k^{th} modes to i^{th} states is given by

$$p_{ki} = \frac{|\Psi_{ik}||\Phi_{ki}|}{\sum_{k=1}^n |\Psi_{ik}||\Phi_{ki}|} \quad (26)$$

3.3.6 Network Equations for Generation and Load Bus

The network equations for generation buses are as follows:

$$P_{Li}(V_i) = \sum_{k=1}^n V_i V_k Y_{ik} \cos(\theta_i - \theta_k - \alpha_{ik}) - I_{di} V_i \sin(\delta_i - \theta_i) - I_{qi} V_i \cos(\delta_i - \theta_i) \quad (27)$$

$$Q_{Li}(V_i) = \sum_{k=1}^n V_i V_k Y_{ik} \sin(\theta_i - \theta_k - \alpha_{ik}) + I_{qi} V_i \sin(\delta_i - \theta_i) - I_{di} V_i \cos(\delta_i - \theta_i) \quad (28)$$

The network equations for load buses are as follows:

$$P_{Li}(V_i) = \sum_{k=1}^n V_i V_k Y_{ik} \cos(\theta_i - \theta_k - \alpha_{ik}) \quad (29)$$

$$Q_{Li}(V_i) = \sum_{k=1}^n V_i V_k Y_{ik} \sin(\theta_i - \theta_k - \alpha_{ik}) \quad (30)$$

3.4 Power Flow Analysis

The power/load flow analysis of the integrated network system is done using Newton Raphson(NR) method. The flow chart for power flow analysis is presented in figure 5. The node voltage and the impedance of each line are subjected to initialize and the mismatch matrices of active and reactive power (Q) are calculated. The mismatch matrices are used to determine the solution of the equations presented in equation (27) and (28) for generator bus and equation (29) and (30) for load buses. If the solution is not converged, then the Jacobian matrix (equation 31). is formed to solve the equations and then the voltage and voltage angle are determined.

$$\begin{bmatrix} \Delta Q_3 \\ \Delta P_2 \\ \Delta P_3 \end{bmatrix} = \begin{bmatrix} \frac{\partial Q_3}{\partial V_3} & \frac{\partial Q_3}{\partial \delta_2} & \frac{\partial Q_3}{\partial \delta_3} \\ \frac{\partial P_2}{\partial V_3} & \frac{\partial P_2}{\partial \delta_2} & \frac{\partial P_2}{\partial \delta_3} \\ \frac{\partial P_3}{\partial V_3} & \frac{\partial P_3}{\partial \delta_2} & \frac{\partial P_3}{\partial \delta_3} \end{bmatrix} \begin{bmatrix} \Delta V_3 \\ \Delta \delta_2 \\ \Delta \delta_3 \end{bmatrix} \quad (31)$$

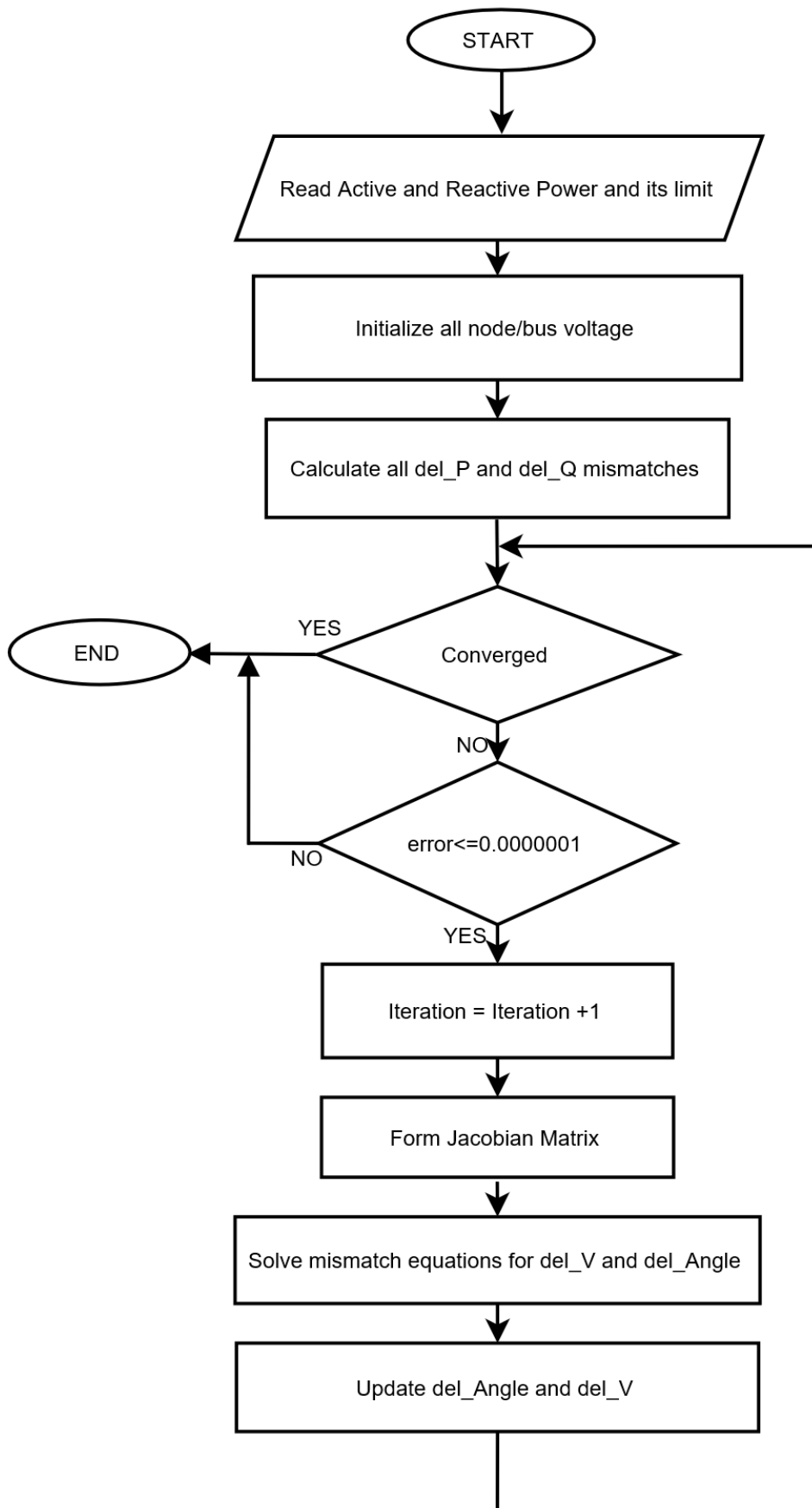


Figure 5: Flow Chart for Newton Raphson Method of Power Flow

3.5 Methodological tool

To verify and perform research on the system, MATLAB (MATrix LABoratory) which is a multi-paradigm numerical computing tool developed by MathWorks Inc. is used. In MATLAB, the computer's cores are used for mathematical operations, and library cells are heavily optimized ("MATLAB Designed For Engineers and Scientists," 2019). The tool is very much able to perform mathematical operations on differential equations and algebraic equations. The testing and debugging is performed in PC after the algorithm is coded in a MATLAB code.

CHAPTER FOUR: RESULTS AND DISCUSSION

4.1 General

As explained in chapter 3, the proposed methodology uses to evaluate the Eigen values and participation factor. The proposed methodology for stability analysis, Eigen vector determination and sensitivity analysis is studied using MATLAB and it is tested for standard IEEE – 9 bus system consisting 3 machines. The IEEE bus test system is used for the base of the study in this thesis and also for authentication and verification of model. Primarily, the proposed methodology is validated using IEEE standard bus systems and then it is applied for Integrated Nepalese Power System network. This study includes integrated power system of Nepal above 66 kV system network is considered for study purpose.

4.1 DFIG integrated to IEEE 9 Bus System

The IEEE 9 bus test system is presented in figure 6 which includes three synchronous machine. In this system, bus 5, 6, and 8 are the load buses. The base case load flow solution is presented in table 2.

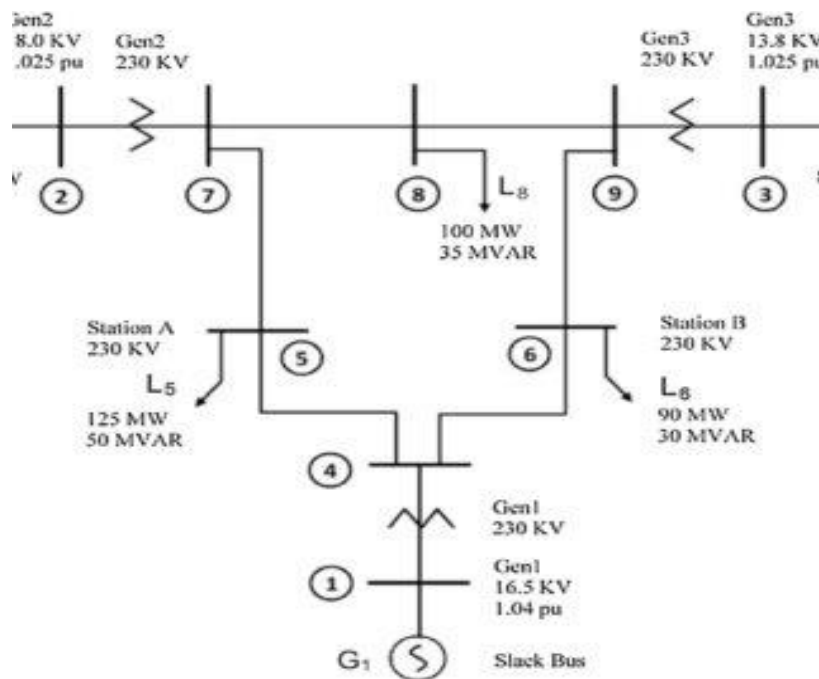


Figure 6: IEEE machine having 9 bus system

Table 2: Base Case load flow solution

Bus Number	V (pu)	Theta(rad)	P (pu)	Q (pu)
1	1.040	0.000	0.716	0.270
2	1.025	0.162	1.630	0.067
3	1.025	0.081	0.850	-0.109
4	1.026	-0.039	0.000	0.000
5	0.996	-0.070	-1.250	-0.500
6	1.013	-0.064	-0.900	-0.300
7	1.026	0.065	0.000	0.000
8	1.016	0.013	-1.000	-0.350
9	1.032	0.034	0.000	0.000

The variation of minimum Eigen values is presented in table 3. Individually, the finest location of wind power-generation is identified to be bus 5 since minimum eigenvalue improvement is highest in this bus. In this system, the optimum loading at bus 5, 6, and 8 are 0.79 pu, 0.96 pu and 1.04 pu respectively. When the DFIG based wind power system connected to bus 5, 6, and 8 simultaneously then the power flow and the Eigen sensitivity is found to be $-0.41693 \pm j 0.4582$ with $P = 0.94$ pu and $-0.40671 \pm j 8.3160$ with $P = 0.94$ pu. The eigen value plot before and after DIFG connection is presented in figure 7 and figure 8 respectively.

Table 3: Eigen Values for IEEE 9 bus system

Bus	P	Q (-ve)	Eigen Values
5	0.5	0.2	$-0.42416 \pm j 9.1278$
6	0.5	0.2	$-0.38835 \pm j 8.8458$
8	0.5	0.2	$-0.41847 \pm j 0.4784$

The DFIG unit of power 0.5 pu is connected to the system then the load flow solution shows the improvement of voltage limit and power flow. The flow solution after DFIG connection is presented in table 4.

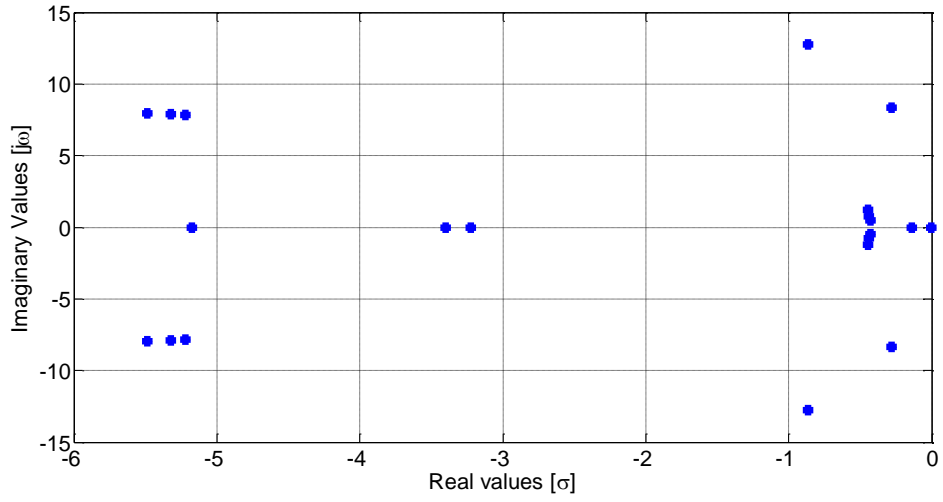


Figure 7: Eigenvalues Without DFIG

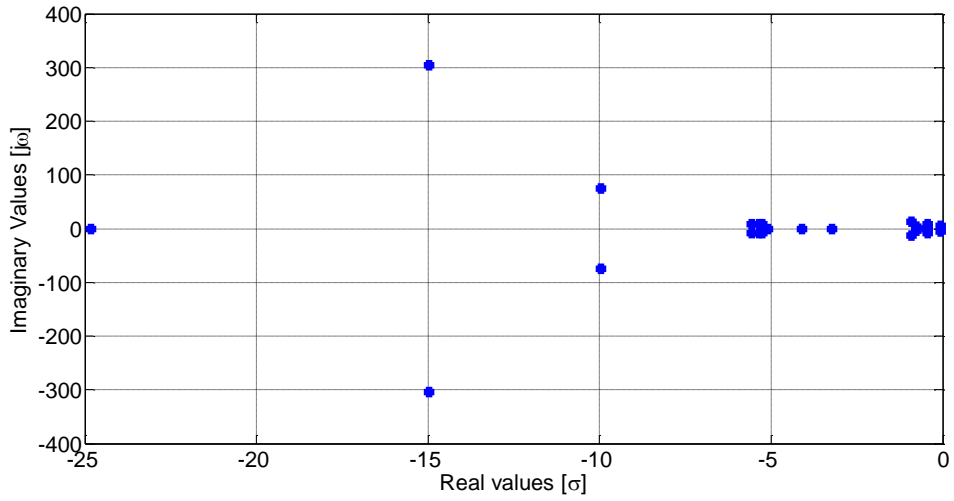


Figure 8: Eigenvalues With DFIG

Table 4: Load flow solution when DFIG connected

Bus Number	V (pu)	Theta(rad)	P (pu)	Q (pu)
1	1.040	0.000	0.722	0.528
2	1.025	0.163	1.630	0.222
3	1.025	0.080	0.850	-0.033
4	1.012	-0.040	0.000	0.000
5	0.958	-0.070	-1.750	-0.700
6	1.001	-0.066	-0.900	-0.300
7	1.016	0.065	0.000	0.000
8	1.008	0.012	-1.000	-0.350
9	1.028	0.033	0.000	0.000
10	0.951	-0.051	0.500	-0.190

4.2 DFIG integrated to INPS System

In this dissertation, the 66 kV bus and higher voltage bus system is considered for the Integrated Nepalese Power System (INPS). The total sixty – six bus is included in the system. In eastern region and western region of Nepal, the INPS system is almost radial structure which is lumped to a point to get minimum errors in load flow solution. The eastern region power generation and load are lumped to Dhalkebar substation and western region power generation and load are lumped to Butwal substation. After this, the total bus in the system is forty-three and analysis is performed for the forty-three bus system. The INPS map is presented in appendix A and the corresponding load and line data are presented in appendix B and C respectively. The base load flow solution for 43 bus INPS system and voltage profile are presented in table 5 and figure 9 respectively.

Table 5: Base load flow solution of INPS system

Bus Number	V (pu)	Theta (Degree)	P (pu)	Q (pu)
1	1.000	0.000	2.810	-0.249
2	1.000	-5.881	-0.608	0.250
3	1.000	-8.162	0.150	0.239
4	1.000	-14.436	0.141	0.114
5	1.018	-24.860	0.700	0.436
6	1.000	-27.797	0.690	0.061
7	1.000	-42.104	-0.079	1.477
8	1.000	-57.868	-0.538	0.521
9	1.000	-41.339	0.320	0.459
10	1.000	-38.798	0.414	-0.032
11	1.000	-34.873	0.240	-0.363
12	1.050	-34.598	0.200	0.330
13	1.000	-35.525	0.141	0.203
14	1.000	-33.505	0.100	-0.015
15	1.000	-33.339	0.075	-0.018
16	1.000	-32.286	0.600	0.016
17	1.000	-31.283	0.360	0.144
18	0.984	-5.492	-0.147	-0.073
19	0.990	-8.295	-0.434	-0.217
20	0.981	-8.983	-0.133	-0.066
21	0.988	-14.864	0.000	0.000
22	0.984	-15.005	-0.241	-0.121
23	0.984	-14.907	-0.128	-0.064
24	0.988	-23.417	-0.096	-0.048

25	0.986	-29.425	-0.229	-0.114
26	0.945	-51.559	-0.334	-0.167
27	0.942	-49.091	-0.035	-0.017
28	0.916	-49.944	-0.213	-0.106
29	0.868	-52.204	-0.527	-0.271
30	0.923	-48.188	-0.295	-0.147
31	0.960	-45.048	-0.010	-0.005
32	0.962	-39.078	-0.059	-0.030
33	0.958	-38.789	-0.286	-0.143
34	0.945	-38.129	-0.343	-0.171
35	0.943	-37.785	-0.411	-0.206
36	0.939	-38.057	-0.216	-0.108
37	0.943	-38.238	-0.119	-0.060
38	0.954	-39.033	-0.126	-0.063
39	0.941	-38.891	-0.177	-0.089
40	0.946	-39.019	-0.160	-0.080
41	0.989	-34.616	-0.063	-0.031
42	0.926	-37.237	-0.117	-0.058
43	0.982	-32.588	-0.150	-0.075

In the base case without DFIG, most of the Eigen values are falling on imaginary axis with complex value as presented in figure 10. The Eigen value on imaginary axis shows the system is critically stable.

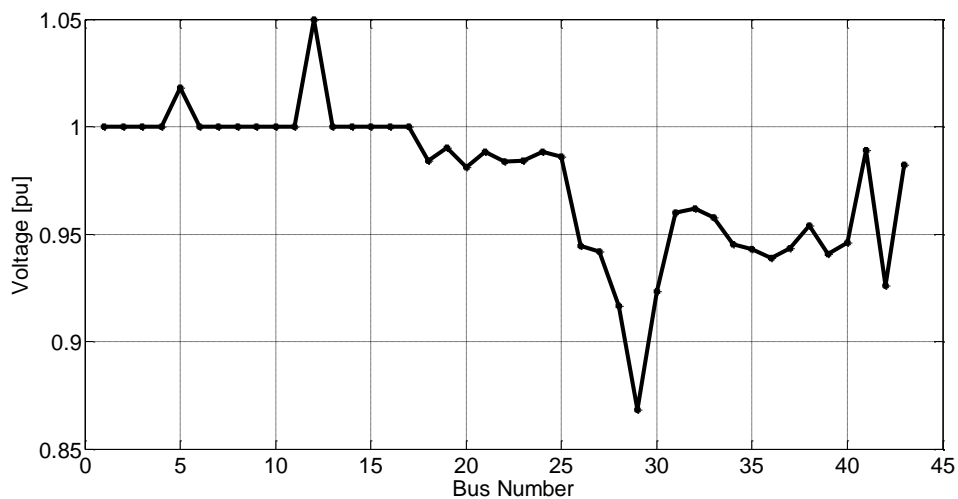


Figure 9: Voltage profile for base load flow solution of INPS system

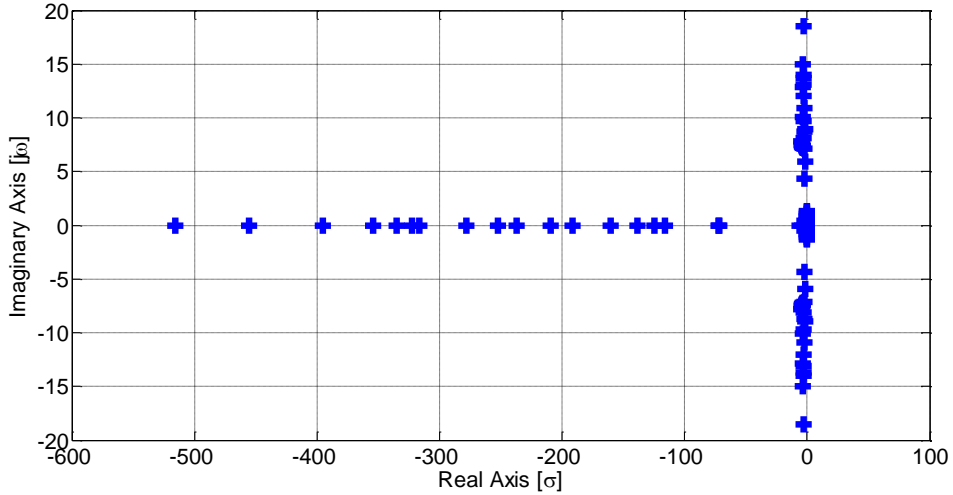


Figure 10: Eigen value plot of INPS system without DFIG

The DFIG connection in the INPS system is considered with five cases for the stability of small signal. The DFIG is connected to the bus which is nearest to feasible wind power generation or available wind power generation. In INPS, the five bus selected for DIFG connection are: Balaju 132, Bhaktapur, Nawalparasi, Makwanpur, and Acham. The DFIG active power is variant form 0.1 pu to 0.5 pu for the connection bus and reactive power is variant in respective of active power. The power factor approximately varies from 0.85 to 0.9 lagging and, therefore, the system has maximum value of Q is 0.4 times of value of P.

4.2.1 Case 1: [Balaju] DFIG Connected to Bus 5 with P=0.5 and Q=0.2

In this Case, the DFIG based wind power is connected to bus 5 with P and Q value of 0.5 pu and 0.2 pu respectively. The minimum Eigen value in this case is found to be -0.05155 which is real and lies in real axis. The figure 11 shows the plot of Eigen values on imaginary plane which shows that most of the Eigen values are lies on real axis and also at origin. Some of the Eigen values are complex conjugate. The system is more stable than the base case because most of the Eigen values are lies on real axis and also at origin. The farthest pole at real axis is -517.13 and the complex conjugate poles $\pm j300$ are farthest from the origin. The voltage profile is presented in table 6 and the bus voltage at bus 44 is 1.011 pu which is in stable range of (1 ± 0.10) pu. The active and reactive power injected by DFIG system are 0.5 pu and 0.19 pu respectively. In figure 12, Eigen sensitivity is plotted for case 1: Balaju. In this case, the DFIG power is varied from 10 kW to 50 kW and corresponding Eigen value are plotted and it shows that the

Eigen value is not so sensitive for 10 kW to 25 kW but the Eigen value increases when power varies from 25 kW to 50 kW. It is recommended to use DFIG of variable power up to 25 kW can be connected at the Balaju location but DFIG of higher power than 25 kW should be connected wisely because these power are highly sensitivity for the system.

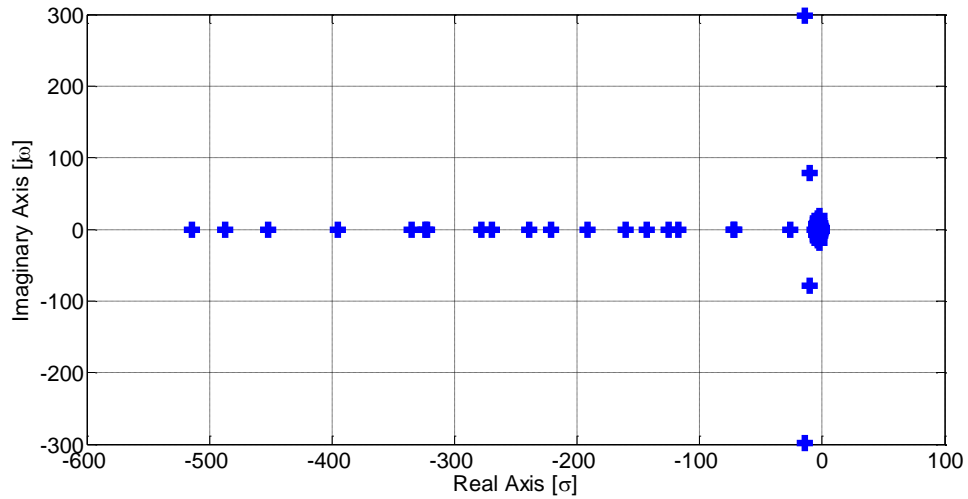


Figure 11: Eigen value plot of INPS system with DFIG for case 1: Balaju

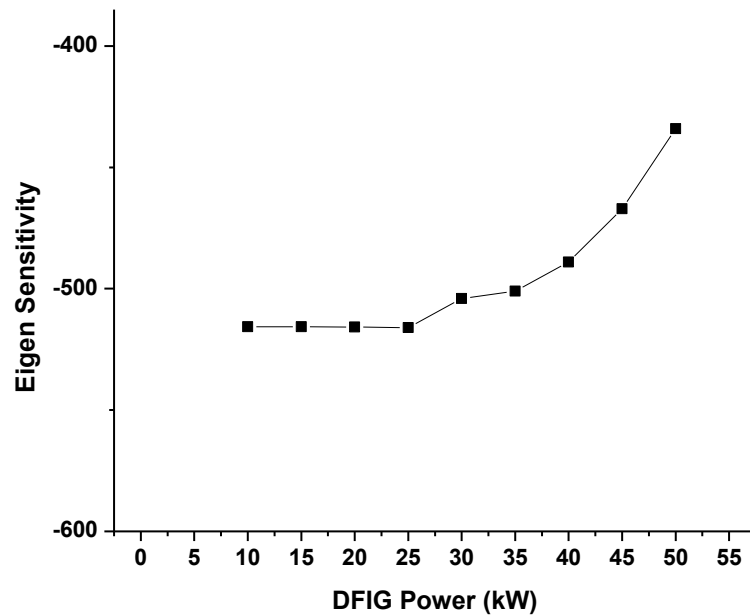


Figure 12: Eigen sensitivity plot for Balaju

Table 6: Load flow solution with DFIG Integration for Balaju

Bus Number	V (pu)	Theta (Degree)	P (pu)	Q (pu)
1	1.000	0.000	2.810	-0.249
2	1.000	-5.881	-0.608	0.250
3	1.000	-8.162	0.150	0.239
4	1.000	-14.436	0.141	0.114
5	1.018	-24.860	0.200	0.636
6	1.000	-27.797	0.690	0.061
7	1.000	-42.104	-0.079	1.477
8	1.000	-57.868	-0.538	0.521
9	1.000	-41.339	0.320	0.459
10	1.000	-38.798	0.414	-0.032
11	1.000	-34.873	0.240	-0.363
12	1.050	-34.598	0.200	0.330
13	1.000	-35.525	0.141	0.203
14	1.000	-33.505	0.100	-0.015
15	1.000	-33.339	0.075	-0.018
16	1.000	-32.286	0.600	0.016
17	1.000	-31.283	0.360	0.144
18	0.984	-5.492	-0.147	-0.073
19	0.990	-8.295	-0.434	-0.217
20	0.981	-8.983	-0.133	-0.066
21	0.988	-14.864	0.000	0.000
22	0.984	-15.005	-0.241	-0.121
23	0.984	-14.907	-0.128	-0.064
24	0.988	-23.417	-0.096	-0.048
25	0.986	-29.425	-0.229	-0.114
26	0.945	-51.559	-0.334	-0.167
27	0.942	-49.091	-0.035	-0.017
28	0.916	-49.944	-0.213	-0.106
29	0.868	-52.204	-0.527	-0.271
30	0.923	-48.188	-0.295	-0.147
31	0.960	-45.048	-0.010	-0.005
32	0.962	-39.078	-0.059	-0.030
33	0.958	-38.789	-0.286	-0.143
34	0.945	-38.129	-0.343	-0.171
35	0.943	-37.785	-0.411	-0.206
36	0.939	-38.057	-0.216	-0.108
37	0.943	-38.238	-0.119	-0.060
38	0.954	-39.033	-0.126	-0.063
39	0.941	-38.891	-0.177	-0.089
40	0.946	-39.019	-0.160	-0.080

41	0.989	-34.616	-0.063	-0.031
42	0.926	-37.237	-0.117	-0.058
43	0.982	-32.588	-0.150	-0.075
44	1.011	-23.914	0.500	-0.190

4.2.2 Case 2: [Bhaktapur] DFIG Connected to Bus 10 with P=0.5 and Q=0.2

In this Case, the DFIG based wind power is connected to bus 10 which is Bhaktapur in INPS system. The DFIG power to be integrated with the P and Q value of 0.5 pu and 0.2 pu respectively. The minimum Eigen value in this case is found to be -0.0137. The figure 13 shows the plot of Eigen values on imaginary plane which shows that most of the Eigen values are lies on real axis and also at origin. Some of the Eigen values are complex conjugate. Some Eigen values are lies on right side of the imaginary axis. The system is not stable than the base case because some of the Eigen values are lies on right side of the imaginary axis. The farthest from the origin are beyond -500 on left half plane and within 100 on right half plane. The voltage profile is presented in table 7 and the bus voltage at bus 44 is 0.947 pu which is in stable range of (1 ± 0.10) pu. The active and reactive power injected by DFIG system are 0.5 pu and 0.101 pu respectively.

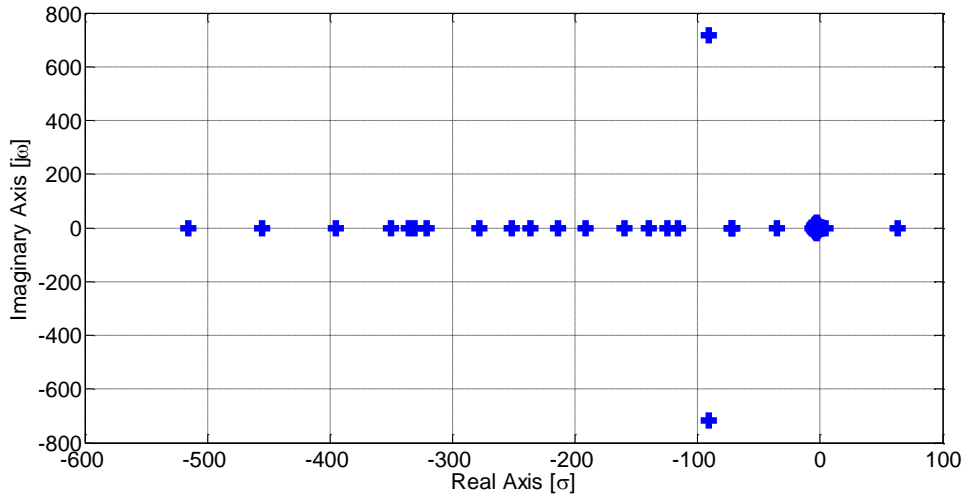


Figure 13: Eigen value plot of INPS system with DFIG for case 2: Bhaktapur

Figure 14 shows the Eigen sensitivity in respect of DFIG power injected and is randomly varies for 25 to 50 kW but stable and insensitive from 10 to 25 kW. This bus is highly vulnerable to connect higher DFIG power system. It is not recommended to

connect DFIG at this location because the system is unstable in this case and also the sensitivity shows vulnerability of the bus while DFIG connected.

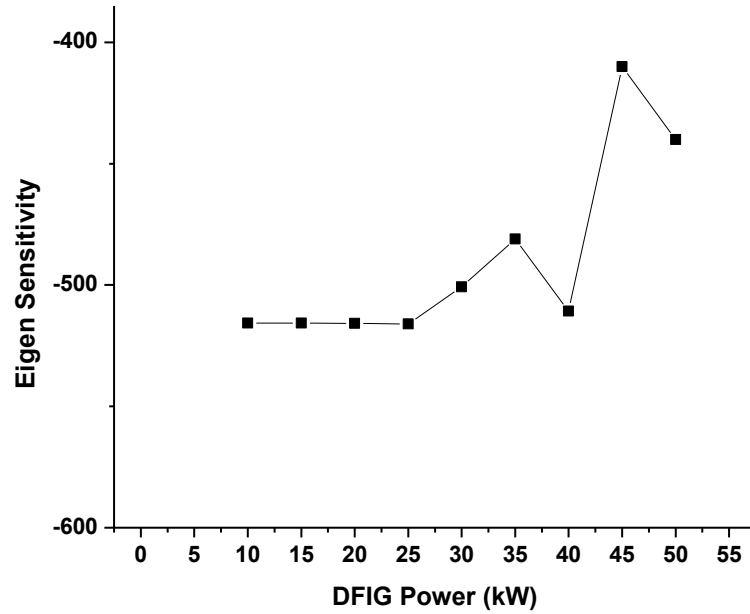


Figure 14: Eigen sensitivity for Bhaktapur

Table 7: Load flow solution with DFIG Integration for Bhaktapur

Bus Number	V (pu)	Theta (Degree)	P (pu)	Q (pu)
1	1.000	0.000	2.810	-0.249
2	1.000	-5.881	-0.608	0.250
3	1.000	-8.162	0.150	0.239
4	1.000	-14.436	0.141	0.114
5	1.018	-24.860	0.700	0.436
6	1.000	-27.797	0.690	0.061
7	1.000	-42.104	-0.079	1.477
8	1.000	-57.868	-0.538	0.521
9	1.000	-41.339	0.320	0.459
10	1.000	-38.798	-0.086	0.168
11	1.000	-34.873	0.240	-0.363
12	1.050	-34.598	0.200	0.330
13	1.000	-35.525	0.141	0.203
14	1.000	-33.505	0.100	-0.015
15	1.000	-33.339	0.075	-0.018
16	1.000	-32.286	0.600	0.016

17	1.000	-31.283	0.360	0.144
18	0.984	-5.492	-0.147	-0.073
19	0.990	-8.295	-0.434	-0.217
20	0.981	-8.983	-0.133	-0.066
21	0.988	-14.864	0.000	0.000
22	0.984	-15.005	-0.241	-0.121
23	0.984	-14.907	-0.128	-0.064
24	0.988	-23.417	-0.096	-0.048
25	0.986	-29.425	-0.229	-0.114
26	0.945	-51.559	-0.334	-0.167
27	0.942	-49.091	-0.035	-0.017
28	0.916	-49.944	-0.213	-0.106
29	0.868	-52.204	-0.527	-0.271
30	0.923	-48.188	-0.295	-0.147
31	0.960	-45.048	-0.010	-0.005
32	0.962	-39.078	-0.059	-0.030
33	0.958	-38.789	-0.286	-0.143
34	0.945	-38.129	-0.343	-0.171
35	0.943	-37.785	-0.411	-0.206
36	0.939	-38.057	-0.216	-0.108
37	0.943	-38.238	-0.119	-0.059
38	0.954	-39.033	-0.126	-0.063
39	0.941	-38.891	-0.177	-0.089
40	0.946	-39.019	-0.160	-0.080
41	0.989	-34.616	-0.063	-0.031
42	0.926	-37.237	-0.117	-0.058
43	0.982	-32.588	-0.150	-0.075
44	0.947	-28.460	0.500	-0.101

The cases first and second are selected arbitrarily to show the stability concept using eigen value analysis. The both cases are compared the base case and shows stability and instability differences. The other three real sites are considered as cases where the wind turbines are installed and also the sensitivity analysis for power and stability is considered. According to Alternative Energy Promotion Centre (AEPCC), the wind power running locations are listed in table 8. Among these, the three sites Nawalparasi, Acham, and Makwanpur are selected. The installed wind turbine power to corresponding locations are 10 kW, 10 kW and 20 kW respectively. The reactive power is not installed at those locations but considered for the DFIG system. For DFIG system,

base value of power is chosen 100 kVA and therefore the power varies as $P = 0.1$ pu, and $P = 0.2$ pu for 10 kW and 20 kW respectively.

Table 8: Wind Turbine Capacity and Location in Nepal

S.N.	Location	Wind Power Capacity (kW)	Remarks
1	Nawalparasi	10	Running
2	Makwanpur	10	Running
3	Tatopani, Jumla	15	Running
4	Acham	20	Running
5	Surkhet	5	Running
6	Bajhang	15	Running
7	Palpa	10	Running
8	Jumla	30	Running
9	Pachthar	20	Running
10	Sindhuli	20	Running
11	Bhojpur	10	In Progress
12	Nisti, Palpa	15	In Progress

Source: Interview, Wind Section, AEPC 2076/12/15

4.2.3 Case 3: [Nawalparasi] DFIG Connected to Bus 31 with $P=0.1$ and $Q=0.04$

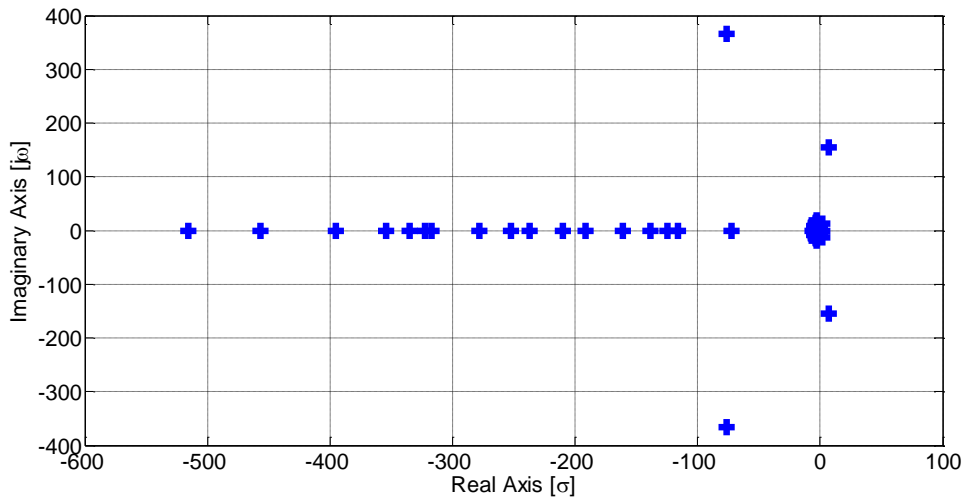


Figure 15: Eigen value plot of INPS system with DFIG for case 3: Nawalparasi

In this Case , the DFIG based wind power is connected to bus 31 (Kawasoti S/S bus) in INPS system. The DFIG power to be integrated with the P and Q value of 0.10 pu and 0.04 pu respectively. The minimum Eigen value in this case is found to be 0.0726. The figure 15 presents the plot of Eigen values on imaginary plane which shows that most of the Eigen values are lies on real axis and also at origin. Some of the Eigen values are

complex conjugate. Some eigenvalues lie on right hand side of imaginary axis in s-plane. The system is not stable than the base case because some of the Eigen values are lies on right side of the imaginary axis. The Eigen value poles farthest from the origin is at -515.575 on left half plane and $0.0727 + j1.5482$ on right half plane. The complex conjugate poles farthest from the origin are $-76.56+j365.9$ and $-76.56-j365.9$. The voltage at bus 44 is 0.940 pu which is in stable range of (1 ± 0.10) pu. The active and reactive power injected by DFIG system are 0.5 pu and 0.101 pu respectively. In figure 16, Eigen sensitivity is shown form Nawalparasi and it is found that the Eigen value increases while increasing the DFIG power and therefore, it is recommended to connect DFIG of constant power at this location. If the wind power changes then the bus parameters also affected and therefore the system is affected from DFIG power.

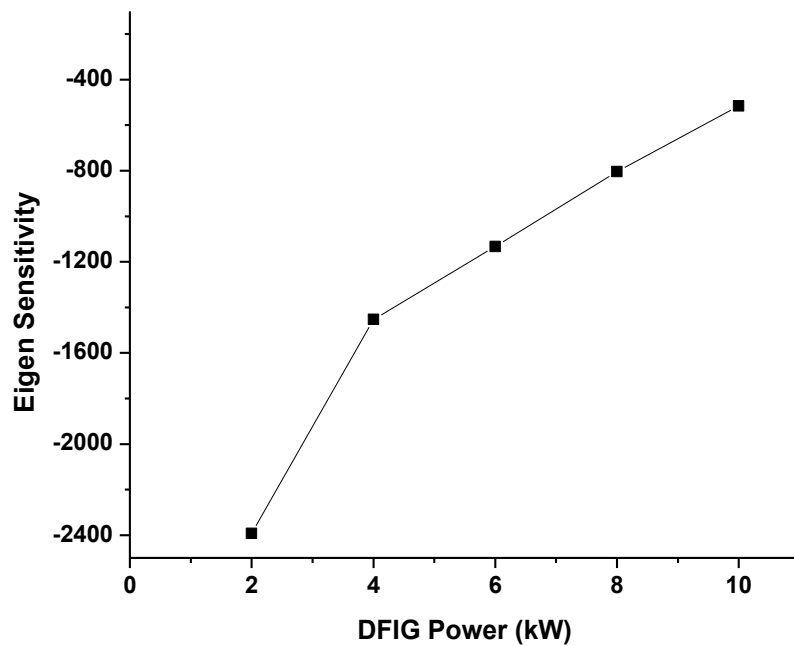


Figure 16: Eigen sensitivity plot for different DFIG Power for Nawalparasi

Table 9: : Load flow solution with DFIG Integration for Nawalparasi

Bus Number	V (pu)	Theta (Degree)	P (pu)	Q (pu)
1	1.000	0.000	2.814	-0.249
2	1.000	-5.881	-0.608	0.250
3	1.000	-8.162	0.150	0.239
4	1.000	-14.472	0.141	0.114
5	1.018	-24.926	0.700	0.437

6	1.000	-27.868	0.690	0.062
7	1.000	-42.193	-0.079	1.558
8	1.000	-57.997	-0.538	0.529
9	1.000	-41.427	0.320	0.459
10	1.000	-38.885	0.414	-0.032
11	1.000	-34.957	0.240	-0.363
12	1.050	-34.682	0.200	0.330
13	1.000	-35.609	0.141	0.203
14	1.000	-33.590	0.100	-0.015
15	1.000	-33.424	0.075	-0.018
16	1.000	-32.370	0.600	0.016
17	1.000	-31.367	0.360	0.144
18	0.984	-5.504	-0.147	-0.073
19	0.990	-8.295	-0.434	-0.217
20	0.981	-8.983	-0.133	-0.066
21	0.988	-14.900	0.000	0.000
22	0.984	-15.040	-0.241	-0.121
23	0.984	-14.942	-0.128	-0.064
24	0.988	-23.475	-0.096	-0.048
25	0.986	-29.496	-0.229	-0.114
26	0.943	-51.660	-0.334	-0.167
27	0.940	-49.180	-0.035	-0.017
28	0.914	-50.026	-0.213	-0.106
29	0.866	-52.299	-0.527	-0.271
30	0.919	-48.215	-0.295	-0.147
31	0.954	-44.996	-0.110	-0.045
32	0.962	-39.162	-0.059	-0.030
33	0.958	-38.873	-0.286	-0.143
34	0.945	-38.213	-0.343	-0.171
35	0.943	-37.869	-0.411	-0.206
36	0.939	-38.141	-0.216	-0.108
37	0.943	-38.322	-0.119	-0.059
38	0.954	-39.117	-0.126	-0.063
39	0.941	-38.975	-0.177	-0.089
40	0.946	-39.103	-0.160	-0.080
41	0.989	-34.701	-0.063	-0.031
42	0.926	-37.321	-0.117	-0.058
43	0.982	-32.672	-0.150	-0.075
44	0.941	-42.826	0.100	-0.036

4.2.4 Case 4: [Makwanpur] DFIG Connected to Bus 26 with P=0.1 and Q=0.04

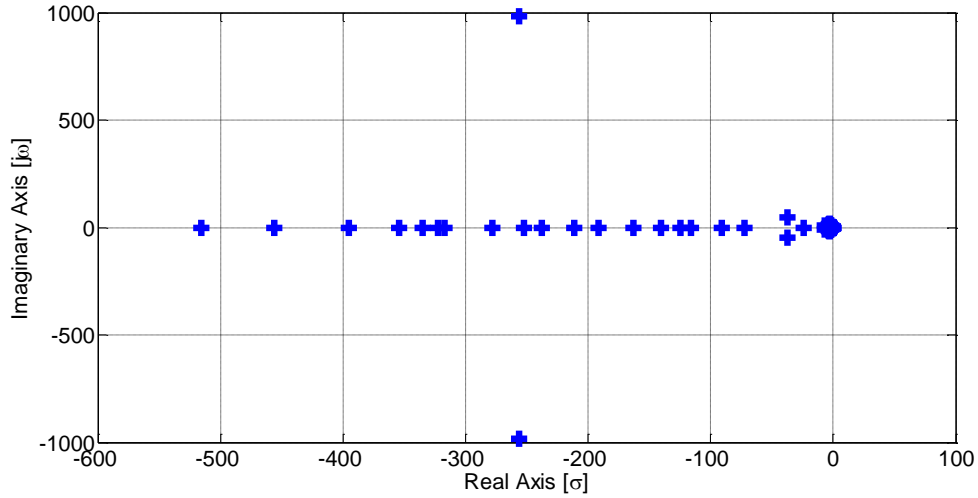


Figure 17: Eigen value plot of INPS system with DFIG for case 4: Makwanpur

In this case , the DFIG based wind power is connected.to bus 26 with the P and Q value of 0.100pu and 0.04 pu respectively. The minimum Eigen value in this case is found to be 0.0955. The figure 17 shows the plot of eigenvalues on imaginary plane which shows that most of the Eigen values are lies on real axis and also at origin. Some of the eigen values are complex conjugate. The system is more stable than the base case, and case 3 because most of the Eigen values are lies on real axis and also at origin. The farthest pole at real axis is -515.5877 and the complex conjugate poles $-256.17 \pm j 981.74$ are farthest from the origin. The voltage profile is at bus 44 is 0.9824 pu which is in stable range of (1 ± 0.10) pu. The active and reactive power injected by the DFIG based wind power system are 0.1 pu and 0.031 pu respectively. In sensitivity analysis, DFIG power is varied and the Eigen sensitivity is considered to identify the sensitivity of the system. In this case, the DFIG power is varied from 2 kW to 10 kW and the DFIG sensitivity is recorded. The sensitivity plot is presented in figure 18 and shows that the DFIG is insensitive to variation of DFIG power so maximum power integration can be recommended for this location.

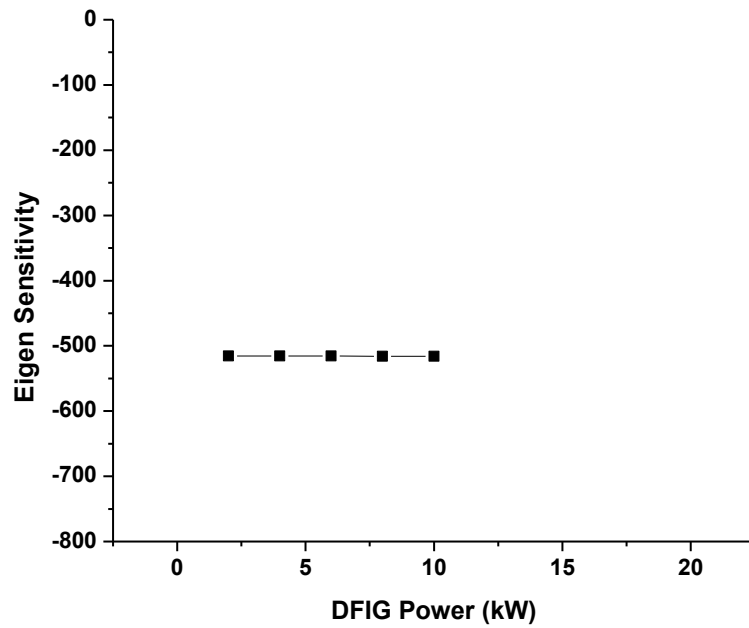


Figure 18: Eigen sensitivity plot for different DFIG Power for Makwanpur

Table 10: : Load flow solution with DFIG Integration for Makwanpur

Bus Number	V (pu)	Theta (Degree)	P (pu)	Q (pu)
1	1.000	0.000	2.815	-0.249
2	1.000	-5.881	-0.608	0.250
3	1.000	-8.162	0.150	0.239
4	1.000	-14.482	0.141	0.115
5	1.018	-24.945	0.700	0.437
6	1.000	-27.887	0.690	0.062
7	1.000	-42.217	-0.079	1.531
8	1.000	-58.082	-0.538	0.559
9	1.000	-41.452	0.320	0.459
10	1.000	-38.909	0.414	-0.032
11	1.000	-34.980	0.240	-0.363
12	1.050	-34.706	0.200	0.330
13	1.000	-35.632	0.141	0.203
14	1.000	-33.613	0.100	-0.015
15	1.000	-33.447	0.075	-0.018
16	1.000	-32.394	0.600	0.016
17	1.000	-31.391	0.360	0.144
18	0.984	-5.507	-0.147	-0.073
19	0.990	-8.295	-0.434	-0.217
20	0.981	-8.983	-0.133	-0.066
21	0.988	-14.910	0.000	0.000

22	0.984	-15.050	-0.241	-0.121
23	0.984	-14.952	-0.128	-0.064
24	0.988	-23.491	-0.096	-0.048
25	0.986	-29.516	-0.229	-0.114
26	0.939	-51.638	-0.434	-0.207
27	0.938	-49.176	-0.035	-0.017
28	0.913	-50.036	-0.213	-0.106
29	0.865	-52.314	-0.527	-0.271
30	0.921	-48.286	-0.295	-0.147
31	0.959	-45.150	-0.010	-0.005
32	0.962	-39.185	-0.059	-0.030
33	0.958	-38.896	-0.286	-0.143
34	0.945	-38.236	-0.343	-0.171
35	0.943	-37.892	-0.411	-0.206
36	0.939	-38.165	-0.216	-0.108
37	0.943	-38.345	-0.119	-0.059
38	0.954	-39.140	-0.126	-0.063
39	0.941	-38.998	-0.177	-0.089
40	0.946	-39.126	-0.160	-0.080
41	0.989	-34.724	-0.063	-0.031
42	0.926	-37.345	-0.117	-0.058
43	0.982	-32.695	-0.150	-0.075
44	0.925	-49.395	0.100	-0.036

4.2.5 Case 5: [Acham] DFIG Connected to Bus 15 with P=0.2 and Q=0.08

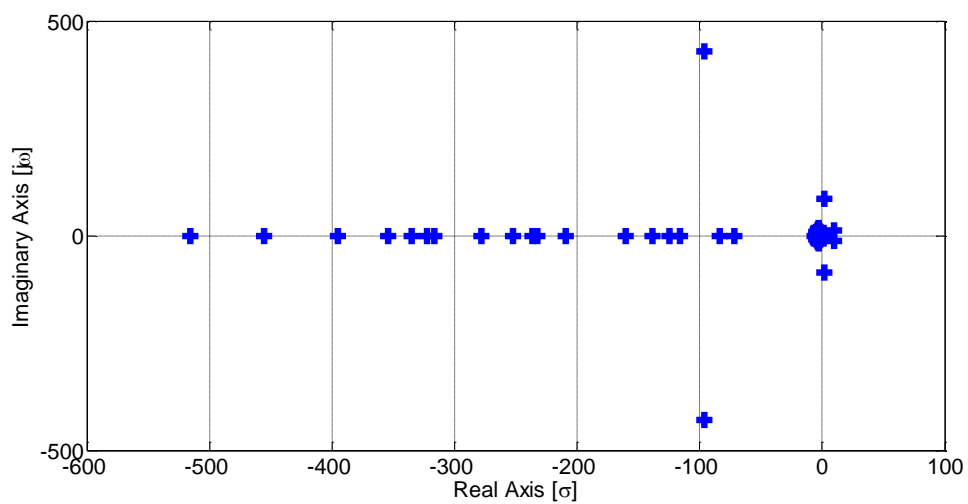


Figure 19: Eigen value plot of INPS system with DFIG for case 5: Acham

In this Case , the DFIG is connected to bus 15 with the P and Q value of 0.2 pu and 0.08 pu respectively. The minimum eigenvalue in this case 5 is found to be 0.0724. The figure 19 shows the plot of Eigen values on imaginary plane which shows that most of the Eigen values are lies on real axis and also at origin. Some of the eigenvalues are complex conjugate. The system is more stable than the base case, and case 3 because most of the Eigen values are lies on real axis and also at origin. The farthest pole at real axis is -515.4718 and the complex conjugate poles $-98.14 \pm j 409.36$ are farthest from the origin. The voltage profile is at bus 44 is 0.9772 pu which is in stable range of (1 ± 0.10) pu. The active and reactive power injected by DFIG wind power system are 0.18 pu and 0.059 pu respectively. In sensitivity analysis, DFIG power is varied and the Eigen sensitivity is considered to identify the sensitivity of the system. In this case, the DFIG power is varied from 2 kW to 20 kW and the DFIG sensitivity is recorded. The sensitivity plot is presented in figure 20 and shows that the DFIG is minimal sensitive to variation of DFIG power from 2 kW to 18 kW and drastic variation when DFIG power varies from 18 kW to 20 kW. Maximum power of 18 kW integration can be recommended for this location.

Table 11: : Load flow solution with DFIG Integration for Acham

Bus Number	V (pu)	Theta (Degree)	P (pu)	Q (pu)
1	1.000	0.000	2.810	-0.249
2	1.000	-5.881	-0.608	0.250
3	1.000	-8.162	0.150	0.239
4	1.000	-14.436	0.141	0.114
5	1.018	-24.860	0.700	0.436
6	1.000	-27.797	0.690	0.061
7	1.000	-42.104	-0.079	1.477
8	1.000	-57.868	-0.538	0.521
9	1.000	-41.339	0.320	0.459
10	1.000	-38.798	0.414	-0.032
11	1.000	-34.873	0.240	-0.363
12	1.050	-34.598	0.200	0.330
13	1.000	-35.525	0.141	0.203
14	1.000	-33.505	0.100	-0.015
15	1.000	-33.339	-0.125	0.062
16	1.000	-32.286	0.600	0.016
17	1.000	-31.283	0.360	0.144
18	0.984	-5.492	-0.147	-0.073
19	0.990	-8.295	-0.434	-0.217

20	0.981	-8.983	-0.133	-0.066
21	0.988	-14.864	0.000	0.000
22	0.984	-15.005	-0.241	-0.121
23	0.984	-14.907	-0.128	-0.064
24	0.988	-23.417	-0.096	-0.048
25	0.986	-29.425	-0.229	-0.114
26	0.945	-51.559	-0.334	-0.167
27	0.942	-49.091	-0.035	-0.017
28	0.916	-49.944	-0.213	-0.106
29	0.868	-52.204	-0.527	-0.271
30	0.923	-48.188	-0.295	-0.147
31	0.960	-45.048	-0.010	-0.005
32	0.962	-39.078	-0.059	-0.030
33	0.958	-38.789	-0.286	-0.143
34	0.945	-38.129	-0.343	-0.171
35	0.943	-37.785	-0.411	-0.206
36	0.939	-38.057	-0.216	-0.108
37	0.943	-38.238	-0.119	-0.060
38	0.954	-39.033	-0.126	-0.063
39	0.941	-38.891	-0.177	-0.089
40	0.946	-39.019	-0.160	-0.080
41	0.989	-34.616	-0.063	-0.031
42	0.926	-37.237	-0.117	-0.058
43	0.982	-32.588	-0.150	-0.075
44	0.975	-29.341	0.200	-0.064

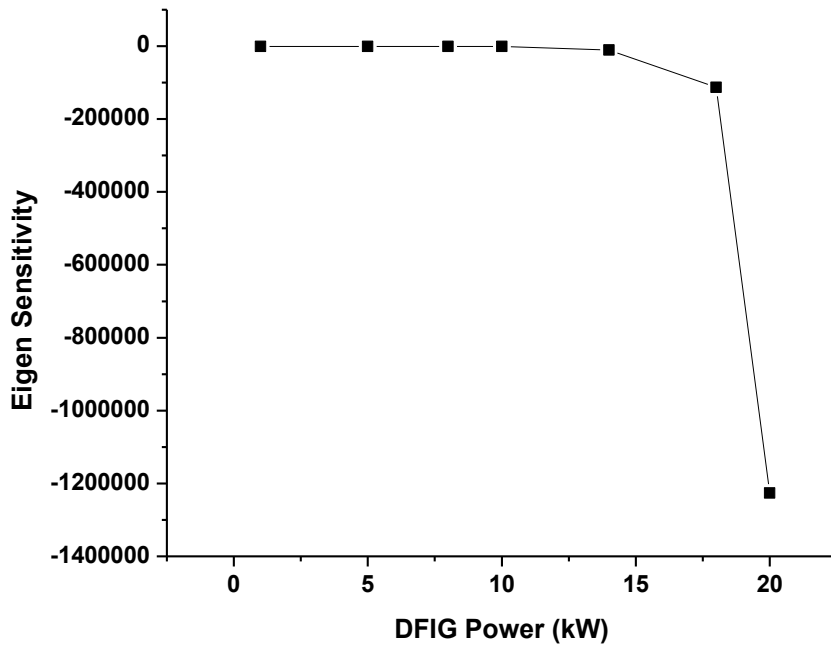


Figure 20: Eigen sensitivity plot for different DFIG Power for Acham

4.3 Financial Analysis of Wind Energy

The financial analysis for integrating wind power system is performed centered on data available from AEPC. The analysis is performed on per kilowatt data. The basic data used are per kilowatt cost of system, capacity factor, energy price of other renewable sources. Financial indicators like internal rate of return (IRR), Benefit cost ratio, normal payback period and discounted payback period are considered during the analysis.

Levelized cost is the price of energy for which the project is just feasible under the assumed conditions. The levelized cost of energy varies with the energy production and is depicted in figure 21. The project capacity factor shows the variation on energy production and corresponding levelized cost is presented. The levelized cost of energy decreases when the capacity factor increases and thus the higher capacity of generation provides the lower cost of energy.

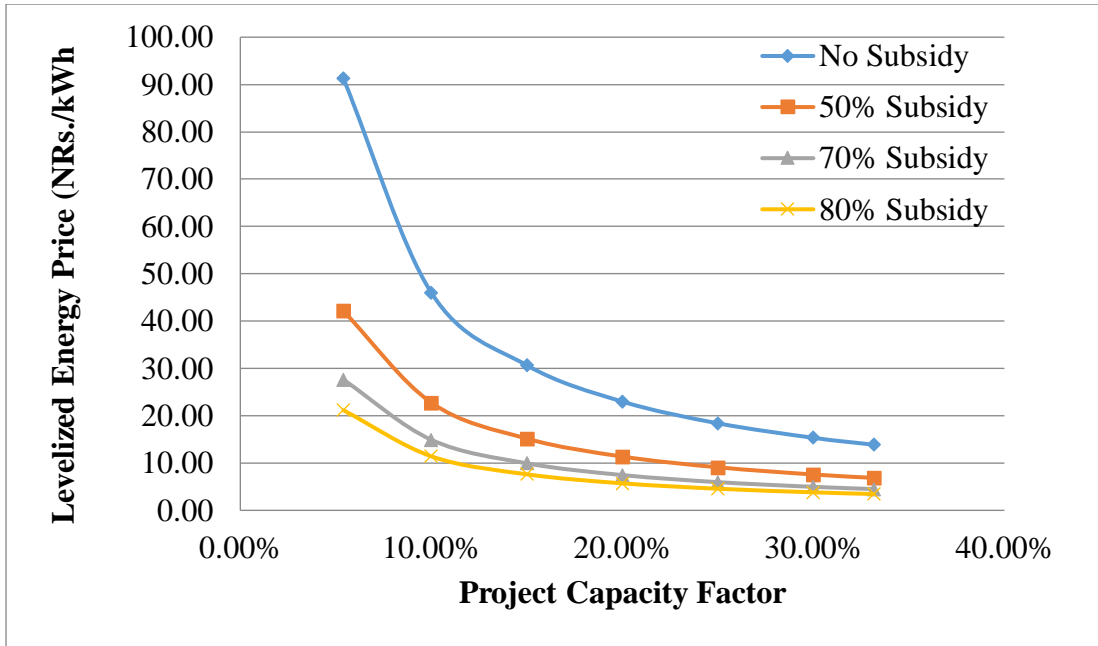


Figure 21: Levelized cost of energy versus project capacity factor

Figure 22 presents the approximate cumulative cash flow for 22% project capacity factor which also assumes the various conditions of subsidy that is provided for wind turbine installation by entities like AEPC. It shows the investment is returned within 5 years from the investment date. The subsidy is not taken as a return value in this calculations. Table 12 shows the summary sheet for financial analysis with consideration of 10% discount rate.

Table 12: Summary Sheet of Financial Analysis

SN	Financial Indicator	Analysis	No Subsidy	50% Subsidy	70% Subsidy	80% Subsidy
1	Internal Rate of Return (IRR)		-2.23%	4.70%	11.58%	18.95%
2	Benefit Cost Ratio (B/C Ratio)		0.33	0.67	1.11	1.66
3	Payback Period (Years)		>20	12.78	7.67	5.11
4	Discounted Payback Period		>20	>20	15.30	7.53
5	Net Present Value (NPV in NRs.)		(173429.32)	(43429.32)	8570.68	34570.68

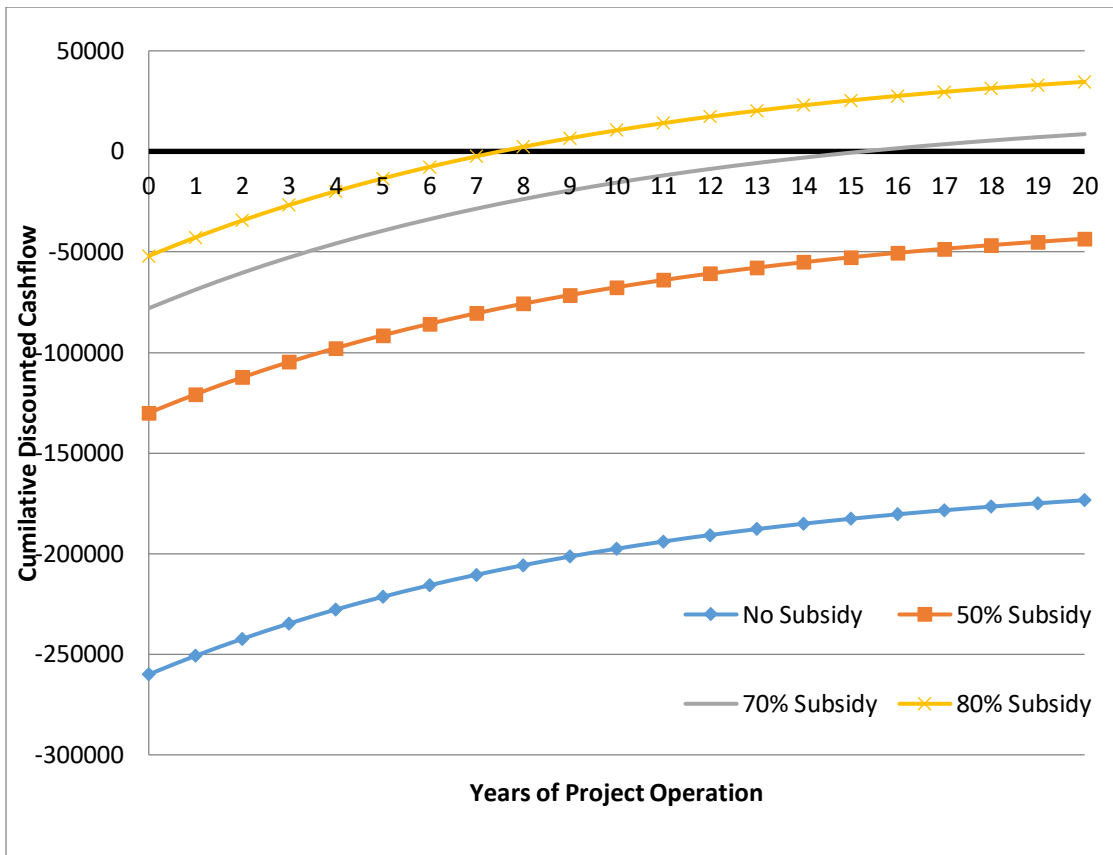


Figure 22: Approximate Cumulative Cash Flow versus project year

The financial analysis has been performed for cases of no subsidy to 80% subsidy on total project cost. The financial analysis indicates that the project is viable only above the subsidy of 70%. The financial indicators are positive only with 70% subsidy on the total cost.

Discussion:

In this chapter, the discussion of the research is presented with reference to findings of the research and objectives set during the research.

1. The impact on voltage profile due to DFIG integration in IEEE standard 9 bus system and INPS has been studied. On both existing systems, base case load flow was conducted and after this, DFIG was added and number of bus has been increased by one and again the load flow in this new system has been conducted. It has been found that, voltage is all buses in both cases are under 10% voltage limit which is acceptable in Transmission Line under Electricity Act, 2049. It can be concluded that the addition of DFIG on INPS has resulted a slight increase of voltage on its neighbor buses and are perfectly under the considered limit. This means that voltage stability is maintained in both systems and DFIG integration has been successful.
2. The impact of small signal stability with participation factor and Eigen value analysis in IEEE system and INPS system has been studied due to wind power integration. The method of analyzing the absolute stability of any control system can be done by analyzing eigenvalues in S-domain, which has been performed for five different test cases of Nepal. Any eigenvalue lying on RHP of S-plane makes the system unstable. Further, if the number of Eigen values lying on imaginary axis of S-plane is reduced, then, it is concluded that small signal stability of the power system has been enhanced and if all the Eigen values lies on real axis of S-plane, the system is fairly stable from small signal stability viewpoint. The results showed that no any Eigen value appeared on RHP in case of Balaju (50 kW), Makwanpur (P=10 kW). This means we can integrate DFIG for specified wind power extraction at these locations and are more stable than base case system. But, in case of and Acham (P= 20 kW), Bhaktapur (P=50 kW) and Nawalparasi (P=50 kW), some eigenvalues were found lying on RHP of s-plane, so we cannot add DFIG for wind power extraction of specified power on these locations. Addition of such capacity DFIG may result the system more vulnerable and may result instability of the system. So, Eigen sensitivity for rated power below the specified values were checked and suitable capacity and type of DFIG should be selected.
3. The effect of wind power sensitivity in the integrated power system has been studied wrt wind power integration. Eigen sensitivity plotted for case 1: Balaju showed that

the DFIG power when varied from 10 kW to 50 kW and results showed the eigen value is not much sensitive for 10 kW to 25 kW, but the Eigen value increases when power varies from 25 kW to 50 kW. It is recommended to use DFIG of variable power up to 25 kW can be connected at the Balaju substation location but DFIG of higher power than 25 kW is not recommended for connection. This concludes that size of DFIG should be chosen in a way where the eigenvalue sensitivity is less for that value than it was previous which means, wind power size is determined by less sensitive values from stability point of view and must be fulfilled in an integrated system. Similarly, the Eigen sensitivity in Nawalparasi showed that the Eigen value increases while increasing the DFIG power and therefore, it is recommended to connect DFIG of constant power at this location. If the wind power changes then the bus parameters also affected and therefore the system is affected from variable DFIG power. These cases conclude that if the Eigen value is highly sensitive for a region, though the system may not have any eigenvalue in RHP of the s-plane, integration of variable power generation DFIG for that region may affect the stability and constant power DFIG should be selected.

4. Similarly, from the case of Makwanpur and Achham, Size and nature of DFIG power is selected in the region of less Eigenvalue sensitive areas. VER DFIG up to 10 kW can be connected in Makwanpur whereas up to 15 kW can be connected in Achham. The sensitivity analysis resulted nature of DFIG to be integrated on system.

CHAPTER FIVE: CONCLUSION AND RECOMMENDATIONS

Conclusions:

In this chapter, the conclusion of the research is presented with reference to findings of the research and objectives set during the research.

1. On both existing systems, base case load flow was conducted and after this, DFIG was added and number of bus has been increased by one and again the load flow in this new system has been conducted, voltage stability is maintained in both systems and DFIG integration has been successful from voltage stability point of view.
2. The study concludes that for Balaju, Bhaktapur, Makwanpur and Achham, variable powered DFIG can be integrated. Whereas, in case of Nawalparasi, constant power DFIG can only be penetrated.
3. Financial Analysis concluded that subsidy is must for wind energy systems. If 50% subsidy is provided, the payback period has been found to be 12.78 years, 70% subsidy reduces payback period to 7.67 years, and for 80% subsidy, payback period is found 5.11 years.

Recommendations:

- The validated analysis could be always used for study of small signal stability before wind power integration as the integrated transmission network of Nepal is expanding as per plans and targets set by Government of Nepal.
- The research considers Absolute Stability of the system. Further, studying Relative Stability criterion like RH-Criteria, Nyquist stability, Root Locus technique etc...In INPS. The extended method can propose to adjust the free parameters of a system to avoid conditional stability. The proposed technique can safeguard the system against relative instability and are done for the complex systems which are prone.
- The wind power system is only attractive with a subsidy of more than 70% of total cost, although, change in energy pricing and costs of wind power system shall change the situation.
- The effect of wind energy on economy of the community as well as overall system shall have to be studied further.

REFERENCES

1. Akhmatov, V. (2003) “Analysis of dynamic behaviour of electric power systems with large amount of wind power”, *Technical University of Denmark (DTU)*, Denmark.
2. NEA, (2019), “Annual report of Nepal Electricity Authority, 2018/19”.
3. Bieker, K., Peitz, S. *et al*, (2019) “Deep Model Predictive Control with Online Learning for Complex Physical Systems” Retrieved from <http://arxiv.org/abs/1905.10094>.
4. Che, Y., Xu, J. *et al*, (2017), “Stability Analysis of Aircraft Power Systems Based on a Unified Large Signal Model”, *Energies* 10(11), 1739.
5. Chi-Tsong, T. C., (1998), “Linear Systems Theory and Design”, *Oxford University Press*, 3rd Edition, New York.
6. Dheer, D. K., Doolla, S. *et al*, (2017), “Effect of placement of droop based generators in distribution network on small signal stability margin and network loss”, *International Journal of Electrical Power and Energy Systems* (88), 108–118.
7. Erlich, I., Kretschmann, J. *et al*, (2007), “Modeling of wind turbines based on doubly-fed induction generators for power system stability studies”, *IEEE Transactions on Power Systems*, 22(3), 909–919. <https://doi.org/10.1109/TPWRS.2007.901607>
8. Ghennam, T., Berkouk, E. M., and François, B., (2009) “Modeling and control of a doubly fed induction generator based wind conversion system”, *2nd International Conference on Power Engineering, Energy and Electrical Drives (POWERENG) Proceedings*, 507–512. <https://doi.org/10.1109/POWERENG.2009.4915230>.
9. Hauer, J. F, (1991), “Application of Prony analysis to the determination of modal content and equivalent models for measured power system response”, *IEEE Transactions on Power Systems*, (6), 1062–1068.
10. Haung, D., Chen, Q. *et al*, (2018), “Wide-Area Measurement—Based Model-Free Approach for Online Power System Transient Stability Assessment”, *Energies*, (11), 958.
11. Lei, Y., Mullane, A., Lightbody, G., and Yacamini, R., (2006), “Modeling of the wind turbine with a doubly fed induction generator for grid integration studies”, *IEEE Transactions on Energy Conversion*, 21(1), 257–264.

12. Lima, F. K. a, Luna, A. *et al*, (2010), “Rotor Voltage Dynamics in the Doubly Fed Induction Generator During Grid Faults” *IEEE Transaction on Power Electronics*, 25(1), 118–130.
13. MATLAB Designed for Engineers and Scientists. (2019). Retrieved October 14, 2016, from https://www.mathworks.com/products/matlab/whymatlab.html?s_tid=hpbrand_whymatlab#reason5.
14. Slootweg, J. G., De Haan, S. *et al*, (2001), “Modeling wind turbines in power system dynamics simulations”, *Proceedings of the IEEE Power Engineering Society Transmission and Distribution Conference, 1(SUMMER)*, 22–26.
15. Tapia, A., Tapia, G., Xabier Ostolaza, J., and Sáenz, J. R., (2003), “Modeling and control of a wind turbine driven doubly fed induction generator”, *IEEE Transactions on Energy Conversion*, 18(2), 194–204. <https://doi.org/10.1109/TEC.2003.811727>.
16. Taylor, C. W., (1994), “Power Systems Voltage Stability”, *Electric Power Research Institute*, New York.
17. Wilems, J. L., (1971), “Stability Theory of Dynamical Systems”, *Springer*, London.

Analysis of Small Signal Stability on Wind Power Integration to Integrated Nepal Power System (INPS)

Bishwas Pokhrel, Assoc. Prof. Dr. Shreeraj Shakya, Assoc. Prof. Dr. Nawraj Bhattarai

Abstract- With large wind energy integration into power systems, wind farms begin to influence power systems in a much more significant manner. As wind energy systems utilize different generator technologies from the one utilized in the conventional power plants, the steady-state, transient and small-signal dynamics, as well as, power system stability will thus be significantly affected. The impact of wind energy systems on the power system dynamics and stability is thus of practical importance.

As there is a significant increase in installation of wind turbines equipped with doubly-fed induction generator (DFIG) in recent years, a dynamic model of the DFIG wind turbine is firstly developed in this study. The model is validated against field measurement data, and the validation gives confidence about the accuracy and applicability of the developed model. DFIG wind farms consist of tens to hundreds of identical DFIG wind turbines increasing the complexity of the wind farm model and simulation time.

In this study, the steady-state behavior of the DFIG is examined. Comparison is made with the conventional synchronous generators (SG) and squirrel-cage induction generators to highlight the differences between the machines. The initialization of the DFIG dynamic variables and other operating quantities is then discussed. Various methods are briefly reviewed and a step-by-step procedure is taken to avoid the iterative computations in initial condition.

The dynamical behavior of the DFIG is studied with eigen value analysis. Modal analysis is performed for both open-loop and closed-loop situations. The effect of parameters and operating point variations on small signal stability is observed. Financial analysis has been done using CREST model tool, which shows that the project is feasible in case of Nepalese subsidiaries.

Keywords – Wind Turbine Generation, Small Signal Stability, Integrated Nepal Power System.

I. INTRODUCTION

The small signal stability is the ability of power system remains in operating equilibrium when small disturbances are created such that the oscillations created in the system are suppressed and the deviations of system state variables remain small for a long time. If the magnitude of oscillations continues to increase or sustain indefinitely, this is the case for system unstable. The small signal stability of power system is affected by many factors such as initial operating conditions, characteristics of various control devices and strength of electrical connections among different components of system. It is inevitable that the power system cannot be operated if the system is unstable in terms of small signal stability. The stability of power system consisting synchronous machine has a major attention in past and also will obtain an immense attention in future too. The small signal stability programs and its simulation programs can be used for controller design, stability status

and system dynamics. The present trend in power system restructuring and deregulation has increased operation efficiency. The high penetration of distributed generation (DG) like renewable such as wind turbine generators (WTGs) has an impact on system stability. The use of controllers on WTGs or use of FACT devices at an appropriate position enables the system stability and security.

Small signal stability is the ability of power system to maintain synchronism when the system is subjected to small disturbances. The small disturbances may be either change in consumer's load or generation power of generating stations. The system may be unstable due to steady increase in generator rotor angle due to lack of synchronizing torque or rotor oscillations of increasing amplitude due to lack of sufficient damping torque. In integrated power system with newer technologies, specially wind turbines, power systems may adversely be affected due to the requirement of scheduling of spinning reserves and energy storage because wind power is variable and difficult to predict. Wind power may have problems of frequent occurrence of voltage dips, grid frequency variations and low power factor due to the location and intermittent nature of wind turbine generators. Therefore, the disturbances due to integration of wind turbine in integrated power system must be studied to imply the problems and also probable solutions to overcome the problem.

The wind turbines are very much using in the world as well as in Nepal. The wind turbine standalone is useful but when it is connected to the grid then it impacts on the stability of the grid. The research gap in the thesis is how the stability changes while wind turbines are added to grid and how much power can be integrated at the prescribed location and is not studied in Nepalese power system. The more the connection point of wind turbine into the grid, then how it affects the participation factor and small signal stability of the grid should be studied.

This study focuses on study of the impact on voltage profile and stability of the grid and analyzes small signal stability with participation factor and Eigen value analysis and determine wind power sensitivity in INPS due to wind power integration.

Further, the latter sections of this paper discusses on the WTG impact on the system stability but limited to technical discussion on voltage profile Eigen value analysis and Eigen sensitivity analysis. It does not consider thermal limit, current handling capacity, network sensitivity effect of impedance matching and harmonic resonance. It only provides information about whether system is stable or not

while integration or adding a wind power to the grid. It does not specify the protection system that can be used for WTG unit in association with grid system. The reconfiguration of grid distribution system affects the power flow in networks and this reconfiguration is also not studied in this study. The variable renewable energy (VRE) cannot supply constant power at all the times and that effect is not considered.

II. Problem Formulation and Methodology

The outline of this work begins from the literature review, in which the wind power generation and the impact on the grid, when integrated to the existing grid is studied. At the review stage, issues of wind farm integration are investigated, the methodologies for system impact study relevant to small signal stability integration is explored.

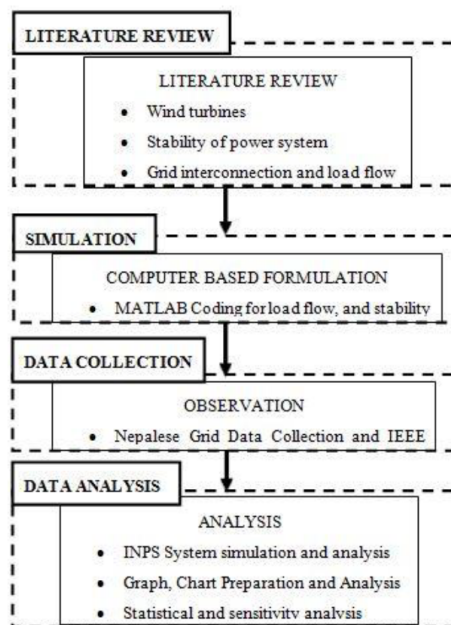


Fig 1: Methodological Block Diagram for Study

In Literature, wind turbine characteristics, wind turbine power generation capability, power system stability and methods for power flow are studied. The prescribed process of methods to study the stability is formulated and simulated in MATLAB. The data of wind turbine power generation and its feasibility is collected from Alternative Energy Promotion Centre (AEPCC) and the integrated Nepalese power system data is collected from Nepal Electricity Authority (NEA). A formulated simulation is done into the INPS and WTG data and analysis is performed for the integrated system.

Small Signal Stability Analysis

The stability analysis for the power system is performed under the condition that the DFIG is added to the grid. In stability analysis, the Eigen values and its vector, participation factor are important for the study. The system data is arranged and then the load flow is performed without and integration of DFIG and stability of the system is studied. After that, the DFIG is integrated to the grid and then the load flow is performed to check the power flow in the network and stability is checked from Eigen value analysis. If the system is found stable, then the results are saved so can be used further. If system is not found to be stable, then the DFIG parameters are varied with respect to the power and the DFIG reactance. The figure 2 shows the flow chart for the stability analysis and other subsections in this section are used to describe the involved equations and mathematical formulations.

Formation of System State Matrix:

The non-linear model of whole system can be represented by non-linear equations. The equations are in state space form are as follows:

$$\dot{x} = f(x, y, u) \dots \dots \dots (1)$$

$$0 = g(x, y) \dots \dots \dots (2)$$

Where x is state variables, y is output variables and u is input variables.

The equations (1) and (2) are linearized and system state matrix A_{sys} is formed.

$$\Delta \dot{x} = A_{sys} \Delta x \dots \dots \dots (3)$$

The Eigen value of A_{sys} is calculated for the computation for the small signal stability. The Eigen values are may be real or complex or zero. The complex Eigen values appear always in complex conjugate pair. For stable operation, all Eigen values λ_i must be in the left half plane.

$$\lambda_i = (\sigma_i \pm j\omega_i) \text{ and } \sigma_i < 0$$

The time constant T [s], damping ratio ζ and oscillating frequency f [Hz] of Eigen value is given by:

$$T = \frac{1}{|\sigma|} \dots \dots \dots (4)$$

$$\zeta = \frac{-\sigma}{\sqrt{\sigma^2 + \omega^2}} \dots \dots \dots (5)$$

$$f = \frac{\omega}{2\pi} \dots \dots \dots (6)$$

The DFIG is connected to load (PQ) bus through a transformer and a bus. If n_{dfg} is the number of DFIGs then the total number of buses is increased by n_{dfg} . The set of

Differential Algebraic Equations (DAE) of DFIG has been performed in MATLAB coding.

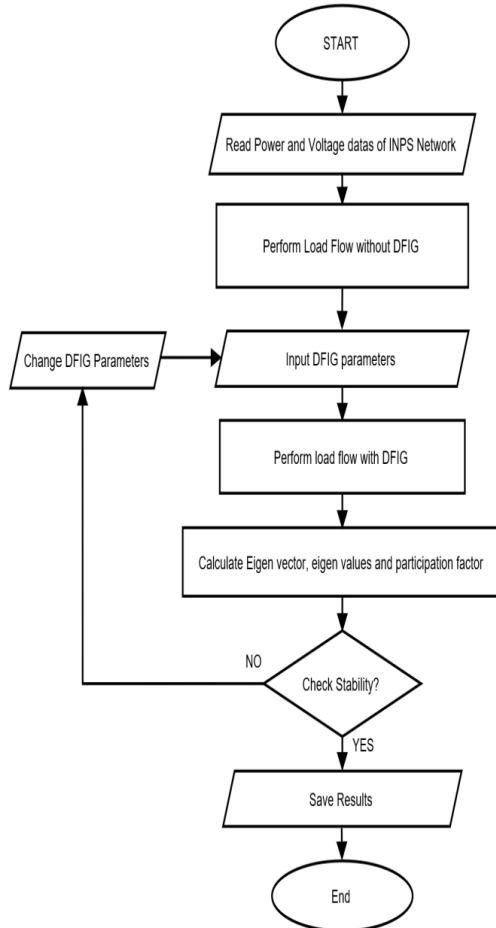


Figure 2: Flow Chart for Stability Analysis

Then, the modal matrices were introduced to express the Eigen properties of A_{sys} . Eigen Value Sensitivity has been performed by taking partial derivative of all eigen values λ_i to a_{kj} where, a_{kj} be the element of matrix \tilde{A}_{sys} (k-th row and j-th column element of \tilde{A}_{sys}).

Similarly, the participation factor (pf) determines the contribution of dominant states (row-wise) to particular modes (Eigen value in column-wise). The participation matrix (P) was generated which is the combination of right eigenvector and left eigenvector.

Network Equations for Generation and Load Bus:

The network equations for generation buses are as follows:

$$P_{Li}(V_i) = \sum_{k=1}^n V_i V_k Y_{ik} \cos(\theta_i - \theta_k - \alpha_{ik}) - I_{di} V_i \sin(\delta_i - \theta_i) - I_{qi} V_i \cos(\delta_i - \theta_i) \quad (7)$$

$$Q_{Li}(V_i) = \sum_{k=1}^n V_i V_k Y_{ik} \sin(\theta_i - \theta_k - \alpha_{ik}) + I_{qi} V_i \sin(\delta_i - \theta_i) - I_{di} V_i \cos(\delta_i - \theta_i) \quad (8)$$

The network equations for load buses are as follows:

$$P_{Li}(V_i) = \sum_{k=1}^n V_i V_k Y_{ik} \cos(\theta_i - \theta_k - \alpha_{ik}) \quad (9)$$

$$Q_{Li}(V_i) = \sum_{k=1}^n V_i V_k Y_{ik} \sin(\theta_i - \theta_k - \alpha_{ik}) \quad (10)$$

Power Flow Analysis

Newton Raphson method is used for the power flow analysis of the integrated network system. The flow chart of the power flow analysis is presented in figure 3. The node voltage and the impedance of each line are subjected to initialize and the mismatch matrices of active power (P) and reactive power (Q) are calculated. The mismatch matrices are used to determine the solution of the equations presented in equation (7) and (8) for generator bus and equation (9) and (10) for load buses. If the solution is not converged, then the Jacobian matrix is formed to solve the equations and then the voltage and voltage angle are determined. The Jacobian matrix for 3-bus system is presented in equation 11.

$$\begin{bmatrix} \Delta Q_3 \\ \Delta P_2 \\ \Delta P_3 \end{bmatrix} = \begin{bmatrix} \frac{\partial Q_3}{\partial V_3} & \frac{\partial Q_3}{\partial \delta_2} & \frac{\partial Q_3}{\partial \delta_3} \\ \frac{\partial P_2}{\partial V_3} & \frac{\partial P_2}{\partial \delta_2} & \frac{\partial P_2}{\partial \delta_3} \\ \frac{\partial P_3}{\partial V_3} & \frac{\partial P_3}{\partial \delta_2} & \frac{\partial P_3}{\partial \delta_3} \end{bmatrix} \begin{bmatrix} \Delta V_3 \\ \Delta \delta_2 \\ \Delta \delta_3 \end{bmatrix} \quad (11)$$

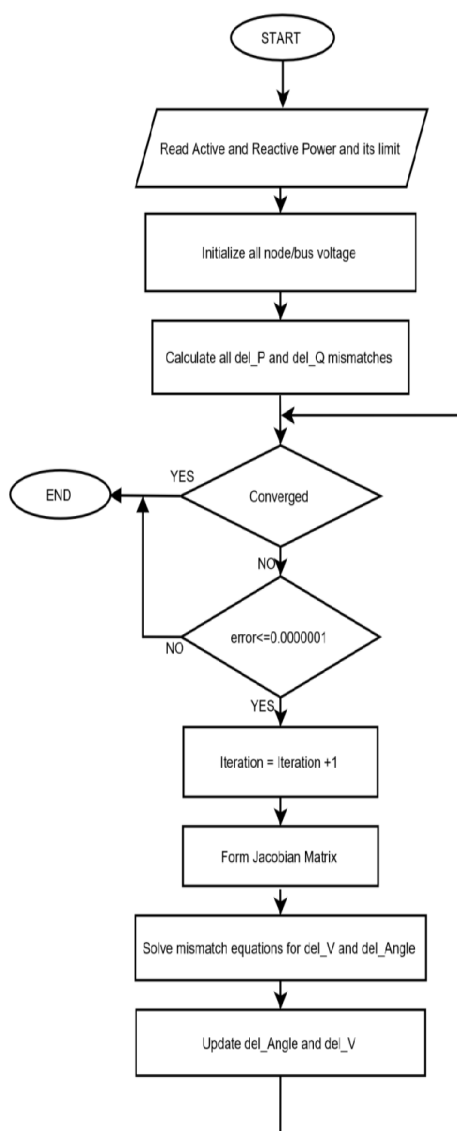


Figure 3: Flow Chart for Newton Raphson Method of Power Flow

III. Model Development and Results

The proposed methodology, which has been described in section II of this paper, uses to evaluate the Eigen values and participation factor. The proposed methodology for stability analysis, Eigen vector determination and sensitivity analysis is coded in MATLAB scripting language and is tested for standard IEEE – 9 bus system consisting 3

machines. The IEEE bus test system is considered for the benchmark of the study in this research for validation and verification of the model and method. The proposed methodology code is firstly verified for IEEE standard bus systems and then it is applied for Integrated Nepalese Power System networks. Cost of Renewable Energy Spreadsheet Tool (CREST Tool) has been used in order to check financial viability of the technology. The obtained results are described in subsections below.

A. Model Building

IEEE 9 Bus System is used as a Test System for this study. Modeling of IEEE 9 bus system and INPS of Nepal is carried out on using MATLAB.

The IEEE 9 bus test system is presented in figure 5 which includes three synchronous machines. In this system, bus 5, 6, and 8 are the load buses.

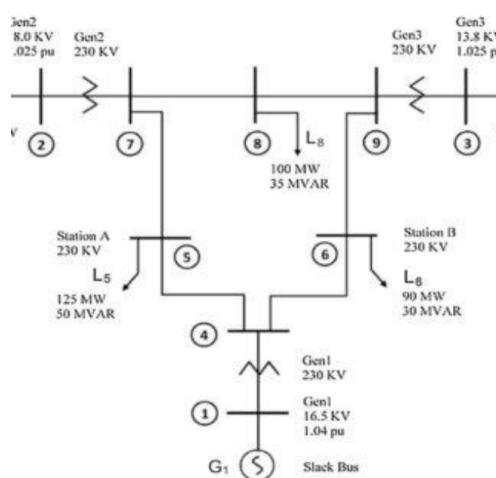


Fig 4: IEEE 3 machine 9 bus system

The following assumptions are made during the modeling INPS and study:

1. The 66 kV bus and higher voltage bus system is considered for the Integrated Nepalese Power System (INPS).
2. The total sixty – six bus is included in the system. In eastern region and western region of Nepal, the INPS system is almost radial structure which is lumped to a point to get minimum errors in load flow solution. The eastern region power generation and load are lumped to Dhalkebar substation and western region power generation and load are lumped to Butwal substation. After this, the total bus in the system is forty-three and analysis is performed for the forty-three bus system

Table 1: Base Case load flow solution

Bus No.	V (pu)	Theta (rad)	P (pu)	Q (pu)
1	1.040	0.000	0.716	0.270
2	1.025	0.162	1.630	0.067
3	1.025	0.081	0.850	-0.109
4	1.026	-0.039	0.000	0.000
5	0.996	-0.070	-1.250	-0.500
6	1.013	-0.064	-0.900	-0.300
7	1.026	0.065	0.000	0.000
8	1.016	0.013	-1.000	-0.350
9	1.032	0.034	0.000	0.000

The variation of minimum Eigen values is presented in table 2. Individually, the best location of DFIG is found to be bus 5 since minimum Eigen value improvement is highest in this bus. In this system, the optimum loading at bus 5, 6, and 8 are 0.79 pu, 0.96 pu and 1.04 pu respectively. When the DFIG connected to bus 5, 6, and 8 simultaneously then the power flow and the Eigen sensitivity is found to be $-0.41693 \pm j 0.4582$ with $P = 0.94$ pu and $-0.40671 \pm j 8.3160$ with $P = 0.94$ pu. The Eigen value plot before and after DFIG connection is presented in figure 5 and figure 6 respectively.

Table 2: Eigen Values for IEEE 9 bus system

Bus	P	Q (-ve)	Eigen Values
5	0.5	0.2	$-0.42416 \pm j 9.1278$
6	0.5	0.2	$-0.38835 \pm j 8.8458$
8	0.5	0.2	$-0.41847 \pm j 0.4784$

The DFIG unit of power 0.5 pu is connected to the system then the load flow solution shows the improvement of voltage limit and power flow. The flow solution after DFIG connection is presented in table 3.

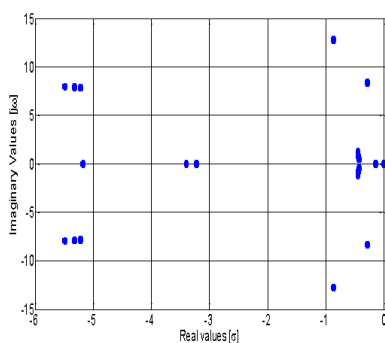


Figure 5: Eigen values Without DFIG

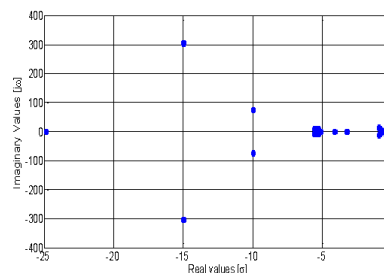


Figure 6: Eigen values With DFIG

Table 3: Load flow solution when DFIG connected

Bus No.	V (pu)	Theta (rad)	P (pu)	Q (pu)
1	1.040	0.000	0.722	0.528
2	1.025	0.163	1.630	0.222
3	1.025	0.080	0.850	-0.033
4	1.012	-0.040	0.000	0.000
5	0.958	-0.070	-1.750	-0.700
6	1.001	-0.066	-0.900	-0.300
7	1.016	0.065	0.000	0.000
8	1.008	0.012	-1.000	-0.350
9	1.028	0.033	0.000	0.000
10	0.951	-0.051	0.500	-0.190

DFIG integrated to INPS System

With the assumptions, the total bus in the system is forty-three and analysis has been performed for the forty-three bus system. The INPS map parameters were used for simulation. The base load flow solution for 43 bus INPS system and the voltage profile was observed. In the base case without DFIG, most of the Eigen values are falling on imaginary axis with complex value as presented in figure 9. The Eigen value on imaginary axis shows the system is critically stable.

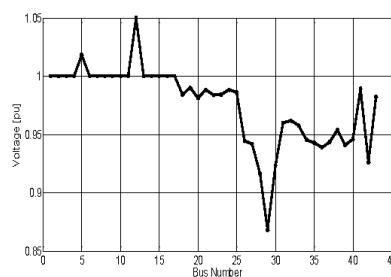


Figure 1: Voltage profile for base load flow solution of INPS system

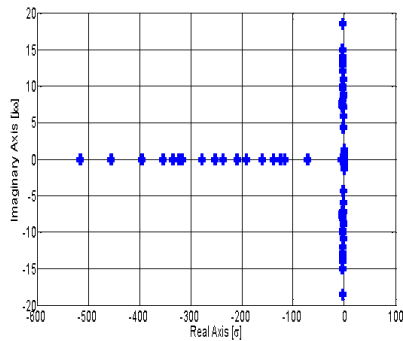


Figure 2: Eigen value plot of INPS system without DFIG

The DFIG connection in the INPS system is considered with five cases for the small signal stability. The DFIG is connected to the bus which is nearest to feasible wind power generation or available wind power generation. In INPS, the six bus selected for DFIG connection are: Balaju 132, Bhaktapur, Nawalparasi, Makwanpur, and Acham. The DFIG active power is variant form 0.1 pu to 0.5 pu for the connection bus and reactive power is variant in respective of active power. The active and reactive power has power factor approximately varies from 0.85 to 0.9 lagging and thus the system has maximum value of Q is 0.4 times of value of P.

Case 1: [Balaju] DFIG Connected to Bus 5 with P=0.5 and Q=0.2

In this case, the DFIG is connected to bus 5 with the P and Q value of 0.5 pu and 0.2 pu respectively. The minimum Eigen value in this case is found to be -0.05155 which is real and lies in real axis. The figure 10 shows the plot of Eigen values on imaginary plane which shows that most of the Eigen values are lies on real axis and also at origin and figure 11 shows the Eigen sensitivity. Some of the Eigen values are complex conjugate. The system is more stable than the base case because most of the Eigen values are lies on real axis and also at origin. The farthest pole at real axis is -517.13 and the complex conjugate poles $\pm j300$ are farthest from the origin. The voltage profile is presented in table 5 and the bus voltage at bus 44 is 1.011 pu which is in stable range of (1 ± 0.5) pu. The active and reactive power injected by DFIG system are 0.5 pu and 0.19 pu respectively.

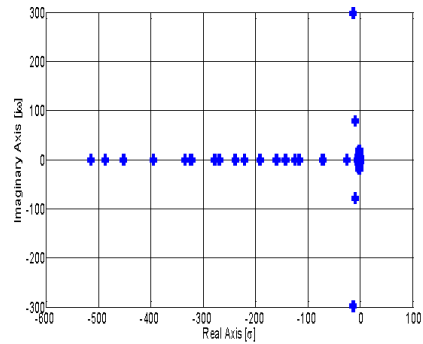


Figure 3: Eigen value plot of INPS system with DFIG for case 1: Balaju

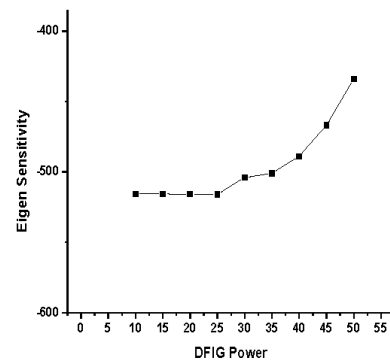


Figure 4: Eigen sensitivity plot for case 1

Case 2: [Bhaktapur] DFIG Connected to Bus 10 with P=0.5 and Q=0.2

In this case, the DFIG is connected to bus 10 which is Bhaktapur in INPS system. The DFIG power to be integrated with the P and Q value of 0.5 pu and 0.2 pu respectively. The minimum Eigen value in this case is found to be -0.0137. The figure 12 shows the plot of Eigen values on imaginary plane which shows that most of the Eigen values are lies on real axis and also at origin. Some of the Eigen values are complex conjugate. Some Eigen values are lies on right side of the imaginary axis. The system is not stable than the base case because most of the Eigen values are lies on right side of the imaginary axis. The farthest from the origin are beyond -500 on left half plane and within 100 on right half plane. The voltage profile is presented in table 6 and the bus voltage at bus 44 is 0.947 pu which is not in stable range of (1 ± 0.5) pu. The active and

reactive power injected by DFIG system are 0.5 pu and 0.101 pu respectively.

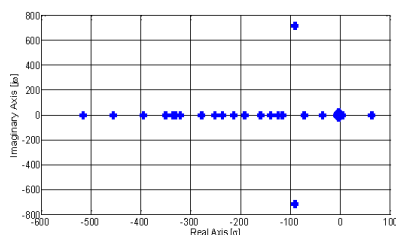
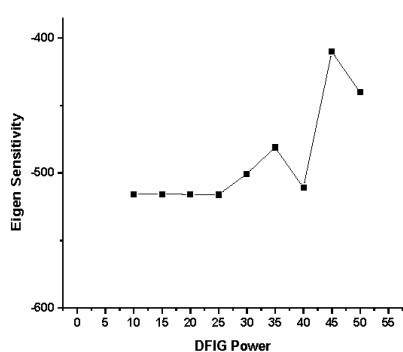


Figure 5: Eigen value plot of INPS system with DFIG for case 2: Bhaktapur



The cases 1 and 2 are selected arbitrarily to show the stability concept using Eigen value analysis. The both cases are compared the base case and shows stability and instability differences. The reactive power is not installed at those locations but considered for the DFIG system. For DFIG system, base value of power is chosen 100 kVA and therefore the power varies as $P = 0.1$ pu, and $P = 0.2$ pu for 10 kW and 20 kW respectively. The load flow for 44 bus (one added due to DFIG penetration) was conducted and results showed that voltage profile was within the limit and voltage stability has been observed.

Financial Analysis of Wind Energy

The financial analysis is performed to show the economic reasonability for wind turbine integration and also the variation on energy cost is presented. The financial calculations and certain assumptions are based on reference of National Renewable Energy Laboratory (NREL) and spreadsheet of NREL is used for wind energy calculations. The levelized cost of energy varies with the energy production and is depicted in figure 19. The project capacity factor shows the variation on energy production and corresponding levelized cost is presented. The levelized cost of energy decreases with the increase in capacity factor increment and thus the higher capacity of generation provide the lower cost of energy.

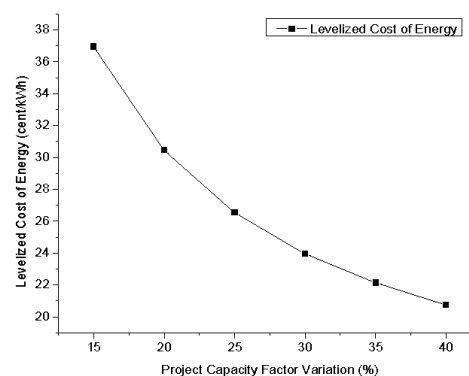


Figure 19: Levelized cost of energy versus project capacity variation

Figure 20 presents the approximate cumulative cash flow for 35% project capacity factor variation which also assumes the subsidy that is provided for wind turbine installation by AEP. It shows the investment is returned within 5 years from the investment date. The subsidy is not taken as a return value in this calculation. The detail financial analysis has been performed and annual cash flows were plotted to obtain the graph in figure 20.

In financial analysis, project life is considered 25 year and wind energy production variation is considered from 15 % to 40 %. The equity of subsidy is 90% for the installation cost and other cost are financed. In this analysis, it was found that the cost of energy goes on decreasing while increasing of the energy production variation. The analysis shows that the project is feasible in case of Nepalese subsidiaries. The project has NPV zero in 3.14 years and the payback period of the system is 3.14 years and project seems financially feasible.

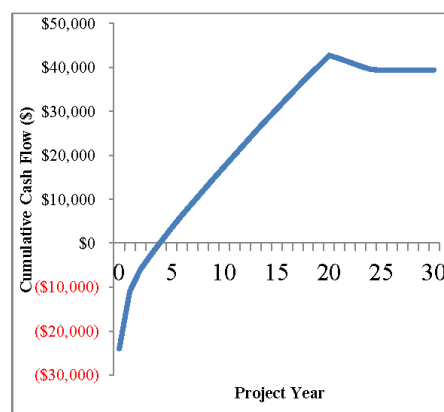


Figure 6: Approximate Cumulative Cash Flow versus project year

CONCLUSION

The minimum Eigen values for the nine bus and INPS bus systems are compared with that of the corresponding systems with DFIG at different locations, one at a time and also in combination. After connection of DFIGs at load buses of such large multi-machine systems, the improvement in Eigen values occurs. This means the rate of reaching the overall system to steady state becomes faster when DFIG is connected one at a time or in combination. These improvements in Eigen values are location dependent as indicated in the result. The Eigen value sensitivity analysis is done to find the optimum loading at load bus where the DFIG is connected. The more the powers P_{tot} and Q_{tot} feed by DFIG to grid, the more the improvement in Eigen values. By observing the negative sign in Eigen value sensitivity, the maximum limit of power or the optimum loading to the grid can be determined. In financial analysis, project life is considered 25 years and found acceptable payback period.

ACKNOWLEDGEMENT

The authors extend their hearty gratitude to the faculties and colleagues at Tribhuvan University, Institute of Engineering, Pulchowk Campus, AEPC and engineers of Nepal Electricity Authority for their constant help, support and recommendations.

REFERENCES

1. Akhmatov, V. (2003). *Analysis of dynamic behaviour of electric power systems with large amount of wind power*.
2. *Annual report of Nepal Electricity Authority, 2018/19*. (2019).
3. Bieker, K., Peitz, S., Brunton, S. L., Kutz, J. N., & Dellnitz, M. (2019). *Deep Model Predictive Control with Online Learning for Complex Physical Systems*. Retrieved from <http://arxiv.org/abs/1905.10094>
4. C. W., T. (1994). *Power Systems Voltage Stability*. New York: Electric Power Research Institute.
5. Che, Y., Xu, J., Shi, K., Liu, H., Chen, W., & Yu, D. (2017). Stability Analysis of Aircraft Power Systems Based on a Unified Large Signal Model. *Energies*, 10.
6. Chi-Tsong, T. C. (1984). *Linear Systems Theory and Design*. New York.
7. Dher, D. K., Doolla, S., & Bandyopadhyay, S. (2017). Electrical Power and Energy Systems Effect of placement of droop based generators in distribution network on small signal stability margin and network loss. *International Journal of Electrical Power and Energy Systems*, (88), 108–118.
8. Erlich, I., Kretschmann, J., Fortmann, J., Mueller-Engelhardt, S., & Wrede, H. (2007). Modeling of wind turbines based on doubly-fed induction generators for power system stability studies. *IEEE Transactions on Power Systems*, 22(3), 909–919. <https://doi.org/10.1109/TPWRS.2007.901607>
9. Ghennam, T., Berkouk, E. M., & François, B. (2009). Modeling and control of a doubly fed induction generator (dfig) based wind conversion system. *POWERENG 2009 - 2nd International Conference on Power Engineering, Energy and Electrical Drives Proceedings*, 507–512. <https://doi.org/10.1109/POWERENG.2009.4915230>
10. Global wind energy council report 2018. (2019). In *Global Wind Energy Council*. Retrieved from www.gwec.net
11. Hauer, J. F. (1991). Application of Prony analysis to the determination of modal content and equivalent models for measured power system response. *IEEE Transactions on Power Systems*, (6), 1062–1068.
12. Haug, D., Chen, Q., Ma, S., Zhang, Y., & Chen, S. (2018). Wide-Area Measurement—Based Model-Free Approach for Online Power System Transient Stability Assessment. *Energies*, (11), 958.
13. Lei, Y., Mullane, A., Lightbody, G., & Yacimini, R. (2006). Modeling of the wind turbine with a doubly fed induction generator for grid integration studies. *IEEE Transactions on Energy Conversion*, 21(1), 257–264. <https://doi.org/10.1109/TEC.2005.847958>
14. Lima, F. K. a, Luna, A., Member, S., Rodriguez, P., Watanabe, E. H., Member, S., & Blaabjerg, F. (2010). Rotor Voltage Dynamics in the Doubly Fed Induction Generator During Grid Faults. *Power*, 25(1), 118–130.
15. MATLAB Designed For Engineers and Scientists. (2019). Retrieved October 14, 2016, from https://www.mathworks.com/products/matlab/why-atlab.html?s_tid=hp_brand_whyatlab#reason5
16. Parashar, M., & Mō, J. (2009). Real Time Dynamics Monitoring System (RTDMSTM): Phasor applications for the control room. *Annual Hawaii International Conference on System Sciences (HICSS-42)*, 5–8. Big Island, USA.
17. Slootweg, J. G., De Haan, S. W. H., Polinder, H., & Kling, W. L. (2001). Modeling wind turbines in power system dynamics simulations. *Proceedings of the IEEE Power Engineering Society Transmission and Distribution Conference*, 1(SUMMER), 22–26. <https://doi.org/10.1109/pess.2001.969976>
18. Tapia, A., Tapia, G., Xabier Ostolaza, J., & Sáenz, J. R. (2003). Modeling and control of a wind turbine driven doubly fed induction generator. *IEEE Transactions on Energy Conversion*, 18(2), 194–204. <https://doi.org/10.1109/TEC.2003.811727>
19. Wilems, J. L. (1971). *Stability Theory of Dynamical Systems*. London.

Bishwas Pokhrel, Dept. of Mechanical Engineering, Institute of Engineering, Pulchowk Campus, TU, Pulchowk, Lalitpur.

Assoc. Prof. Dr. Shreeraj Shakya, Dept. of Mechanical Engineering, Institute of Engineering, Pulchowk Campus, TU, Pulchowk, Lalitpur.

Assoc. Prof. Dr. Nawraj Bhattarai, Dept. of Mechanical Engineering, Institute of Engineering, Pulchowk Campus, TU, Pulchowk, Lalitpur.

APPENDIX B: Load and Generation Data of INPS System

Bus	Type	Vsp	del	Pgi	Qgi	Pli	Qli	Qmin	Qmax	Bus name
1	3	1	0	0	0	0.99	0.495	0	0	Amlekhgunj
2	2	1	0	6.2	0	27.43	13.715	-1	2	Anarmani
3	3	1	0	0	0	5.35	2.68	0	0	Atariya
4	3	1	0	0	0	34.29	17.145	0	0	Balaju
5	3	1	0	0	0	0	0	0	0	Balaju132
6	3	1	0	0	0	11.66	5.83	0	0	Banepa
7	3	1	0	0	0	17.72	8.86	0	0	Baneshwor
8	3	1	0	0	0	0	0	0	0	Banskot
9	3	1	0	0	0	43.44	21.72	0	0	Bardghat
10	3	1	0	0	0	41.15	20.57	0	0	Bhaktapur
11	3	1	0	0	0	0	0	0	0	Bhaktapur 132
12	3	1	0	0	0	22.86	11.43	0	0	Bharatpur
13	2	1	0	36	0	0	0	-10.9	21.8	Bhotekoshi
14	3	1	0	0	0	52.74	27.12	0	0	Birgunj
15	2	1	0	5.1	0	56.24	28.12	-1	2.1	Butwal
16	3	1	0	0	0	33.38	16.69	0	0	Chandranighapur
17	3	1	0	0	0	13.35	6.675	0	0	Chdrauta/Shivapur
18	3	1	0	0	0	0	0	0	0	Chapali
19	2	1	0	20	0	0	0	-6.8	13.6	Chilime
20	3	1	0	0	0	0	0	0	0	Damak
21	3	1	0	0	0	9.65	4.825	0	0	Damauli
22	2	1	0	14.1	0	0	0	-4.5	9	Devighat
23	3	1	0	0	0	30.64	15.32	0	0	Dhalkebar
24	2	1	0	39	0	82.08	41.04	-12	24	Duhabi
25	2	1	0	15	0	0	0	-4.5	9	Gandak
26	3	1	0	0	0	0	0	0	0	Hetauda
27	2	1	0	12.7	0	20.58	10.29	-1.6	3.2	Hetauda 66
28	2	1	0	7.5	0	0	0	-0.5	1	Indrawati
29	2	1	0	12	0	0	0	-4.5	9	Jhimruk
30	1	1	0	144	0	0	0	-44.4	89.3	Kali gandaki
31	2	1	0	0	0	13.26	6.63	0	0	Kawasoti
32	2	1	0	60	0	0	0	-18	36.3	Khimti

33	3	1	0	0	0	2.5	1.25	0	0	Kohalpur
34	2	1	0	60	0	18.59	9.29	-18	36	Kulekhali I
35	2	1	0	32	0	0	0	-9.1	19.6	Kulekhali II
36	2	1	0	80	0	0	0	-30	60	Kushaha
37	3	1	0	0	0	38.87	19.435	0	0	Lahan
38	3	1	0	0	0	11.89	5.95	0	0	Lainchaur
39	3	1	0	0	0	26.98	13.49	0	0	Lamahi
40	3	1	0	0	0	15.04	7.52	0	0	Lamosanghu
41	3	1	0	0	0	12.8	6.4	0	0	Lekhnath
42	2	1	0	6	0	0	0	-2	4	Lucknow
43	3	1	0	0	0	3.57	1.78	0	0	Lumki
44	3	1	0	0	0	5.95	2.97	0	0	Mahendranagar 1
45	3	1	0	0	0	0	0	0	0	Mailung
46	2	1	0	69	0	0	0	-22.5	45	Marsyangdi
47	3	1	0	0	0	5.94	2.97	0	0	Matatirtha
48	2	1	0	70	0	0	0	-22.5	45	M. Marsyangdi
49	3	1	0	0	0	0	0	0	0	Mirchaiya
50	2	1	0	14.1	0	0	0	-3.2	6.8	Modi
51	3	1	0	0	0	21.6	10.8	0	0	New Chabel
52	3	1	0	0	0	0	0	0	0	New Parwanipur
53	3	1	0	0	0	16	8	0	0	New Patan
54	3	1	0	0	0	0	0	0	0	New Marsyangdi
55	3	1	0	0	0	6.29	3.145	0	0	Paanchkhal
56	3	1	0	0	0	21.26	10.63	0	0	Parwanipur
57	3	1	0	0	0	3.5	1.75	0	0	Pathlaiya
58	3	1	0	0	0	24.14	12.07	0	0	Pokhara
59	3	1	0	0	0	14.69	7.345	0	0	Syanja
60	3	1	0	0	0	29.49	14.745	0	0	Simara
61	2	1	0	10	0	0	0	-3	6	Sunkoshi
62	2	1	0	30	0	0	0	-6.5	15	Tanakpur 2
63	3	1	0	0	0	12.57	6.29	0	0	Teku
64	2	1	0	24	0	0	0	-5.3	10.5	Trishuli
65	3	1	0	0	0	0	0	0	0	Siuchatar-132
66	3	1	0	0	0	28.58	14.29	0	0	Siuchatar-66

APPENDIX C: Line Data of INPS System

Line Num.	From bus	To bus	R	X	B/2	TAP ratio	Ycap
1	3	43	0.04551	0.016648	0.03643	1	0
2	39	29	0.09878	0.13648	0.02299	1	0
3	30	15	0.02179	0.09301	0.01962	1	0
4	30	59	0.01254	0.05352	0.01129	1	0
5	21	48	0.02743	0.10035	0.02196	1	0
6	9	25	0.01089	0.03318	0.00672	1	0
7	41	58	0.00622	0.01448	0.0028	1	0
8	15	25	0.02681	0.09807	0.0216	1	0
9	21	41	0.04162	0.09688	0.01875	1	0
10	12	31	0.02179	0.06636	0.01344	1	0
11	33	39	0.05985	0.021894	0.0479	1	0
12	37	24	0.04523	0.16548	0.03621	1	0
13	20	2	0.01746	0.06386	0.01397	1	0
14	47	35	0.01908	0.06941	0.01539	1	0
15	41	59	0.02287	0.09762	0.02059	1	0
16	46	54	0.00381	0.01628	0.00343	1	0
17	58	8	0.00623	0.02345	0.00485	1	0
18	24	20	0.02992	0.10947	0.02395	1	0
19	37	36	0.03678	0.13456	0.02944	1	0
20	23	16	0.04115	0.15052	0.03293	1	0
21	43	33	0.04987	0.18245	0.03992	1	0
22	37	49	0.01745	0.06386	0.01397	1	0
23	34	27	0.06659	0.13397	0.00208	1	0
24	57	16	0.0106	0.03877	0.00848	1	0
25	40	11	0.03005	0.11165	0.02369	1	0
26	36	24	0.01683	0.06158	0.01347	1	0
27	57	52	0.0106	0.03877	0.00848	1	0
28	66	34	0.1207	0.2537	0.00377	1	0
29	50	8	0.0197	0.07035	0.01457	1	0
30	54	48	0.01295	0.0629	0.02516	1	0
31	44	3	0.02307	0.08438	0.01846	1	0

32	9	31	0.032684	0.09954	0.02016	1	0
33	4	64	0.18265	0.292	0.00036	1	0
34	56	14	0.03746	0.07873	0.00117	1	0
35	1	60	0.04162	0.08748	0.0013	1	0
36	44	62	0.02998	0.1083	0.02196	1	0
37	60	56	0.03746	0.07873	0.00117	1	0
38	35	26	0.00499	0.01814	0.00402	1	0
39	66	63	0.01022	0.0361	0.00053	1	0
40	66	53	0.0136	0.03563	0.00051	1	0
41	66	4	0.02721	0.06066	0.00089	1	0
42	33	42	0.0374	0.13684	0.02994	1	0
43	64	45	0.08275	0.17297	0.00257	1	0
44	53	7	0.01753	0.02533	0.00039	1	0
45	10	7	0.05914	0.08857	0.00136	1	0
46	6	10	0.09495	0.12756	0.00199	1	0
47	10	51	0.04252	0.12817	0.0177	1	0
48	39	17	0.03179	0.11631	0.02545	1	0
49	51	22	0.19525	0.31214	0.00386	1	0
50	5	18	0.00623	0.02281	0.00499	1	0
51	18	11	0.00748	0.027	0.00607	1	0
52	57	26	0.02307	0.08438	0.01846	1	0
53	47	65	0.00212	0.00771	0.00171	1	0
54	40	13	0.01869	0.07035	0.01456	1	0
55	17	15	0.03803	0.13912	0.03044	1	0
56	32	40	0.02868	0.01049	0.02295	1	0
57	6	55	0.6179	0.08301	0.0013	1	0
58	55	28	0.19564	0.257	0.004	1	0
59	61	55	0.131	0.17598	0.00275	1	0
60	38	4	0.00716	0.01784	0.00034	1	0
61	22	64	0.0208	0.04348	0.00065	1	0
62	4	22	0.20784	0.33227	0.0411	1	0
63	23	49	0.01995	0.07298	0.01597	1	0
64	19	45	0.0587	0.1227	0.0018	1	0
65	11	5	0.00748	0.027	0.00607	1	0

66	65	5	0.00383	0.01598	0.0034	1	0
67	12	26	0.052136	0.15879	0.03216	1	0
68	21	12	0.04056	0.09441	0.01827	1	0
69	46	65	0.04578	0.19502	0.04116	1	0
70	66	65	0.01	0.2421	0	1	0
71	26	27	0.01	0.244	0	1	0
72	10	11	0.01	0.222	0	1	0
73	5	4	0.01	0.2491	0	1	0
74	52	56	0.01	0.174	0	1	0
75	46	12	0.011986	0.051154	0.010789	1	0
76	45	22	0.0208	0.04348	0.0065	1	0
77	1	27	0.06659	0.13997	0.00208	1	0

APPENDIX D: Financial Analysis

SN	Description	Amount	Remarks
<u>Cost of Wind Power System</u>			
1	Cost per Kilowatt for Wind power system	650,000.00	AEPC, cost including battery installation
2	Battery, Storage & Distribution system Component in wind power system	60%	
3	Cost per kilowatt for wind power system excluding Battery installation	260,000.00	
<u>Benefit From wind Power System</u>			
1	Peak annual generation per kilowatt Installation (Kilowatt-Hour)	8,760.00	Theoretical Capacity
2	Capacity Factor for Wind Power System	5.4% to 33.16%	IOEGC 2015 pp 169-179
3	Capacity Factory for wind power system	22.00%	AEPC
4	Annual Generation From Wind Power System (Kilowatt-Hour)	1,927.20	
5	Rate of Energy Sales (NRs./kW-Hr)	7.30	NEA PPA Rate for Solar Plants
6	Annual Revenue from Energy Sales	14,068.56	
7	Operation & Maintenance Cost	3,900.00	@1.5% of Total Cost of System
8	Depreciation	13,000.00	Straight Line method with No Scrap value at end of 20 yrs
9	Profit From Revenue before tax (EBIT)	(2,831.44)	
10	Corporate Tax	-	@25% of Net Profit
11	Net Profit from the Project	(2,831.44)	
12	CashFlow to the equity Holder	10,168.56	
<u>Assumptions</u>			
	Minimum Attractive Rate of Return	10%	

APPENDIX E: MATLAB Codes

File 1

```
%clc
clear all

%% bus data
% Type of Bus 1-Slack, 2-PV, 3-PQ

%          Bus  Type  V  theta  PGi  QGi  PLi  QLi
busdata = [1   1   1   0   1.44  0.893  0   0   ;
           2   2   1   0   0.531 0.301 1.1394 0.56965
           ;
           3   2   1   0   0.15  0.09  0   0   ;
           4   2   1   0   0.141 0.068 0   0   ;
           5   2   1.018 0   0.7   0.45  0   0   ;
           6   2   1   0   0.69  0.45  0   0   ;
           ;
           7   2   1   0   0.127 0.032 0.2058 0.1029
           ;
           8   2   1   0   1.252 0.86  1.7902 0.8951
           ;
           9   2   1   0   0.32  0.196 0   0   ;
           10  2   1   0   0.6   0.36  0.1859 0.0929
           ;
           11  2   1   0   0.24  0.105 0   0   ;
           12  2   1.05  0   0.2   0.136 0   0   ;
           13  2   1   0   0.141 0.09  0   0   ;
           14  2   1   0   0.1   0.06  0   0   ;
           15  2   1   0   0.075 0.01  0   0   ;
           16  2   1   0   0.6   0.363 0   0   ;
           17  2   1   0   0.36  0.218 0   0   ;
           18  3   1   0   0     0     0.1469 0.07345
           ;
           19  3   1   0   0     0     0.4344 0.2172
           ;
           20  3   1   0   0     0     0.1326 0.0663
           ;
           21  3   1   0   0     0     0     0   ;
           22  3   1   0   0     0     0.2414 0.1207
           ;
           23  3   1   0   0     0     0.128 0.064 ;
           24  3   1   0   0     0     0.0965 0.04825
           ;
```

```

; 25 3 1 0 0 0 0.2286 0.1143
;
; 26 3 1 0 0 0 0.3338 0.1669
;
; 27 3 1 0 0 0 0.035 0.0175 ;
; 28 3 1 0 0 0 0.2126 0.1063
;
; 29 3 1 0 0 0 0.5274 0.2712
;
; 30 3 1 0 0 0 0.2949 0.14745
;
; 31 3 1 0 0 0 0.0099 0.00495
;
; 32 3 1 0 0 0 0.0594 0.0297
;
; 33 3 1 0 0 0 0.2858 0.1429
;
; 34 3 1 0 0 0 0.3429 0.17145
;
; 35 3 1 0 0 0 0.4115 0.2057
;
; 36 3 1 0 0 0 0.216 0.108 ;
; 37 3 1 0 0 0 0.1189 0.0595
;
; 38 3 1 0 0 0 0.1257 0.0629
;
; 39 3 1 0 0 0 0.1772 0.0886
;
; 40 3 1 0 0 0 0.16 0.08 ;
; 41 3 1 0 0 0 0.0629 0.03145
;
; 42 3 1 0 0 0 0.1166 0.0583
;
; 43 3 1 0 0 0 0.1504 0.0752
];

```

```

% 10 3 1.0 0 0.5 0.2 0.5 0.2];
%% line data
% From To R X B/2 tap ratio
% Bus Bus pu pu pu (a)
linedata = [31 7 0.04162 0.08748 0.0013 1 ;
34 33 0.02721 0.06066 0.00089 1 ;
34 35 0.00748 0.027 0.00607 1 ;

```

34	37	0.00716	0.01784	0.00034	1	;
42	35	0.09495	0.12756	0.00199	1	;
39	35	0.05914	0.08857	0.00136	1	;
21	22	0.00623	0.02345	0.00485	1	;
19	20	0.032684	0.09954	0.02016	1	;
25	7	0.052136	0.15879	0.03216	1	;
17	43	0.01869	0.07035	0.01456	1	;
2	19	0.02681	0.09807	0.0216	1	;
26	27	0.0106	0.03877	0.00848	1	;
12	11	0.0587	0.1227	0.0018	1	;
24	25	0.04056	0.09441	0.01827	1	;
13	34	0.20784	0.33227	0.0411	1	;
13	36	0.19525	0.31214	0.00386	1	;
8	26	0.04115	0.15052	0.03293	1	;
3	19	0.01089	0.03318	0.00672	1	;
15	41	0.19564	0.257	0.004	1	;
1	18	0.01254	0.05352	0.01129	1	;
1	2	0.02179	0.09301	0.01962	1	;
16	43	0.02868	0.01049	0.02295	1	;
10	7	0.06659	0.13397	0.00208	1	;
10	33	0.1207	0.2537	0.00377	1	;
9	7	0.00499	0.01814	0.00402	1	;
9	32	0.01908	0.06941	0.01539	1	;
43	35	0.03005	0.11165	0.02369	1	;
23	24	0.04162	0.09688	0.01875	1	;
5	24	0.02743	0.10035	0.02196	1	;
5	6	0.01295	0.0629	0.02516	1	;
6	25	0.011986	0.051154	0.010789	1	;
6	33	0.04578	0.19502	0.04116	1	;
32	33	0.00212	0.00771	0.00171	1	;
4	21	0.0197	0.07035	0.01457	1	;
36	35	0.04252	0.12817	0.0177	1	;
40	39	0.01753	0.02533	0.00039	1	;
41	42	0.6179	0.08301	0.0013	1	;
28	29	0.03746	0.07873	0.00117	1	;
28	30	0.03746	0.07873	0.00117	1	;
27	28	0.0106	0.03877	0.00848	1	;
27	7	0.02307	0.08438	0.01846	1	;
22	23	0.00622	0.01448	0.0028	1	;
30	31	0.04162	0.08748	0.0013	1	;


```

33 38 0.01022 0.0361 0.00053 1 ;
33 40 0.0136 0.03563 0.00051 1 ;
14 41 0.131 0.17598 0.00275 1 ;
18 23 0.02287 0.09762 0.02059 1 ;
11 13 0.0208 0.04348 0.00065 1 ;
11 34 0.18265 0.292 0.00036 1 ];

```

```
%% machine data
```

```

% m/c bus x_d x'_d T'_do x_q x'_q T'_qo H D
% no no
%
mac= [ 1 1 1.6560 0.3190 4.8960 1.6490
0.6380 0.0191 2.847 0.0127 ;
2 2 1.3480 0.1300 4.3389 1.3480
0.2600 0.0117 1.983 0.0532 ;
3 3 1.3560 0.1900 4.6839 1.3560
0.3800 0.0197 2.082 0.0309 ;
4 4 1.3480 0.1300 4.3389 1.3480
0.2600 0.0117 1.983 0.0532 ;
5 5 1.3320 0.1160 4.3089 1.3320
0.2320 0.0110 1.8873 0.0493 ;
6 6 1.2800 0.1000 4.2370 1.2980
0.2010 0.0109 1.883 0.0292 ;
7 7 1.1510 0.1140 3.9948 1.5490
0.3300 0.0172 1.8934 0.0436 ;
8 8 1.1510 0.1140 3.9948 1.5490
0.3300 0.0172 1.8934 0.0436 ;
9 9 1.5100 0.1400 4.4648 1.4800
0.3000 0.0097 2.434 0.032 ;
10 10 1.3480 0.1300 4.3389 1.3480
0.2600 0.0117 1.983 0.0532 ;
11 11 1.6200 0.1800 3.6448 1.5300
0.5000 0.0099 1.9434 0.0561 ;
12 12 1.3320 0.1160 4.3089 1.3320
0.2320 0.0110 1.8873 0.0493 ;
13 13 1.3390 0.1250 4.2170 1.3430
0.2600 0.0199 1.763 0.0541 ;
14 14 1.5500 0.1900 4.9660 1.5950
0.4380 0.0219 2.107 0.0299 ;
15 15 1.3480 0.1300 4.3389 1.3480
0.2600 0.0117 1.983 0.0532 ;

```

```

    16 16    1.2980    0.1310    4.3890    1.2980
0.2620    0.0110    1.85  0.04992    ;
    17 17    1.3480    0.1300    4.3389    1.3480
0.2600    0.0117    1.983 0.0532    ];

```

```

%   exc  K_A  T_A   K_E   T_E   K_F   T_F
%   no

```

```

exc= [  1  25.0000    0.2000   -0.0582    0.6544    0.1050
       0.3500    ;
       2  25.0000    0.2000   -0.0582    0.6544    0.1050
       0.3500    ;
       3  25.0000    0.2000   -0.0582    0.6544    0.1050
       0.3500    ;
       4  25.0000    0.2000   -0.0582    0.6544    0.1050
       0.3500    ;
       5  25.0000    0.2000   -0.0582    0.6544    0.1050
       0.3500    ;
       6  25.0000    0.2000   -0.0582    0.6544    0.1050
       0.3500    ;
       7  25.0000    0.2000   -0.0582    0.6544    0.1050
       0.3500    ;
       8  25.0000    0.2000   -0.0582    0.6544    0.1050
       0.3500    ;
       9  25.0000    0.2000   -0.0582    0.6544    0.1050
       0.3500    ;
      10  25.0000    0.2000   -0.0582    0.6544    0.1050
       0.3500    ;
      11  25.0000    0.2000   -0.0582    0.6544    0.1050
       0.3500    ;
      12  25.0000    0.2000   -0.0582    0.6544    0.1050
       0.3500    ;
      13  25.0000    0.2000   -0.0582    0.6544    0.1050
       0.3500    ;
      14  25.0000    0.2000   -0.0582    0.6544    0.1050
       0.3500    ;
      15  25.0000    0.2000   -0.0582    0.6544    0.1050
       0.3500    ;
      16  25.0000    0.2000   -0.0582    0.6544    0.1050
       0.3500    ;
      17  25.0000    0.2000   -0.0582    0.6544    0.1050
       0.3500 ];

```

```

BMVA=100;
Wel = 2*pi*60;

mach = mac(:,1); fbus = mac(:,2); Xd = mac(:,3); Xdd = mac(:,4);
Td0d = mac(:,5);
Xq = mac(:,6); Xqd = mac(:,7); Tq0d = mac(:,8); H = mac(:,9);
D = mac(:,10);
nmac=length(mach);

KA= exc(:,2); TA= exc(:,3); KE= exc(:,4); TE= exc(:,5); KF=
exc(:,6);TF= exc(:,7);
Ra=zeros(1,17);

```

File 2

```
% Load flow analysis of basic 9-bus system
% using NR method
Busdata_1

p=linedata(:,1);
q=linedata(:,2);
r=linedata(:,3);
x=linedata(:,4);
b=linedata(:,5);
a=linedata(:,6);
j=0 + 1.0000i;
b=j*b;

z=r+j*x;
y=1./z;

nb=max(max(p),max(q));
nl=length(p);

%% Bus-admittance matrix

Y=zeros(nb,nb);

for k=1:nl
    Y(p(k),q(k))=Y(p(k),q(k))- y(k)/a(k);
    Y(q(k),p(k))=Y(p(k),q(k));
end

for k=1:nb
    for n=1:nl
        if p(n)==k
            Y(k,k)=Y(k,k)+(y(n)/(a(n)^2))+b(n);
        elseif q(n)==k
            Y(k,k)=Y(k,k)+y(n)+b(n);
        end
    end
end
end
Y;
```

```

G=real(Y);
B=imag(Y);

%% bus data evaluation
bus=busdata(:,1);
type=busdata(:,2);
V=busdata(:,3);
theta=busdata(:,4);
Pg=busdata(:,5);%/BMVA;
Qg=busdata(:,6);%/BMVA;
Pl=busdata(:,7);%/BMVA;
Ql=busdata(:,8);%/BMVA;

Psp=Pg-Pl;
Qsp=Qg-Ql;

pv=find(type==2);
pq=find(type==3);
pqv=find(type==2 | type==3);

npv=length(pv);
npq=length(pq);
npqv=length(pqv);

iter=1;
tol=1;

%% Load flow using N-R method
% Iteration starts

while (tol>0.0000001)

    P = zeros(nb,1);
    Q = zeros(nb,1);

    for i=1:nb
        for k=1:nb
            P(i) = P(i) + V(i)* V(k)*(G(i,k)*cos(theta(i)-theta(k))
+ B(i,k)*sin(theta(i)-theta(k)));
            Q(i) = Q(i) + V(i)* V(k)*(G(i,k)*sin(theta(i)-theta(k))
- B(i,k)*cos(theta(i)-theta(k)));

```

```

        end
    end

    dP1=Psp-P;
    dQ1=Qsp-Q;

    dQ=zeros(npq,1);
    k=1;
    for i=1:nb
        if type(i)==3
            dQ(k,1)=dQ1(i);
            k=k+1;
        end
    end

    dP=zeros(npqv,1);
    k=1;
    for i=1:nb
        if type(i)==2 || type(i)==3
            dP(k,1)=dP1(i);
            k=k+1;
        end
    end

    error=[dP; dQ];

    % Jacobian

    J1=zeros(nb-1,nb-1);
    for i=1:nb-1
        k=pqv(i);
        for m=1:nb-1
            n=pqv(m);
            if n==k
                J1(i,m)=-Q(k)-B(k,k)*(V(k)^2);
            else
                J1(i,m)=V(k)*V(n)*(G(k,n)*sin(theta(k)-theta(n))-
                B(k,n)*cos(theta(k)-theta(n)));
            end
        end
    end
end

```

```

end

J2=zeros(nb-1,npq);
for i=1:nb-1
    k=pqv(i);
    for m=1:npq
        n=pq(m);
        if n==k
            J2(i,m)=P(k)+G(k,k)*(V(k)^2);
        else
            J2(i,m)=V(k)*V(n)*(G(k,n)*cos(theta(k)-
theta(n))+B(k,n)*sin(theta(k)-theta(n)));
        end
    end
end

J3=zeros(npq,nb-1);
for i=1:npq
    k=pq(i);
    for m=1:nb-1
        n=pqv(m);
        if n==k
            J3(i,m)=P(k)-G(k,k)*(V(k)^2);
        else
            J3(i,m)=V(k)*V(n)*(-G(k,n)*cos(theta(k)-theta(n))-
B(k,n)*sin(theta(k)-theta(n)));
        end
    end
end

J4=zeros(npq,npq);
for i=1:npq
    k=pq(i);
    for m=1:npq
        n=pq(m);
        if n==k
            J4(i,m)=Q(k)-B(k,k)*(V(k)^2);
        else
            J4(i,m)=V(k)*V(n)*(G(k,n)*sin(theta(k)-theta(n))-
B(k,n)*cos(theta(k)-theta(n)));
        end
    end
end

```

```

        end
    end

    JCB=[J1 J2;J3 J4];

    % calculation of deviations

    X=inv(JCB)*error;
    dtheta=X(1:nb-1);
    dV=X(nb:end);

    k=1;
    for i=1:nb
        if type(i)==3
            V(i)=V(i)+dV(k)*V(i);
            k=k+1;
        end
    end
    k=1;
    for i=1:nb
        if type(i)==2 || type(i)==3
            theta(i)=theta(i)+dtheta(k);
            k=k+1;
        end
    end

    iter=iter+1;
    tol=max(abs(error));
    THETA=180*theta/pi;

end

P(1)=0;
Q(1)=0;

for m=1:nb
    P(1)=P(1)+V(1)*V(m)*(G(1,m)*cos(theta(1)-theta(m))+B(1,m)*sin(theta(1)-theta(m)));
    Q(1)=Q(1)+V(1)*V(m)*(G(1,m)*sin(theta(1)-theta(m))-B(1,m)*cos(theta(1)-theta(m)));
end

```



```

v=zeros(nb,1);
nn=1;
for i=1:nb
    v(nn,1)= V(i)*(cos(theta(i))+j*sin(theta(i)));
    nn=nn+1;
end
[V THETA P Q]
Y_mag=abs(Y);
alpha=angle(Y);
save N_R_value V theta P Q Y_mag alpha

%% Initial condition of the machine

m=nmac;    % No of PV buses
PL=zeros(1,m);
QL=zeros(1,m);

for i=1:m
    PG(i)=P(i)-PL(i);
    QG(i)=Q(i)-QL(i);
    IG(i)=(PG(i)-1i*QG(i))/(V(i)*(exp(-1i*theta(i))));
    gama(i)=angle(IG(i));
    beeta(i)=angle(V(i)*exp(1i*theta(i))+(Ra(i)+1i*Xq(i))*IG(i)); %
    this is delta ( rotor angle)=beeta(here) of the machine
    Id(i)=real(IG(i)*exp(-1i*(beeta(i)-pi/2))); %
    Id and Iq currents
    Iq(i)=imag(IG(i)*exp(-1i*(beeta(i)-pi/2)));
    Vd(i)=real(V(i)*exp(1i*theta(i))*exp(-1i*(beeta(i)-pi/2))); %
    This is Vd
    Vq(i)=imag(V(i)*exp(1i*theta(i))*exp(-1i*(beeta(i)-pi/2))); %
    This is Vq
    Edd(i)=Vd(i)+Ra(i)*Id(i)-Xqd(i)*Iq(i); %
    Ed'=(called Edd)
    Eqd(i)=Vq(i)+Ra(i)*Iq(i)+Xdd(i)*Id(i); %
    Eq'=(called Eqd)
    Efd(i)=Eqd(i)+(Xd(i)-Xdd(i))*Id(i); %
    Efd
    VR(i)=(KE(i)+0.0039*exp(1.555*Efd(i)))*Efd(i); %
    VR

```

```

    Rf(i)=KF(i)/TF(i)*Efd(i); %
Rf
    Vref(i)=V(i)+VR(i)/KA(i); %
Vref
    TM(i)=Edd(i)*Id(i)+Eqd(i)*Iq(i)+(Xqd(i)-Xdd(i))*Id(i)*Iq(i); %
TM
end
% [beeta' Id' Iq' Vd' Edd' Eqd' Efd' VR' Rf' Vref' TM']

save machinedata beeta Id Iq Vd Vq Edd Eqd Efd VR Rf Vref TM

```

File 3

```
% connected with a load bus through a parallel tr line and a
transformer,
% using NR method

N_R_method_2

%% DFIG connection

dbus=44;          % bus num.
dbuscncd=20;     % bus at which DFIG connected
% prompt={'DFIG Conn. to Bus','Reactance of DFIG','DFIG Act. Power (pu)
','DFIG React. Power (pu) ' };
% dlg_title='INPUT';
% num_lines=1;
% def={' ',' ',' ',' ',' '};
% answer=inputdlg(prompt,dlg_title,num_lines,def);
%
% dbuscncd=str2num(answer{1});
% x_dg=str2num(answer{2});
% pdg=str2num(answer{3});
% qdg=str2num(answer{4});
x_dg=0.034;

pdg = 2.0;
qdg = -pdg*0.4;

pl=-pdg;
ql=-qdg-((((pdg)^2+(qdg)^2)^0.5)/V(dbuscncd))^2*x_dg;

for k=1:length(p)
    if p(k)>=dbus
        p(k)=p(k)+1;
    elseif q(k)>=dbus
        q(k)=q(k)+1;
    elseif p(k)>=dbus & q(k)>=dbus
        p(k)=p(k)+1;
        q(k)=q(k)+1;
    end
end
```

```

end

linedata1=[dbuscncctd dbus 0 x_dg 0 1 0];
linedata=[p q r x b a zeros(nl,1)];linedata1];

% Load flow with DFIG using N-R method

p=linedata(:,1);
q=linedata(:,2);
r=linedata(:,3);
x=linedata(:,4);
b=linedata(:,5);
a=linedata(:,6);

z=r+j*x;

nb=max(max(p),max(q));
nl=length(p);

y=ones(nl,1)./z;

% Bus-admittance matrix

Y=zeros(nb,nb);

for k=1:nl
    if a(k) <= 0
        a(k) = 1;
    end
    Y(p(k),q(k))=Y(p(k),q(k)) - (y(k)/a(k));
    Y(q(k),p(k))=Y(p(k),q(k));
end

for k=1:nb
    for n=1:nl
        if p(n)==k
            Y(k,k)=Y(k,k) + (y(n)/(a(n)^2)) + b(n);
        elseif q(n)==k

```

```

        Y(k,k)=Y(k,k)+y(n)+b(n);
    end
end
end
Y;
G=real(Y);
B=imag(Y);

mac(:,2)=mac(:,2)+1;
fbus=mac(:,2);

busdata2=busdata(1:17,1:8);
busdata1=busdata(18:43,1:8);

busdata_dg=[dbus 3 1 0 0 0 pl ql];

busdata2(:,1)=busdata2(:,1)+1;
busdata=[busdata2;busdata1;busdata_dg];

bus=busdata(:,1);
type=busdata(:,2);
V=busdata(:,3);
theta=busdata(:,4);
Pg=busdata(:,5);
Qg=busdata(:,6);
Pl=busdata(:,7);
Ql=busdata(:,8);

Pl(dbuscncld)=Pl(dbuscncld)+pdg;
Ql(dbuscncld)=Ql(dbuscncld)-qdg;

P = Pg - Pl;
Q = Qg - Ql;
Psp = P;
Qsp = Q;

pv=find(type==2);
pq=find(type==3);
pqv=find(type==2 | type==3);

```

```

npv=length(pv);
npq=length(pq);
npqv=length(pqv);

iter=1;
tol=1;

% Iteration starts

while(tol>0.0000001)

    P = zeros(nb,1);
    Q = zeros(nb,1);

    for i=1:nb
        for k=1:nb
            P(i) = P(i) + V(i)* V(k)*(G(i,k)*cos(theta(i)-theta(k))
+ B(i,k)*sin(theta(i)-theta(k)));
            Q(i) = Q(i) + V(i)* V(k)*(G(i,k)*sin(theta(i)-theta(k))
- B(i,k)*cos(theta(i)-theta(k)));
        end
    end

    dP1=Psp-P;
    dQ1=Qsp-Q;

    dQ=zeros(npq,1);
    k=1;
    for i=1:nb
        if type(i)==3
            dQ(k,1)=dQ1(i);
            k=k+1;
        end
    end

    dP=zeros(npqv,1);
    k=1;
    for i=1:nb
        if type(i)==2 || type(i)==3
            dP(k,1)=dP1(i);
            k=k+1;
        end
    end
end

```

```

        end
    end

    error=[dP; dQ];

    % Jacobian

    J1=zeros(nb-1,nb-1);
    for i=1:nb-1
        k=pqv(i);
        for m=1:nb-1
            n=pqv(m);
            if n==k
                J1(i,m)=-Q(k)-B(k,k)*(V(k)^2);
            else
                J1(i,m)=V(k)*V(n)*(G(k,n)*sin(theta(k)-theta(n))-
B(k,n)*cos(theta(k)-theta(n)));
            end
        end
    end

    J2=zeros(nb-1,npq);
    for i=1:nb-1
        k=pqv(i);
        for m=1:npq
            n=pq(m);
            if n==k
                J2(i,m)=P(k)+G(k,k)*(V(k)^2);
            else
                J2(i,m)=V(k)*V(n)*(G(k,n)*cos(theta(k)-
theta(n))+B(k,n)*sin(theta(k)-theta(n)));
            end
        end
    end

    J3=zeros(npq,nb-1);
    for i=1:npq
        k=pq(i);
        for m=1:nb-1
            n=pqv(m);
            if n==k

```

```

        J3(i,m)=P(k)-G(k,k)*(V(k)^2);
    else
        J3(i,m)=V(k)*V(n)*(-G(k,n)*cos(theta(k)-theta(n))-
B(k,n)*sin(theta(k)-theta(n)));
    end
end
end

J4=zeros(npq,npq);
for i=1:npq
    k=pq(i);
    for m=1:npq
        n=pq(m);
        if n==k
            J4(i,m)=Q(k)-B(k,k)*(V(k)^2);
        else
            J4(i,m)=V(k)*V(n)*(G(k,n)*sin(theta(k)-theta(n))-
B(k,n)*cos(theta(k)-theta(n)));
        end
    end
end

JCB=[J1 J2;J3 J4];

% calculation of deviations

X=inv(JCB)*error;
dtheta=X(1:nb-1);
dV=X(nb:end);

k=1;
for i=1:nb
    if type(i)==3
        V(i)=V(i)+dV(k)*V(i);
        k=k+1;
    end
end

k=1;
for i=1:nb
    if type(i)==2 || type(i)==3
        theta(i)=theta(i)+dtheta(k);
    end
end

```



```

        k=k+1;
    end
end

iter=iter+1;
tol=max(abs(error));
THETA=180*theta/pi;

end
P(1)=0;
Q(1)=0;

    for m=1:nb
        P(1)=P(1)+V(1)*V(m)*(G(1,m)*cos(theta(1)-
theta(m))+B(1,m)*sin(theta(1)-theta(m)));
        Q(1)=Q(1)+V(1)*V(m)*(G(1,m)*sin(theta(1)-theta(m))-
B(1,m)*cos(theta(1)-theta(m)));
    end

v=zeros(nb,1);
nn=1;
for i=1:nb
    v(nn,1)= V(i)*(cos(theta(i))+j*sin(theta(i)));
    nn=nn+1;
end
afterloadflow = [V THETA P Q]
Y_mag=abs(Y);
alpha=angle(Y);

save loadflow V theta P Q Y_mag alpha dbus dbuscncd

```

File 4

```
clear all
%(with DFIG 2 mass model)

Loadflow_3
% Finding initial condition of DFIG
%%%%%%%%%%%%%%%%%%%%%%%%%%%%%%%%%%%%%%%%%%%%%%%%%%%%%%%%%%%%%%%%%%%%%%%%
%%%%%%%%%%%%%%%%%%%%%%%%%%%%%%%%%%%%%%%%%%%%%%%%%%%%%%%%%%%%%%%%%%%%%%%%
%(with DFIG 2 mass model)

wel=2*pi*60;
Rs=0.005;
Rr=1.1*Rs;
Lm=4;
Lss=1.01*Lm;
Lrr=1.005*Lss;
Kmrr=Lm/Lrr;
R2=(Kmrr^2)*Rr;
R1=Rs+R2;
Ls1=Lss-(Lm*Kmrr);
Tr=Lrr/Rr;
Kopt=0.5787;
Ht=4;
Hg=0.1*Ht;
Heq=Ht+Hg;
Ksh=0.3;
Csh=0.01;
ws=1;
wr_rated=1.2;

% x_df=[iqs ids iqr idr vqr vdr wr] % DFIG values
x_df = [1 ; 0.5 ; -0.5 ; 1 ; 0.5 ; 0.5 ; 1];

vqs(1,1)= V(dbus,1)*cos(theta(dbus,1));
vds(1,1)= V(dbus,1)*sin(theta(dbus,1));
Ptot(1,1)= -P1(dbus);
Qtot(1,1)= -Q1(dbus);

iter= 0;
tol= 1;
```

```

while(tol>0.000001)

    fn = [-Rs*x_df(1) + Lss*x_df(2) + Lm*x_df(4);
          -Rs*x_df(2) - Lss*x_df(1) - Lm*x_df(3);
          -Rr*x_df(3) + Lrr*x_df(4) - x_df(7)*Lrr*x_df(4) +
Lm*x_df(2) - x_df(7)*Lm*x_df(2) - x_df(5);
          -Rr*x_df(4) - Lrr*x_df(3) + x_df(7)*Lrr*x_df(3) -
Lm*x_df(1) + x_df(7)*Lm*x_df(1) - x_df(6);
          Lm*x_df(1)*x_df(4) - Lm*x_df(2)*x_df(3) - Kopt*(x_df(7)^2);
          vqs(1,1)*x_df(1) + vds(1,1)*x_df(2) + x_df(5)*x_df(3) +
x_df(6)*x_df(4);
          -vqs(1,1)*x_df(2) + vds(1,1)*x_df(1) ];

    del_f = [vqs(1,1)-fn(1);vds(1,1)-fn(2);0-fn(3);0-fn(4);0-
fn(5);Ptot(1,1)-fn(6);Qtot(1,1)-fn(7) ];

    Jac = [-Rs          Lss          0          Lm
0          0          0;
          -Lss          -Rs          -Lm          0
0          0          0;
          0          Lm-(Lm*x_df(7))  -Rr          Lrr-
(Lrr*x_df(7)) -1          0  -(Lrr*x_df(4))-(Lm*x_df(2));
          -Lm+(Lm*x_df(7))  0          -Lrr+(Lrr*x_df(7))  -
Rr          0          -1  (Lrr*x_df(3))+(Lm*x_df(1));
          Lm*x_df(4)          -Lm*x_df(3)          -Lm*x_df(2)
Lm*x_df(1)          0          0  -2*Kopt*x_df(7);
          vqs(1,1)          vds(1,1)          x_df(5)          x_df(6)
x_df(3) x_df(4)          0;
          vds(1,1)          -vqs(1,1)          0          0
0          0          0 ];

    delx_df = inv(Jac)*del_f;

    for k=1:length(x_df)
        x_df(k)=x_df(k)+delx_df(k);
    end

    tol=max(del_f);

    iter=iter+1;

end

```

```

x_df=x_df';

iqs(1,1)=x_df(1);
ids(1,1)=x_df(2);
iqr(1,1)=x_df(3);
idr(1,1)=x_df(4);
vqr=x_df(5);
vdr=x_df(6);
wr(1,1)=x_df(7);
wt(1,1)=wr(1,1);
theta_tw(1,1)=1.7573;

eds1(1,1) = - Lm*(iqr(1,1) + Kmrr*iqs(1,1));
eqs1(1,1) = Lm*(idr(1,1) + Kmrr*ids(1,1));

Te(1,1)=Lm*((iqs(1,1)*idr(1,1)) - (ids(1,1)*iqr(1,1)));

if wr(1,1)>=wr Rated
    iter1= 0;
    toll= 1;
% x_df=[iqs ids iqr idr vqr vdr ] % DFIG values
x_df1 = [1 ; 0.5 ; -0.5 ; 1 ; 0.5 ; 0.5];

while(toll>0.000001)

    fn1 = [-Rs*x_df1(1) + Lss*x_df1(2) + Lm*x_df1(4);
           -Rs*x_df1(2) - Lss*x_df1(1) - Lm*x_df1(3);
           -Rr*x_df1(3) + Lrr*x_df1(4) - wr Rated*Lrr*x_df1(4) +
Lm*x_df1(2) - wr Rated*Lm*x_df1(2) - x_df1(5);
           -Rr*x_df1(4) - Lrr*x_df1(3) + wr Rated*Lrr*x_df1(3) -
Lm*x_df1(1) + wr Rated*Lm*x_df1(1) - x_df1(6);
           vqs(1,1)*x_df1(1) + vds(1,1)*x_df1(2) + x_df1(5)*x_df1(3)
+ x_df1(6)*x_df1(4);
           -vqs(1,1)*x_df1(2) + vds(1,1)*x_df1(1) ];

    del_f1 = [vqs(1,1)-fn1(1);vds(1,1)-fn1(2);0-fn1(3);0-
fn1(4);Ptot(1,1)-fn1(5);Qtot(1,1)-fn1(6)];

    Jac1 = [-Rs          Lss          0          Lm
0          0;
           -Lss        -Rs          -Lm          0
0          0;

```

```

                                0          Lm-(Lm*wr_rated)      -Rr          Lrr-
(Lrr*wr_rated)  -1          0;
-Rr          -Lm+(Lm*wr_rated)          0          -Lrr+(Lrr*wr_rated)
              0          -1;
x_df1(6)      vqs(1,1)          vds(1,1)          x_df1(5)
              x_df1(3) x_df1(4);
              vds(1,1)          -vqs(1,1)          0          0
0          0 ];

```

```
delx_df1 = inv(Jac1)*del_f1;
```

```

for k=1:length(x_df1)
    x_df1(k)=x_df1(k)+delx_df1(k);
end

```

```
toll=max(del_f1);
```

```
iter1=iter1+1;
```

```
end
```

```
x_df1=x_df1';
```

```
iqs(1,1)=x_df1(1);
```

```
ids(1,1)=x_df1(2);
```

```
iqr(1,1)=x_df1(3);
```

```
idr(1,1)=x_df1(4);
```

```
vqr=x_df1(5);
```

```
vdr=x_df1(6);
```

```
wr(1,1)=wr_rated;
```

```
wt(1,1)=wr(1,1);
```

```
theta_tw(1,1)=1.7573;
```

```
eds1(1,1) = - Lm*(iqr(1,1) + Kmrr*iqs(1,1));
```

```
eqs1(1,1) = Lm*(idr(1,1) + Kmrr*ids(1,1));
```

```
Te(1,1)=Ptot(1,1)/wr_rated;
```

```
Terated=Te(1,1);
```

```
end
```

```
Tm=Te(1,1);
```

```
Ws = 2*pi*60;
```

```
P1_mat=[-(wel*R1)/Ls1          wel*ws          (wel*wr)/(ws*Ls1)          -
(wel)/(Ls1*Tr*ws)          (wel*eqs1)/(Ls1*ws)          0          0;

          -(wel*ws)          -(wel*R1)/Ls1          wel/(Ls1*Tr*ws)
(wel*wr)/(ws*Ls1)          (wel*eds1)/(Ls1*ws)          0          0;

          0          wel*ws*R2          -wel/Tr          wel*ws*(1-
wr/ws)          -wel*eds1          0          0;

          -wel*ws*R2          0          -wel*ws*(1-wr/ws)          -wel/Tr
wel*eqs1          0          0;

          -(eqs1)/(2*Hg*ws)          -eds1/(2*Hg*ws)          -iqs/(2*Hg*ws)          -
ids/(2*Hg*ws)          Csh*wel/(2*Hg)          Ksh/(2*Hg)          -Csh*wel/(2*Hg);

          0          0          0          0          0
-wel          0          wel;

          0          0          0          0          0
Csh*wel/(2*Ht)          -Ksh/(2*Ht)          -Csh*wel/(2*Ht)];
```

```
P2_mat=[wel*V(nb)*sin(theta(nb))/Ls1          -wel*cos(theta(nb))/Ls1;
          -wel*V(nb)*cos(theta(nb))/Ls1          -wel*sin(theta(nb))/Ls1;

          0          0;

          0          0;

          0          0;

          0          0;

          0          0];
```

```
Q1_mat=[V(nb)*cos(theta(nb))-Kmrr*vqr          V(nb)*sin(theta(nb))-Kmrr*vdr
vdr/(Lm)          -vqr/(Lm)          0          0          0;

          V(nb)*sin(theta(nb))          -V(nb)*cos(theta(nb))
0          0          0          0          0];
```

```
Q2_mat=[ids*V(nb)*cos(theta(nb))-iqs*V(nb)*sin(theta(nb))
iqs*cos(theta(nb))+ids*sin(theta(nb));

          ids*V(nb)*sin(theta(nb))+iqs*V(nb)*cos(theta(nb))
iqs*sin(theta(nb))-ids*cos(theta(nb))];
```

```
% Calculation of eigen value
```

```
%
```

```
% Asys2=P1_mat-P2_mat*Q2_mat^-1*Q1_mat;
```

```
% lamda2=eig(Asys2)
```

```
save dfig_mat P1_mat P2_mat Q1_mat Q2_mat
```

```

%loadflow          % Load flow data required for finding the initial
condition
%NR9bus
% Given Machine Data

% mach = mac(:,1); fbus = mac(:,2); Xd = mac(:,3); Xdd = mac(:,4);
Td0d = mac(:,5);
% Xq = mac(:,6); Xqd = mac(:,7); Tq0d = mac(:,8); H = mac(:,9);
D = mac(:,10);
% nmac=length(mach);
%
% KA= exc(:,2); TA= exc(:,3); KE= exc(:,4); TE= exc(:,5); KF=
exc(:,6);TF= exc(:,7);
% Ra=[0 0 0];

%%%%%%%%%%%%%%%%%%%%%%%%%%%%%%%%%%%%%%%%%%%%%%%%%%%%%%%%%%%%%%%%%%%%%%%%
%%%%%%%%%%%%%%%%%%%%%%%%%%%%%%%%%%%%%%%%%%%%%%%%%%%%%%%%%%%%%%%%%%%%%%%%

% Program starts from here

% Initial condition of the machine

m=nmac; % No of PV buses
PL=zeros(1,m);
QL=zeros(1,m);

for i=1:m
    PG(i)=P(i)-PL(i);
    QG(i)=Q(i)-QL(i);
    IG(i)=(PG(i)-1i*QG(i))/(V(i)*(exp(-1i*theta(i))));
    gama(i)=angle(IG(i));
    beeta(i)=angle(V(i)*exp(1i*theta(i))+(Ra(i)+1i*Xq(i))*IG(i)); %
    this is delta ( rotor angle)=beeta(here) of the machine
    Id(i)=real(IG(i)*exp(-1i*(beeta(i)-pi/2))); %
    Id and Iq currents
    Iq(i)=imag(IG(i)*exp(-1i*(beeta(i)-pi/2)));
    Vd(i)=real(V(i)*exp(1i*theta(i))*exp(-1i*(beeta(i)-pi/2))); %
    This is Vd
    Vq(i)=imag(V(i)*exp(1i*theta(i))*exp(-1i*(beeta(i)-pi/2))); %
    This is Vq
    Edd(i)=Vd(i)+Ra(i)*Id(i)-Xqd(i)*Iq(i); %
    Ed'=(called Edd)

```

```

    Eqd(i)=Vq(i)+Ra(i)*Iq(i)+Xdd(i)*Id(i); %
Eq'=(called Eqd)
    Efd(i)=Eqd(i)+(Xd(i)-Xdd(i))*Id(i); %
Efd
    VR(i)=(KE(i)+0.0039*exp(1.555*Efd(i)))*Efd(i); %
VR
    Rf(i)=KF(i)/TF(i)*Efd(i); %
Rf
    Vref(i)=V(i)+VR(i)/KA(i); %
Vref
    TM(i)=Edd(i)*Id(i)+Eqd(i)*Iq(i)+(Xqd(i)-Xdd(i))*Id(i)*Iq(i); %
TM
end
save machine_DFIG beeta Id Iq Vd Vq Edd Eqd Efd VR Rf Vref TM
% [beeta' Id' Iq' Vd' Edd' Eqd' Efd' VR' Rf' Vref' TM']

```


File 5

```
%(with DFIG 2 mass model)

%loadflow
Machine_DFIG_5

wel=2*pi*60;
Rs=0.005;
Rr=1.1*Rs;
Lm=4;
Lss=1.01*Lm;
Lrr=1.005*Lss;
Kmrr=Lm/Lrr;
R2=(Kmrr^2)*Rr;
R1=Rs+R2;
Ls1=Lss-(Lm*Kmrr);
Tr=Lrr/Rr;
Kopt=0.5787;
Ht=4;
Hg=0.1*Ht;
Heq=Ht+Hg;
Ksh=0.3;
Csh=0.01;
ws=1;

% x_df=[iqs ids iqr idr vqr vdr wr] % DFIG values
x_df = [1 ; 0.5 ; -0.5 ; 1 ; 0.5 ; 0.5 ; 1];

vqs(1,1)= V(dbus,1)*cos(theta(dbus,1));
vds(1,1)= V(dbus,1)*sin(theta(dbus,1));
Ptot(1,1)= -P1(dbus);
Qtot(1,1)= -Q1(dbus);

iter= 0;
tol= 1;

while(tol>0.000001)
```

```

fn = [-Rs*x_df(1) + Lss*x_df(2) + Lm*x_df(4);
      -Rs*x_df(2) - Lss*x_df(1) - Lm*x_df(3);
      -Rr*x_df(3) + Lrr*x_df(4) - x_df(7)*Lrr*x_df(4) +
Lm*x_df(2) - x_df(7)*Lm*x_df(2) - x_df(5);
      -Rr*x_df(4) - Lrr*x_df(3) + x_df(7)*Lrr*x_df(3) -
Lm*x_df(1) + x_df(7)*Lm*x_df(1) - x_df(6);
      Lm*x_df(1)*x_df(4) - Lm*x_df(2)*x_df(3) - Kopt*(x_df(7)^2);
      vqs(1,1)*x_df(1) + vds(1,1)*x_df(2) + x_df(5)*x_df(3) +
x_df(6)*x_df(4);
      -vqs(1,1)*x_df(2) + vds(1,1)*x_df(1) ];

```

```

del_f = [vqs(1,1)-fn(1);vds(1,1)-fn(2);0-fn(3);0-fn(4);0-
fn(5);Ptot(1,1)-fn(6);Qtot(1,1)-fn(7)];

```

```

Jac = [-Rs          Lss          0          Lm
0      0      0;
      -Lss          -Rs          -Lm          0
0      0      0;
      0          Lm-(Lm*x_df(7))  -Rr          Lrr-
(Lrr*x_df(7)) -1          0  -(Lrr*x_df(4))-(Lm*x_df(2));
Rr      -Lm+(Lm*x_df(7))  0          -Lrr+(Lrr*x_df(7))  -
0          -1  (Lrr*x_df(3))+Lm*x_df(1));
Lm*x_df(1)  Lm*x_df(4)          -Lm*x_df(3)          -Lm*x_df(2)
0          0          -2*Kopt*x_df(7);
x_df(3) x_df(4)  vqs(1,1)  vds(1,1)  x_df(5)  x_df(6)
0          0          0;
0          0          vds(1,1)  -vqs(1,1)  0          0
0          0          0 ];

```

```

delx_df = inv(Jac)*del_f;

```

```

for k=1:length(x_df)
    x_df(k)=x_df(k)+delx_df(k);
end

```

```

tol=max(del_f);

```

```

iter=iter+1;

```

```

end

```

```

x_df=x_df';

```

```

iqs(1,1)=x_df(1);

```

```

ids(1,1)=x_df(2);
iqr(1,1)=x_df(3);
idr(1,1)=x_df(4);
vqr=x_df(5);
vdr=x_df(6);
wr(1,1)=x_df(7);
wt(1,1)=wr(1,1);
theta_tw(1,1)=1.7573;

eds1(1,1) = - Lm*(iqr(1,1) + Kmrr*iqs(1,1));
eqs1(1,1) = Lm*(idr(1,1) + Kmrr*ids(1,1));

Te(1,1)=Lm*((iqs(1,1)*idr(1,1)) - (ids(1,1)*iqr(1,1)));
Tm=Te(1,1);

Ws = 2*pi*60;

```

File 6:

```

clc
clear all
N_R_method_2

% Calculation of eigen value of 39 bus system

load N_R_value
load machinedata
% machD68

Nd=7; % No of differential equations

m=nmac; % No of PV buses
n=length(bus); % Total no of buses
ngb=n-m;
Ws=2*pi*60;

for i=1:m
    M(i)=(2*H(i))/Ws;

```

```

fs(i)=- (KE(i)+(0.0039*exp(1.555*Efd(i)))*(1.555*Efd(i)+1))/TE(i);

end

% Calculation of Matrix A

% Calculation of A1,B1,B2,E1

for i=1:m

A11(:, :, i)=[0      1      0      0      0      0
0;
      0      -D(i)/M(i)      -Iq(i)/M(i)      -Id(i)/M(i)      0
0      0;
      0      0      -1/Td0d(i)      0      1/Td0d(i)
0      0;
      0      0      0      -1/Tq0d(i)      0      0
0;
1/TE(i)      0      0      0      0      fs(i)
-1/TA(i)      0      0      0      0      -(KA(i)*KF(i))/(TA(i)*TF(i))
0      0      0      0      0      KF(i)/(TF(i)^2)
0      -1/TF(i)];

end

A1=zeros(Nd*m,Nd*m);
for i=1:m
for j=1:Nd
for k=1:Nd
A1((Nd*(i-1)+j),(Nd*(i-1)+k))=A11(j,k,i);
end
end
end

for i=1:m
A21(:, :, i)=[0      0;
(Iq(i)*(Xdd(i)-Xqd(i))-Edd(i))/M(i)      (Id(i)*(Xdd(i)-
Xqd(i))-Eqd(i))/M(i);
-(Xd(i)-Xdd(i))/Td0d(i)      0;
0      (Xq(i)-Xqd(i))/Tq0d(i);

```

```

0
0
0

0;
0;
0];

A31(:, :, i)=[0 0;
0 0;
0 0;
0 0;
0 0;
0 -KA(i)/TA(i);
0 0];

E11(:, :, i)=[0 0;
1/M(i) 0;
0 0;
0 0;
0 0;
0 KA(i)/TA(i);
0 0];

end
A2=zeros(Nd*m, 2*m);
A3=zeros(Nd*m, 2*m);
E1=zeros(Nd*m, 2*m);
for i=1:m
    for j=1:Nd
        for k=1:2
            A2((Nd*(i-1)+j), (2*(i-1)+k))=A21(j, k, i);
            A3((Nd*(i-1)+j), (2*(i-1)+k))=A31(j, k, i);
            E1((Nd*(i-1)+j), (2*(i-1)+k))=E11(j, k, i);
        end
    end
end

%%%%% stator Algebraic equations

for i=1:m

```

```

B11(:, :, i) = [-V(i) * cos(beta(i) - theta(i)) 0 0 1 0 0 0;
                V(i) * sin(beta(i) - theta(i)) 0 1 0 0 0 0];

B21(:, :, i) = [-Ra(i) Xqd(i);
                -Xdd(i) -Ra(i)];

B31(:, :, i) = [V(i) * cos(beta(i) - theta(i)) -sin(beta(i) - theta(i));
                -V(i) * sin(beta(i) - theta(i)) -cos(beta(i) - theta(i))];
end

B1=zeros(2*m, Nd*m); % 2 is no of stator equations
B2=zeros(2*m, 2*m);
B3=zeros(2*m, 2*m);

for i=1:m
    for j=1:2
        for k=1:Nd
            B1((2*(i-1)+j), (Nd*(i-1)+k))=B11(j, k, i);
        end
    end
end

for i=1:m
    for j=1:2
        for k=1:2
            B2((2*(i-1)+j), (2*(i-1)+k))=B21(j, k, i);
            B3((2*(i-1)+j), (2*(i-1)+k))=B31(j, k, i);
        end
    end
end

% Network Equations

% Generator Buses

for i=1:m
    C11(:, :, i)=[Id(i)*V(i)*cos(beta(i)-theta(i))-
    Iq(i)*V(i)*sin(beta(i)-theta(i)) 0 0 0 0 0 0;
                -Id(i)*V(i)*sin(beta(i)-theta(i))-
    Iq(i)*V(i)*cos(beta(i)-theta(i)) 0 0 0 0 0 0];

```

```

        C21(:, :, i)=[V(i)*sin(beeta(i)-theta(i))      V(i)*cos(beeta(i)-
theta(i));
                    V(i)*cos(beeta(i)-theta(i))      -V(i)*sin(beeta(i)-
theta(i))];
end

for i=1:m
    for j=1:2
        for k=1:Nd
            C1((2*(i-1)+j), (Nd*(i-1)+k))=C11(j, k, i);
        end
    end
end

for i=1:m
    for j=1:2
        for k=1:2
            C2((2*(i-1)+j), (2*(i-1)+k))=C21(j, k, i);

        end
    end
end

% for matrix C3

for i=1:m
    sum1=0;
    sum2=0;

    for k=1:n
        if (k~=i)
            sum_a=(V(k)*Y_mag(i, k)*sin(theta(i)-theta(k)-
alpha(i, k)));
            sum_b=(V(k)*Y_mag(i, k)*cos(theta(i)-theta(k)-
alpha(i, k)));
            sum1=sum1+sum_a;
            sum2=sum2+sum_b;

        end
    end
end

```

```

    end
    s1(i)=sum1;
    s2(i)=sum2;
end

for i=1:m
    for j=1:m
        if i==j
            C3(2*i-1,2*j-1)=Iq(i)*V(i)*sin(beeta(i)-theta(i))-
            Id(i)*V(i)*cos(beeta(i)-theta(i))+V(i)*s1(i);
            C3(2*i-1,2*j)=Id(i)*sin(beeta(i)-
            theta(i))+Iq(i)*cos(beeta(i)-theta(i))-s2(i)-
            2*V(i)*Y_mag(i,i)*cos(alpha(i,i));
            C3(2*i,2*j-1)=Id(i)*V(i)*sin(beeta(i)-
            theta(i))+Iq(i)*V(i)*cos(beeta(i)-theta(i))-V(i)*s2(i);
            C3(2*i,2*j)=Id(i)*cos(beeta(i)-theta(i))-
            Iq(i)*sin(beeta(i)-theta(i))-s1(i)+2*V(i)*Y_mag(i,i)*sin(alpha(i,i));
        else
            C3(2*i-1,2*j-1)=-V(i)*V(j)*Y_mag(i,j)*sin(theta(i)-
            theta(j)-alpha(i,j));
            C3(2*i-1,2*j)=-V(i)*Y_mag(i,j)*cos(theta(i)-theta(j)-
            alpha(i,j));
            C3(2*i,2*j-1)=V(i)*V(j)*Y_mag(i,j)*cos(theta(i)-theta(j)-
            alpha(i,j));
            C3(2*i,2*j)=-V(i)*Y_mag(i,j)*sin(theta(i)-theta(j)-
            alpha(i,j));
        end
    end
end

for i=1:m
    for j=1:(n-m)
        C4(2*i-1,2*j-1)=-V(i)*V(j+m)*Y_mag(i,j+m)*sin(theta(i)-
        theta(j+m)-alpha(i,j+m));
        C4(2*i-1,2*j)=-V(i)*Y_mag(i,j+m)*cos(theta(i)-theta(j+m)-
        alpha(i,j+m));
        C4(2*i,2*j-1)=V(i)*V(j+m)*Y_mag(i,j+m)*cos(theta(i)-
        theta(j+m)-alpha(i,j+m));
        C4(2*i,2*j)=-V(i)*Y_mag(i,j+m)*sin(theta(i)-theta(j+m)-
        alpha(i,j+m));
    end
end
end

```



```

for i=1:(n-m)
    for j=1:m
        D1(2*i-1,2*j-1)=-V(i+m)*V(j)*Y_mag(i+m,j)*sin(theta(i+m)-
theta(j)-alpha(i+m,j));
        D1(2*i-1,2*j)=-V(i+m)*Y_mag(i+m,j)*cos(theta(i+m)-theta(j)-
alpha(i+m,j));
        D1(2*i,2*j-1)=V(i+m)*V(j)*Y_mag(i+m,j)*cos(theta(i+m)-
theta(j)-alpha(i+m,j));
        D1(2*i,2*j)=-V(i+m)*Y_mag(i+m,j)*sin(theta(i+m)-theta(j)-
alpha(i+m,j));
    end
end

for i=(m+1):n
    sum_3=0;
    sum_4=0;

    for k=1:n
        if (k~=i)
            sum_c1=(V(k)*Y_mag(i,k)*sin(theta(i)-theta(k)-
alpha(i,k)));
            sum_d1=(V(k)*Y_mag(i,k)*cos(theta(i)-theta(k)-
alpha(i,k)));
            sum_3=sum_3+sum_c1;
            sum_4=sum_4+sum_d1;
        end

    end

    s_3(i)=sum_3;
    s_4(i)=sum_4;
end

for i=1:(n-m)
    for j=1:(n-m)
        if (i~=j)
            D2(2*i-1,2*j-1)=-
V(i+m)*V(j+m)*Y_mag(i+m,j+m)*sin(theta(i+m)-theta(j+m)-
alpha(i+m,j+m));
            D2(2*i-1,2*j)=-V(i+m)*Y_mag(i+m,j+m)*cos(theta(i+m)-
theta(j+m)-alpha(i+m,j+m));

```

```

        D2(2*i,2*j-1)=V(i+m)*V(j+m)*Y_mag(i+m,j+m)*cos(theta(i+m)-theta(j+m)-alpha(i+m,j+m));
        D2(2*i,2*j)=-V(i+m)*Y_mag(i+m,j+m)*sin(theta(i+m)-theta(j+m)-alpha(i+m,j+m));

    else

        D2(2*i-1,2*j-1)=V(i+m)*s_3(i+m);
        D2(2*i-1,2*j)=-s_4(i+m)-2*V(i+m)*Y_mag(i+m,i+m)*cos(alpha(i+m,i+m));
        D2(2*i,2*j-1)=-V(i+m)*s_4(i+m);
        D2(2*i,2*j)=-s_3(i+m)+2*V(i+m)*Y_mag(i+m,i+m)*sin(alpha(i+m,i+m));

    end
end
end

% Calculation of eigen value without DFIG

A1_mat=[A1 zeros(119,1);zeros(1,120)];
B1_mat=[A2 A3 zeros(119,52);zeros(1,120)];
C1_mat=[[B1; C1; zeros(52,119)] zeros(120,1)];
D1_mat=[B2 B3 zeros(34,52);
        C2 C3 C4;
        zeros(52,34) D1 D2];

Asys1=A1_mat - B1_mat * inv(D1_mat) *C1_mat;
lamda1=eig(Asys1);
plot(lamda1, '+', 'LineWidth', 4)
title('Eigenvalues Without DFIG', 'Color', 'b', 'FontWeight', 'bold')
grid on

save stab1_9b Asys1 lamda1

```

File 7

```
clc
clear all

Machine_DFIG_5

% Calculation of eigen value of 39 bus system

clear all
Busdata_1
load loadflow
load machine_DFIG
load dfig_mat

Nd=7; % No of differential equations

m=17; % No of PV buses
n=44; % Total no of buses
ngb=n-m;

Ws=2*pi*60;

for i=1:m
    M(i)=(2*H(i))/Ws;
    fs(i)=-((KE(i)+(0.0039*exp(1.555*Efd(i))))*(1.555*Efd(i)+1))/TE(i);
end

% Calculation of Matrix A

% Calculation of A1,B1,B2,E1

for i=1:m

A11(:, :, i)=[0      1      0      0      0      0
0;
```

```

0      0      -D(i)/M(i)      -Iq(i)/M(i)      -Id(i)/M(i)      0
0      0;
0      0      0      -1/Td0d(i)      0      1/Td0d(i)
0;
0      0      0      0      -1/Tq0d(i)      0      0
0;
1/TE(i) 0      0      0      0      0      fs(i)
-1/TA(i) KA(i)/TA(i);      0      0      -(KA(i)*KF(i))/(TA(i)*TF(i))
0      0      0      0      0      KF(i)/(TF(i)^2)
0      -1/TF(i)];

```

```
end
```

```
A1=zeros(Nd*m,Nd*m);
```

```
for i=1:m
```

```
for j=1:Nd
```

```
for k=1:Nd
```

```
A1((Nd*(i-1)+j),(Nd*(i-1)+k))=A11(j,k,i);
```

```
end
```

```
end
```

```
end
```

```
for i=1:m
```

```
A21(:, :, i)=[0 0;
```

```
(Iq(i)*(Xdd(i)-Xqd(i))-Edd(i))/M(i) (Id(i)*(Xdd(i)-Xqd(i))-Eqd(i))/M(i);
```

```
-(Xd(i)-Xdd(i))/Td0d(i) 0;
```

```
0 (Xq(i)-Xqd(i))/Tq0d(i);
```

```
0 0;
```

```
0 0;
```

```
0 0];
```

```
A31(:, :, i)=[0 0;
```

```
0 0;
```

```
0 0;
```

```
0 0;
```

```
0 0;
```

```
0 -KA(i)/TA(i);
```

```
0 0];
```

```

E11(:, :, i)=[0 0;
              1/M(i) 0;
              0 0;
              0 0;
              0 0;
              0 KA(i)/TA(i);
              0 0];

end

A2=zeros(Nd*m, 2*m);
A3=zeros(Nd*m, 2*m);
E1=zeros(Nd*m, 2*m);
for i=1:m
    for j=1:Nd
        for k=1:2
            A2((Nd*(i-1)+j), (2*(i-1)+k))=A21(j, k, i);
            A3((Nd*(i-1)+j), (2*(i-1)+k))=A31(j, k, i);
            E1((Nd*(i-1)+j), (2*(i-1)+k))=E11(j, k, i);
        end
    end
end

end

%% %% stator Algebraic equations

for i=1:m
    B11(:, :, i)=[-V(i)*cos(beeta(i)-theta(i)) 0 0 1 0 0 0;
                 V(i)*sin(beeta(i)-theta(i)) 0 1 0 0 0 0];

    B21(:, :, i)=[-Ra(i) Xqd(i);
                 -Xdd(i) -Ra(i)];

    B31(:, :, i)=[V(i)*cos(beeta(i)-theta(i)) -sin(beeta(i)-theta(i));
                 -V(i)*sin(beeta(i)-theta(i)) -cos(beeta(i)-theta(i))];
end

B1=zeros(2*m, Nd*m); % 2 is no of stator equations
B2=zeros(2*m, 2*m);
B3=zeros(2*m, 2*m);

```

```

for i=1:m
    for j=1:2
        for k=1:Nd
            B1((2*(i-1)+j),(Nd*(i-1)+k))=B11(j,k,i);
        end
    end
end

for i=1:m
    for j=1:2
        for k=1:2
            B2((2*(i-1)+j),(2*(i-1)+k))=B21(j,k,i);
            B3((2*(i-1)+j),(2*(i-1)+k))=B31(j,k,i);
        end
    end
end

%%%%%% Network Equations %%%%

%% %% Generator Buses %%

for i=1:m
    C11(:, :, i)=[Id(i)*V(i)*cos(beeta(i)-theta(i))-
Iq(i)*V(i)*sin(beeta(i)-theta(i))  0 0 0 0 0 0;
                -Id(i)*V(i)*sin(beeta(i)-theta(i))-
Iq(i)*V(i)*cos(beeta(i)-theta(i))  0 0 0 0 0 0];

    C21(:, :, i)=[V(i)*sin(beeta(i)-theta(i))      V(i)*cos(beeta(i)-
theta(i));
                V(i)*cos(beeta(i)-theta(i))      -V(i)*sin(beeta(i)-
theta(i))];
end

for i=1:m
    for j=1:2
        for k=1:Nd
            C1((2*(i-1)+j),(Nd*(i-1)+k))=C11(j,k,i);
        end
    end
end

```

```

for i=1:m
    for j=1:2
        for k=1:2
            C2((2*(i-1)+j),(2*(i-1)+k))=C21(j,k,i);

        end
    end
end

end

% for matrix C3

for i=1:m
    sum1=0;
    sum2=0;

    for k=1:n
        if (k~=i)
            sum_a=(V(k)*Y_mag(i,k)*sin(theta(i)-theta(k)-
alpha(i,k)));
            sum_b=(V(k)*Y_mag(i,k)*cos(theta(i)-theta(k)-
alpha(i,k)));
            sum1=sum1+sum_a;
            sum2=sum2+sum_b;

        end

    end

    s1(i)=sum1;
    s2(i)=sum2;
end

for i=1:m
    for j=1:m
        if i==j
            C3(2*i-1,2*j-1)=Iq(i)*V(i)*sin(beeta(i)-theta(i))-
Id(i)*V(i)*cos(beeta(i)-theta(i))+V(i)*s1(i);

            C3(2*i-1,2*j)=Id(i)*sin(beeta(i)-
theta(i))+Iq(i)*cos(beeta(i)-theta(i))-s2(i)-
2*V(i)*Y_mag(i,i)*cos(alpha(i,i));

```

```

        C3(2*i,2*j-1)=Id(i)*V(i)*sin(beeta(i)-
theta(i))+Iq(i)*V(i)*cos(beeta(i)-theta(i))-V(i)*s2(i);
        C3(2*i,2*j)=Id(i)*cos(beeta(i)-theta(i))-
Iq(i)*sin(beeta(i)-theta(i))-s1(i)+2*V(i)*Y_mag(i,i)*sin(alpha(i,i));
        else
            C3(2*i-1,2*j-1)=-V(i)*V(j)*Y_mag(i,j)*sin(theta(i)-
theta(j)-alpha(i,j));
            C3(2*i-1,2*j)=-V(i)*Y_mag(i,j)*cos(theta(i)-theta(j)-
alpha(i,j));
            C3(2*i,2*j-1)=V(i)*V(j)*Y_mag(i,j)*cos(theta(i)-theta(j)-
alpha(i,j));
            C3(2*i,2*j)=-V(i)*Y_mag(i,j)*sin(theta(i)-theta(j)-
alpha(i,j));

        end
    end
end

```

```

for i=1:m
    for j=1:(n-m-1)
        C4(2*i-1,2*j-1)=-V(i)*V(j+m)*Y_mag(i,j+m)*sin(theta(i)-
theta(j+m)-alpha(i,j+m));
        C4(2*i-1,2*j)=-V(i)*Y_mag(i,j+m)*cos(theta(i)-theta(j+m)-
alpha(i,j+m));
        C4(2*i,2*j-1)=V(i)*V(j+m)*Y_mag(i,j+m)*cos(theta(i)-
theta(j+m)-alpha(i,j+m));
        C4(2*i,2*j)=-V(i)*Y_mag(i,j+m)*sin(theta(i)-theta(j+m)-
alpha(i,j+m));
    end
end

```

```

for i=1:m
    for j=(n-m)
        C5(2*i-1,2*j-53)=-V(i)*V(j+m)*Y_mag(i,j+m)*sin(theta(i)-
theta(j+m)-alpha(i,j+m));
        C5(2*i-1,2*j-52)=-V(i)*Y_mag(i,j+m)*cos(theta(i)-theta(j+m)-
alpha(i,j+m));
        C5(2*i,2*j-53)=V(i)*V(j+m)*Y_mag(i,j+m)*cos(theta(i)-
theta(j+m)-alpha(i,j+m));
        C5(2*i,2*j-52)=-V(i)*Y_mag(i,j+m)*sin(theta(i)-theta(j+m)-
alpha(i,j+m));
    end
end

```



```

end
% for matrix D1 & D2

for i=1:(n-m-1)
    for j=1:m
        D1(2*i-1,2*j-1)=-V(i+m)*V(j)*Y_mag(i+m,j)*sin(theta(i+m)-
theta(j)-alpha(i+m,j));
        D1(2*i-1,2*j)= -V(i+m)*Y_mag(i+m,j)*cos(theta(i+m)-theta(j)-
alpha(i+m,j));
        D1(2*i,2*j-1)=V(i+m)*V(j)*Y_mag(i+m,j)*cos(theta(i+m)-
theta(j)-alpha(i+m,j));
        D1(2*i,2*j)= -V(i+m)*Y_mag(i+m,j)*sin(theta(i+m)-theta(j)-
alpha(i+m,j));
    end
end

%% Calculation of DFIG bus E1 and E2 (bus=10)

for i=(m+1):n
    sum3=0;
    sum4=0;

    for k=1:n
        if (k~=i)
            sum_c=(V(k)*Y_mag(i,k)*sin(theta(i)-theta(k)-
alpha(i,k)));
            sum_d=(V(k)*Y_mag(i,k)*cos(theta(i)-theta(k)-
alpha(i,k)));
            sum3=sum3+sum_c;
            sum4=sum4+sum_d;
        end

    end

    s3(i)=sum3;
    s4(i)=sum4;
end

for i=1:(n-m-1)
    for j=1:(n-m-1)

```

```

        if (i~=j)
            D2(2*i-1,2*j-1)=-
V(i+m)*V(j+m)*Y_mag(i+m,j+m)*sin(theta(i+m)-theta(j+m)-
alpha(i+m,j+m));
            D2(2*i-1,2*j)=-V(i+m)*Y_mag(i+m,j+m)*cos(theta(i+m)-
theta(j+m)-alpha(i+m,j+m));
            D2(2*i,2*j-
1)=V(i+m)*V(j+m)*Y_mag(i+m,j+m)*cos(theta(i+m)-theta(j+m)-
alpha(i+m,j+m));
            D2(2*i,2*j)=-V(i+m)*Y_mag(i+m,j+m)*sin(theta(i+m)-
theta(j+m)-alpha(i+m,j+m));

        else

            D2(2*i-1,2*j-1)=V(i+m)*s3(i+m);
            D2(2*i-1,2*j)=-s4(i+m)-
2*V(i+m)*Y_mag(i+m,i+m)*cos(alpha(i+m,i+m));
            D2(2*i,2*j-1)=-V(i+m)*s4(i+m);
            D2(2*i,2*j)=-
s3(i+m)+2*V(i+m)*Y_mag(i+m,i+m)*sin(alpha(i+m,i+m));

        end
    end
end

for i=1:(n-m-1)
    for j=(n-m)
        if (i~=j)
            D3(2*i-1,2*j-53)=-
V(i+m)*V(j+m)*Y_mag(i+m,j+m)*sin(theta(i+m)-theta(j+m)-
alpha(i+m,j+m));
            D3(2*i-1,2*j-52)=-V(i+m)*Y_mag(i+m,j+m)*cos(theta(i+m)-
theta(j+m)-alpha(i+m,j+m));
            D3(2*i,2*j-
53)=V(i+m)*V(j+m)*Y_mag(i+m,j+m)*cos(theta(i+m)-theta(j+m)-
alpha(i+m,j+m));
            D3(2*i,2*j-52)=-V(i+m)*Y_mag(i+m,j+m)*sin(theta(i+m)-
theta(j+m)-alpha(i+m,j+m));

        else

            D3(2*i-1,2*j-53)=V(i+m)*s3(i+m);
            D3(2*i-1,2*j-52)=-s4(i+m)-
2*V(i+m)*Y_mag(i+m,i+m)*cos(alpha(i+m,i+m));
            D3(2*i,2*j-53)=-V(i+m)*s4(i+m);

```

```

        D3(2*i,2*j-52)=-
s3(i+m)+2*V(i+m)*Y_mag(i+m,i+m)*sin(alpha(i+m,i+m));

        end
    end
end

for i=(m+1):n
    sum5=0;
    sum6=0;

    for k=1:n
        if (k~=i)
            sum_e=(V(k)*Y_mag(i,k)*sin(theta(i)-theta(k)-
alpha(i,k)));
            sum_f=(V(k)*Y_mag(i,k)*cos(theta(i)-theta(k)-
alpha(i,k)));
            sum5=sum3+sum_e;
            sum6=sum4+sum_f;

        end

    end

    s5(i)=sum5;
    s6(i)=sum6;
end

for i=(n-m)
    for j=1:m
        F1(2*i-53,2*j-1)=-V(i+m)*V(j)*Y_mag(i+m,j)*sin(theta(i+m)-
theta(j)-alpha(i+m,j));
        F1(2*i-53,2*j)=-V(i+m)*Y_mag(i+m,j)*cos(theta(i+m)-theta(j)-
alpha(i+m,j));
        F1(2*i-52,2*j-1)=V(i+m)*V(j)*Y_mag(i+m,j)*cos(theta(i+m)-
theta(j)-alpha(i+m,j));
        F1(2*i-52,2*j)=-V(i+m)*Y_mag(i+m,j)*sin(theta(i+m)-theta(j)-
alpha(i+m,j));
    end
end

for i=(n-m)

```

```

    for j=1:(n-m-1)
        if (i~=j)
            F2(2*i-53,2*j-1)=-
V(i+m)*V(j+m)*Y_mag(i+m,j+m)*sin(theta(i+m)-theta(j+m)-
alpha(i+m,j+m));
            F2(2*i-53,2*j)=-V(i+m)*Y_mag(i+m,j+m)*cos(theta(i+m)-
theta(j+m)-alpha(i+m,j+m));
            F2(2*i-52,2*j-
1)=V(i+m)*V(j+m)*Y_mag(i+m,j+m)*cos(theta(i+m)-theta(j+m)-
alpha(i+m,j+m));
            F2(2*i-52,2*j)=-V(i+m)*Y_mag(i+m,j+m)*sin(theta(i+m)-
theta(j+m)-alpha(i+m,j+m));

        else

            F2(2*i-53,2*j-1)=V(i+m)*s5(i+m);
            F2(2*i-53,2*j)=-s6(i+m)-
2*V(i+m)*Y_mag(i+m,i+m)*cos(alpha(i+m,i+m));
            F2(2*i-52,2*j-1)=-V(i+m)*s6(i+m);
            F2(2*i-52,2*j)=-
s5(i+m)+2*V(i+m)*Y_mag(i+m,i+m)*sin(alpha(i+m,i+m));

        end
    end
end

for i=(n-m)
    for j=(n-m)
        if (i~=j)
            F3(2*i-53,2*j-53)=-
V(i+m)*V(j+m)*Y_mag(i+m,j+m)*sin(theta(i+m)-theta(j+m)-
alpha(i+m,j+m));
            F3(2*i-53,2*j-52)=-V(i+m)*Y_mag(i+m,j+m)*cos(theta(i+m)-
theta(j+m)-alpha(i+m,j+m));
            F3(2*i-52,2*j-
53)=V(i+m)*V(j+m)*Y_mag(i+m,j+m)*cos(theta(i+m)-theta(j+m)-
alpha(i+m,j+m));
            F3(2*i-52,2*j-52)=-V(i+m)*Y_mag(i+m,j+m)*sin(theta(i+m)-
theta(j+m)-alpha(i+m,j+m));

        else

            F3(2*i-53,2*j-53)=V(i+m)*s5(i+m);
            F3(2*i-53,2*j-52)=-s6(i+m)-
2*V(i+m)*Y_mag(i+m,i+m)*cos(alpha(i+m,i+m));

```

```

        F3(2*i-52,2*j-53)=-V(i+m)*s6(i+m);
        F3(2*i-52,2*j-52)=-
s5(i+m)+2*V(i+m)*Y_mag(i+m,i+m)*sin(alpha(i+m,i+m));

        end
    end
end

%% Calculation of eigen value including DFIG

A_mat=[A1 zeros(119,7);
        zeros(7,119) P1_mat];

B_mat=[A2 A3 zeros(119,52) zeros(119,2);
        zeros(7,34) zeros(7,34) zeros(7,52) P2_mat];

C_mat=[B1 zeros(34,7);
        C1 zeros(34,7);
        zeros(52,119) zeros(52,7);
        zeros(2,119) Q1_mat];

D_mat=[B2 B3 zeros(34,52) zeros(34,2);
        C2 C3 C4 C5;
        zeros(52,34) D1 D2 D3;
        zeros(2,34) F1 F2 (Q2_mat-F3)];

Asys=A_mat - B_mat* inv(D_mat) *C_mat;
lamda=eig(Asys);
plot(lamda, '+', 'LineWidth', 4)
%title('Eigenvalues With DFIG', 'Color', 'b', 'FontWeight', 'bold')
grid on
save stab12_9b Asys lamda

```

File 8

```
Stability1_withoutDFIG_7
Stability1_withDFIG_8
clc
clear all

load stab1_9b
load stab12_9b

%% Calculation of participation factor

% calculation of pf without DFIG

[RV_1,DIA_1] = eig(Asys1);           % RV_1 right eigen vector
LV_1=inv(RV_1);                     % LV_1 left eigen vector
RV_1 = abs(RV_1); LV_1 = abs(LV_1);

dim_1=max(size(Asys1));             % Dimension of Asys1 matrix
for i=1:dim_1
    for k=1:dim_1
        pfac_1(i,k)=RV_1(i,k)*LV_1(k,i);
    end
end
pf_1=abs(pfac_1);

% calculation of pf with DFIG

[RV,DIA] = eig(Asys);              % RV right eigen vector
LV=inv(RV);                         % LV left eigen vector

dim=max(size(Asys));               % Dimension of Asys matrix
for i=1:dim
    for k=1:dim
        pfac(i,k)=RV(i,k)*LV(k,i);
    end
end
pf=abs(pfac);
```

```

save pfdata pf_1 pf

% % Plot in graph
%
% subplot(2,2,[1 2]) ;
% hold on
% grid on
% plot(lamda1, '+')
%           title('Synchronous Machine Without
DFIG(Lamda1)', 'Color', 'r', 'FontWeight', 'bold')
% hleg1 = legend('Lamda1');
% set(hleg1, 'Location', 'NorthWest')
%
% subplot(2,2,[3 4]);
% plot(lamda, '+')
% grid on
%           title('Synchronous Machine Combine with DFIG
(Lamda)', 'Color', 'r', 'FontWeight', 'bold')
% hleg2 = legend('Lamda');
% set(hleg2, 'Location', 'NorthWest')

% hold off

```

File 10

```
diary on
part_factor_9
clear all

load stab1_9b
load stab12_9b
load pfddata
[s,i] = sort(pf);
[s_1,i_1] = sort(pf_1);

x = size(pf);
y = size(pf_1);

sort_depth = 120;
search_depth = 126;
for j = 1:sort_depth
for k = 1:y(1)
    M(k,1) = k;
    temp = i_1((y(1)-j+1),k);
for n = j:search_depth
for l=1:x(2)
    if temp == i((x(1)-n+1),l)
        M(k,2*(j-1)+2) = temp;
        M(k,2*(j-1)+3) = 1;
    else
    end
end
end
end
end

save sorted M
load sorted

N1 = 17; %no. of sync machines
cod = [cellstr('del') cellstr('w') cellstr('Eqd') cellstr('Edd')
cellstr('Efd') cellstr('Vr') cellstr('Rf')];
```



```

for i = 1:N1;
    for j = 1:length(cod)
        name(i,j) = cellstr([char(cod(j)) '_' num2str(i)]);
    end
end

%adding anmes of dfig states to name matrix
N2 = 1;
cod = [cellstr('i_qs') cellstr('i_ds') cellstr('e_qs') cellstr('e_ds')
cellstr('w_r') cellstr('theta') cellstr('w_t')];
for i = 1:N2;
    for j = 1:length(cod)
        name(N1+i,j) = cellstr([char(cod(j)) '_' num2str(N1+i)]);
    end
end
save name name
% indexing states

load sorted
load name

N1=21;
N2=7;
for mm=1:1
for kk = 1:N1
    temp = M(kk,2*mm);
    ii = ceil(temp/N2);
    jj = temp - (ii-1)*N2;
    index(kk,mm) = name(ii,jj);
end
end

%disp(' Eigen_value_w/oDF(A)    Eigen_value_with_DF(B)    Difference(A-
B)    states')
comp_tabl=[lamda1 lamda(M(:,2)) (lamda1-lamda(M(:,2))) M(:,3)];
tabl=[real(lamda1)    real(lamda(M(:,2)))    real(lamda1-lamda(M(:,2)))
M(:,3)];

% take only reqd matrices

save arrange9 comp_tabl tabl pf pf_1 lamda1 lamda index name M

```

```

clear all
load arrange9

%Plot in graph

subplot(2,2,[1 2]) ;
hold on
grid on
plot(lamda1, '+')
title('Eigenvalues Without DFIG', 'Color', 'b', 'FontWeight', 'bold')
% hleg1 = legend('Lamda1');
% set(hleg1, 'Location', 'NorthWest')

subplot(2,2,[3 4]);
plot(lamda, '+')
grid on
title('Eigenvalues with DFIG', 'Color', 'b', 'FontWeight', 'bold')
%hleg2 = legend('Lamda');
%set(hleg2, 'Location', 'NorthWest')
hold off % sort_depth = 7;
diary off

```

APPENDIX D: Plagiarism Report

Bishwas_VII

ORIGINALITY REPORT

14%

SIMILARITY INDEX

9%

INTERNET SOURCES

8%

PUBLICATIONS

11%

STUDENT PAPERS

PRIMARY SOURCES

1	Submitted to Seoul National University Student Paper	1%
2	res.mdpi.com Internet Source	1%
3	Jadhav, H.T., and Ranjit Roy. "A comprehensive review on the grid integration of doubly fed induction generator", International Journal of Electrical Power & Energy Systems, 2013. Publication	1%
4	ijates.com Internet Source	<1%
5	www.grin.com Internet Source	<1%
6	Submitted to Indian Institute of Technology, Kharagpure Student Paper	<1%
7	K. E. Okedu, S. M. Muyeen, Rion Takahashi, Junji Tamura. "Effectiveness of Current-controlled Voltage Source Converter Excited	<1%

Doubly Fed Induction Generator for Wind Farm Stabilization", Electric Power Components and Systems, 2012

Publication

8	researchbank.swinburne.edu.au Internet Source	<1%
9	Submitted to Tshwane University of Technology Student Paper	<1%
10	Submitted to Engineers Australia Student Paper	<1%
11	Submitted to Institute of Engineering, Pulchock Campus, Tribhuvan University Student Paper	<1%
12	docshare.tips Internet Source	<1%
13	pcmp.springeropen.com Internet Source	<1%
14	flipkarma.com Internet Source	<1%
15	Submitted to Asian Institute of Technology Student Paper	<1%
16	www.inderscienceonline.com Internet Source	<1%
17	Submitted to London School of Marketing Student Paper	<1%
